universität wien

DISSERTATION

Titel der Dissertation

„Novel Role of STAT3 in Hepatocellular Carcinogenesis“

Band 1 von 1

Verfasser

Mag.rer.nat. Georg Machat

angestrebter akademischer Grad

Doktor der Naturwissenschaften (Dr.rer.nat.)

Wien, 2013

Studienkennzahl lt. Studienblatt:	A 091 441
Dissertationsgebiet lt. Studienblatt:	Genetik und Mikrobiologie
Betreuerin / Betreuer:	Ao. Univ. Prof. Mag. Dr. Wolfgang Mikulits

Table of contents:

1 Abstract 1

2 Zusammenfassung 2

3 Introduction 3

3.1 Hepatocellular Carcinoma 3

3.2 $p14^{ARF}/p19^{ARF}$ 14

3.2.1 The ARF-p53 Pathway 14

3.2.2 $p19^{ARF}/p14^{ARF}$ p53-Independent Tumor Suppression 16

3.2.3 $p19^{ARF}/p14^{ARF}$ in HCC 20

3.3 JAK-STAT Pathway and STAT3 21

3.3.1 JAK-STAT 21

3.3.2 The Structure and Function of STAT Proteins 22

3.3.3 STAT3 24

3.4. Aims of the study 35

4 Manuscript 36

4.1 Contribution to this study 37

4.2 Abstract 38

4.3 Introduction 39

4.4 Materials and Methods 41

4.5 Results 43

4.5.1 Stat3 represses tumor growth of Ras-transformed $p19^{ARF-/-}$ hepatocytes 43

4.5.2 Loss of Stat3 promotes tumor formation in $p19^{ARF-/-}$ MIM-R hepatocytes 43

4.5.3 Stat3 acts pro-oncogenic in $p19^{ARF}$-positive Ras-transformed hepatocytes 44

4.5.4 Upregulation of $p19^{ARF}$ is associated with DEN-induced tumor formation in $Stat3^{fl/fl}$ mice 44

4.5.5 $p14^{ARF}$ modulates Stat3 activation during human HCC development 45

4.5.6 $p14^{ARF}$ acts downstream of Jak-mediated Stat3 phosphorylation 45

4.6 Discussion 47

4.7 References 50

4.8 Figures 53

4.9 Supplemetary data 60

4.9.1 Supporting Figures 60

4.9.2 Supporting Material and Methods 63

5 Results 65

5.1 Microarray analysis of murine STAT3-deficient HCC cells expressing STAT3 isoforms 65
5.2 Murine HCC cells show functional p53 pathway 65
5.3 Unphosphorylated STAT3 (U-STAT3) translocates to the nucleus and is transcriptionally active 66
5.4 NFkB translocates to the nucleus irrespective of U-STAT3 67
5.5 Suppression of STAT3 phosphorylation in $p14^{ARF}$ knockdown Hep3B cells occurs early in tumor development 68
5.6 Proliferation of Hep3B cells lacking $p14^{ARF}$ in vitro is independent of STAT3 activation....71
5.7 Exogenous expression of $p14^{ARF}$ leads to decreased tumor formation and vascularization 71
5.8 The impact of STAT3 and/or p14 knockdown is cell line dependent....74
5.8.1 Knockdown of STAT3 in human Hep3B hepatoma cells 74
5.8.2 Hep3B-shSTAT3-shp14 75
5.8.3 PLC-shSTAT3 76
5.9 Detection of $p14^{ARF}$in primary human HCC....77
5.10 The TGF-β-Smad pathway is crucial in murine, but dispensable in human hepatoma cells 78
5.11 Phosphorylation of STAT3 is independent of PTEN 79
6 Discussion....82
6.1 $p19^{ARF}$/$p14^{ARF}$ Controls Oncogenic Functions of STAT3 in HCC – in retrospect....82
6.2 Further investigations of murine model systems 85
6.2.1 Microarray analysis 85
6.2.2 p53 functionality 86
6.2.3 U-STAT3 localization and transactivation 86
6.2.4 The interaction of NFkB and U-STAT3....87
6.2.5 Conclusions and outlook 87
6.3 Investigation on human hepatoma cell lines – facing diversity....88
6.3.1 Early down-regulation of active STAT3 in Hep3B-shp14ARF cells 88
6.3.2 Impact of $p14^{ARF}$ expression....89
6.3.3 Intervention with STAT3....90
6.3.4 Double knockdown of STAT3/p14ARF in human hepatoma cells 90
6.3.5 Analysis of p14ARF in primary human HCC 91
6.3.6 The role of STAT3 in TGF-β signaling....92
6.3.7 Investigations on PTEN/STAT3 interactions in human HCC 93
6.4 Concluding remarks 95
7 References....98
8 Materials and Methods....119

9 Acknowledgements 125
10 Curriculum Vitae 126

1 Abstract

Hepatocellular carcinoma (HCC) is a leading cause of cancer-related death. Chronic liver disease caused by viral hepatitis infection, steatohepatitis or intoxication by Aflatoxin or alcohol represents the main background for HCC development. Deregulation of various signaling cascades such as aberrations in Ras and STAT (signal transducer and activator of transcription) signaling generates heterogeneous molecular patterns of HCC. This study addressed the role of STAT3 in HCC. Albeit known as an oncogene in HCC, STAT3 showed both pro- and anti-oncogenic features in Ras-transformed murine hepatoma cells which are under the control of $p19^{ARF}$. Knockout of STAT3 as well as exogenous expression of STAT3 lacking the phosphorylation site on Tyr^{705} (U-STAT3) caused enhanced tumor formation, demonstrating a tumor-suppressive function of STAT3 in Ras-transformed hepatocytes that are deficient for $p19^{ARF}$. Furthermore, the knockout of STAT3 abrogated the anti-proliferative effect of transforming growth factor-β (TGF-β) in $p19^{ARF}$-deficient murine hepatocytes, corroborating its tumor suppressive effects. Importantly, $p19^{ARF}$ expressing hepatocytes exhibited the reversed phenotype by displaying tumor promoting properties through the synergy of STAT3 and $p19^{ARF}$. Further investigations showed the ability of U-STAT3 to translocate into the nucleus and to enhance transcriptional transactivation. Analysis of STAT3 and $p14^{ARF}$ (the human homologue of $p19^{ARF}$) in several human hepatoma cell lines suggested their crosstalk also in human HCC. In summary, these data show tumor-promoting and novel tumor-suppressive functions of STAT3 in malignant hepatocytes which are modulated by Ras-signaling and the availability of $p14^{ARF}$/$p19^{ARF}$. Several lines of evidence further indicate that U-STAT3 is crucially involved in HCC development. These findings implicate a detailed examination of the genetic changes prior to individualized anti-HCC therapy, as treatment modalities targeting STAT3 might cause adverse effects.

2 Zusammenfassung

Das hepatozelluläre Karzinom (HCC) ist eine der häufigsten Krebserkrankungen, die zum Tode führen. Chronische Lebererkrankungen, die durch virale Hepatitis-Infektionen oder Steatohepatitis beziehungsweise durch permanente Alkoholintoxikationen verursacht werden, sind die häufigste Ursache für die Entwicklung eines HCC. Veränderungen in den verschiedenen Signalkaskaden, wie dem Ras- oder STAT (Signal Transducer and Activator of Transcription)-Signalweg, führen zu einem heterogenen molekularen Muster in HCCs. Die Studie im Rahmen der Dissertation befasst sich mit der Rolle von STAT3 im HCC. Obwohl als Onkogen bekannt, zeigt STAT3 in Ras-transformierten Hepatom-Zelllinien pro- aber auch anti-onkogene Eigenschaften in Abhängigkeit von $p19^{ARF}$. Sowohl der Verlust wie auch die exogene Expression von STAT3, welchem die Phosphorylierungsstelle am Tyr^{705} fehlt (U-STAT3), verursachten erhöhtes Tumorwachstum. Dies beweist eine tumor-suppressive Funktion von STAT3 in Ras-transformierten, $p19^{ARF}$-defizienten Hepatozyten. Weiters zeigt die Deletion von STAT3 eine Aufhebung des von TGF-β (Transforming Growth Factor-β) bedingten anti-proliferativen Effekts in $p19^{ARF-/-}$-Hepatozyten, was die tumor-suppressive Eigenschaft von STAT3 unterstreicht. Wichtig in diesem Zusammenhang ist, dass der beobachtete Phänotyp in $p19^{ARF}$-exprimierenden Hepatozyten zu einem onkogenen Effekt umgekehrt wird. Weitere Untersuchungen zeigten die Fähigkeit von U-STAT3 zur Translokation in den Zellkern und zur Aktivierung der Transkription. Zudem weist die Analyse von STAT3 und $p14^{ARF}$ (dem humanen Homolog zu $p19^{ARF}$) in verschiedenen humanen Zelllinien auf deren synergistische Interaktion in humanen HCC Zellen hin. Zusammenfassend zeigen die Resultate dieser Studie, dass STAT3 sowohl eine tumor-fördernde als auch eine tumor-suppressive Funktion in Ras-transformierten Hepatozyten ausübt, die von $p14^{ARF}$/$p19^{ARF}$ abhängig ist. Darüber hinaus hat U-STAT3 einen entscheidenden Einfluss auf die HCC-Entwicklung. Diese Ergebnisse legen eine detaillierte Untersuchung der genetischen Veränderungen im Vorfeld einer individualisierten anti-HCC Therapie nahe, da andernfalls gezielte STAT3 Behandlungen negative Auswirkungen mit sich bringen können.

3 Introduction

3.1 Hepatocellular Carcinoma

Hepatocellular carcinoma (HCC) shows the sixth most common incidence of neoplasms and holds the third place in cancer-related mortality (Forner et al. 2012). Among other hepatic cancers, such as cholangiocellular carcinoma, HCC represents 90% of all malignant diseases in the liver (Nordenstedt et al. 2010). Its etiology is highly variable and ranges from hepatitis infection to lifestyle indication, such as alcohol abuse (El-Serag 2011). Accordingly, the origin of liver cancer is also dependent on the geographic region. For example, 75% of all hepatitis B virus (HBV) infected cases occur in Asia and half of them finally develops HCC (El-Serag 2012). Japan represents a particular case, since approximately 90% of HCC derived from hepatitis C virus (HCV) infection (Yoshizawa 2002). In the United States, alcohol abuse leads the ranking of risk factors of HCC (Altekruse et al. 2009). Further important risk factors are provided by underlying liver diseases such as nonalcoholic fatty liver disease (NAFLD) and nonalcoholic steatohepatitis (NASH), which are predominately the consequence of type II diabetes mellitus and obesity (Ascha et al. 2010). Chronic liver disease and its endstage cirrhosis results from the factors mentioned above and are considered as a premalignant state (Alazawi et al. 2010).

Several staging systems have been developed for HCC to provide evaluation for proper therapeutic options. Nowadays, therapeutic management is given by the Barcelona Clinic Liver Cancer (BCLC) staging system (Cabrera and Nelson 2010). Early stage options are surgical resection, liver transplantation, percutaneous ethanol injection (PEI) and radiofrequency ablation (RFA). PEI causes necrosis of tumor tissue and represents a low-cost application with high efficacy. However, local recurrence has been observed in tumors larger than 3 cm, as the ethanol failed to reach the whole tumor volume (Khan et al. 2000). Therefore, PEI has been replaced by RFA that yields to more rigorous tumor ablation. Transarterial chemoembolization (TACE) represents the major therapy for intermediate stage tumors. The main advantage of TACE is that the main blood supply of liver tumors is arterial (Cabrera and Nelson 2010). Drawbacks of TACE are its possibly contraindicative role observed in patients harboring portal vein invasion, advanced cirrhosis or thrombosis (Georgiades et al. 2005). In addition to palliative treatment, targeted therapies are applied for patients with advanced stage HCC. Most notably, the “Sorafenib Hepatocellular Carcinoma Assessment Randomized Protocol (SHARP)” attracted great attention. Sorafenib inhibits

tyrosine kinases of platelet-derived growth factor receptor-β (PDGFR-β), vascular endothelial growth factor receptors 1-3 (VEGFR1-3) as well as serine–threonine kinases of Raf-1 and B-Raf. It prolongs the survival of late-stage HCC patients for almost three months, but also side effects occur upon treatment (Llovet et al. 2008).

A large body of evidence is available that aberrant signaling from ligands and their respective receptors to cytoplasmic effector molecules plays a pivotal role in HCC. Some important regulatory factors and pathways are listed below and their implications in HCC are introduced.

Insuline-Like Growth Factor. Insulin-like growth factors (IGFs) and IGF receptors (IGFRs) provide an indispensable axis for cell homeostasis and cell growth in healthy organisms and some neoplasms. In the latter, mostly deregulated ligand expression rather than mutations of the receptors leads to aberrant signaling (Pollak 2012). IGFR acts upstream of Ras-Raf-MAPK and Akt/mTOR signaling (Samani et al. 2007). In HCC, a recent clinical study suggested that high serum levels of IGF1 correlate with better prognosis of patients receiving anti-angiogenic therapy (Shao et al. 2012). Another investigation revealed that microRNA (miR)-145 targets several genes along the IGF pathway, such as IGFR1 and insulin receptor substrate (IRS)-1 and -2, leading to cell cycle arrest and apoptosis (Law et al. 2012). Overexpression of IGF2 that is commonly observed in liver cancer is regulated by a specific pattern of promoter activation. This event is epigenetically modulated via hypomethylation. Thus, IGF2 might be used as a prognostic marker (Tang et al. 2006). An antibody targeting specifically IGFR1 showed promising results by reducing proliferation and tumor formation in a HCC xenograft model (Tovar et al. 2010). Since efficacy of this antibody (IMC-A12, cixutumumab) was limited in some cancers, further studies revealed a role of EGFR (epidermal growth factor receptor) via Akt/mTOR signaling in bypassing the potency of cixutumumab (Shin et al. 2011).

Epidermal Growth Factor. The epidermal growth factor (EGF) family consists of four receptors and 13 ligands, wherein EGF and transforming growth factor alpha (TGF-α) are the most prominent ones (Higashiyama et al. 2008). Dysregulation of EGFR signaling in various epithelial cancers via mutation and subsequent enhancement of tyrosine kinase activity is well-known (Humphrey et al. 1990). Many EGFR mutants have been identified in several tumors, such as EGFR variant 3 (EGFR vIII), which is frequently expressed in glioblastoma, lung, prostate and ovarian cancer (Kuan et al. 2001).

There is a plethora of pathways being activated by EGFRs. Among them are the Ras-MAPK, Grb-2, Shc, PLC-γ, PI3-K, Src and JAK-STAT pathways (Jorissen et al. 2003). Several direct

targeting compounds, such as monoclonal antibodies or kinase inhibitors, are available against EGFRs, as listed in Table 1.

Drug	Target	Type	Application
Cetuximab (Erbitux)	EGFR	Chimeric mAb	CRC, and head and neck cancer
Panitumumab (Vecitibix, ABX-EGF)	EGFR	Fully human mAb	CRC
Gefinitib (Iressa, ZD1839)	EGFR	TKI	NSCLC
Erlotinib (Tarceva)	EGFR	TKI	NSCLC and panvreas cancer
Trastuzumab (Herceptin)	ErbB2	Humanized mAb	Breast cancer

CRC, colorectal cancer; mAb, monoclonal antibody; NSCLC, non-small cell lung carcinoma; TKI, tyrosine kinase inhibitor.

Table 1. Approved therapeutics targeting EGFRs; taken from Higashiyama 2008.

EGFR is overexpressed in more than 50% of HCC cases. It was shown that Erlotinib and Gefitinib, two tyrosine kinase inhibitors, exhibit promising results in a phase II study and in cell growth inhibition, respectively (Buckley et al. 2008). Amphiregulin, an EGFR ligand, was found upregulated in pre-malignant HCC stages such as chronic liver disease and as a mitogenic and anti-apoptotic factor in HCC cells, indicating amphiregulin as a potent therapeutic target (Castillo et al. 2006). Interestingly, EGFR activity governs the efficacy of Sorafenib. Upon EGFR inhibition, better results in proliferation control were achieved, suggesting RAF kinase as a key player in this respect (Ezzoukhry et al. 2012). A further study focusing on the interaction of EGFR and Sorafenib confirmed these results, indicating that EGFR-dependent activation of ERK and AKT is targeted by Sorafenib (Blivet-Van Eggelpoel et al. 2012).

Hepatocyte Growth Factor/c-Met. This signaling drives several proto-oncogenic features, such as proliferation, angiogenesis and cell motility (Kaposi-Novak et al. 2006). Increased levels of hepatocyte growth factor (HGF) and its corresponding receptor c-Met have been previously found in several tumor tissues, such as colorectal, thyroid, gastric and prostate cancer. In HCC, high c-Met expression indicated lower 5-year survival and enhanced intrahepatic metastases (Ueki et al. 1997). A recent study proposed high levels of HGF/c-Met expression as a reliable marker for disease recurrence. Notably, in contrast to other solid cancers, no gene amplification was observed in HCC (Kondo et al. 2012). Foretinib, a small molecule inhibitor targeting tyrosine kinases of c-Met but also VEGFR, achieved reduction of tumor growth in xenograft models. The authors also suggested an interplay of c-Met and VEGFR in HCC regarding angiogenesis (Huynh et al. 2012). Ivanovska and co-workers performed comparative microarray analysis of a transgenic c-Met mouse model and a collection of human HCC samples. This interesting study showed similar gene signatures between murine and human tissues and suggested mouse disease models as a valuable source for biomarkers (Ivanovska et al. 2011).

Vascular Endothelial Growth Factor. The VEGF/VEGFR system is composed of several ligands (VEGFA-D) and 3 receptors (VEGFR1-3). This pathway plays a crucial role both in physiological and malignant formation of new blood vessels. After a balance is achieved between cell growth and cell death, vascularization is indispensable for further proliferation and spread of the tumor (Leite de Oliveira et al. 2011). Major efforts have been aimed at inhibiting this axis. For example, bevacizumab showed promising reduction of vessel formation in several tumor tissues (Crawford and Ferrara 2009), however, it failed to significantly prolong survival of HCC patients (Leite de Oliveira et al. 2011). Sunitinib, another tyrosine kinase inhibitor targeting VEGFR is applied in gastrointestinal tumors showing resistance against imatinib treatment (Crawford and Ferrara 2009). Importantly, there is increasing evidence that early tumor growth is attenuated, yet invasion and metastasis more frequently occurs upon VEGFR inhibition, suggesting a dual role in carcinogenesis (Loges et al. 2009). In line with these findings, a HCC model showed that treatment with Sorafenib inhibits VEGF receptors, however, led to increased amount of tumor-associated macrophages and concomitant pro-oncogenic factors. Co-therapy of Sorafenib and macrophage inhibitors could attenuate this effect (Zhang et al. 2010). In addition, a recent study showed that VEGFR-1, that was initially thought to be expressed predominately in endothelial cells, indicates poor prognosis in HCC (Li et al. 2012). Another study reported that VEGFR-1 was capable to induce epithelial to mesenchymal transition (EMT) upon treatment with VEGF-B (Yi et al. 2011). Recently, the knockdown of VEGF showed a reduced proliferation, survival and migration in hepatoma cell lines (Zhang et al. 2012). Interestingly, these effects were accompanied by enhanced p53 expression, indicating that VEGF actions might be mediated by p53.

Platelet-Derived Growth Factor. Platelet-Derived Growth Factor (PDGF) ligands exist in four different isoforms, PDGF-A-D, and homo- and hetero-dimerization (only between A and B) must take place to gain functionality (Wang et al. 2009). Dimers bind to their respective PDGFR-α or -β receptors which in turn also form homo- or hetero-dimers and activate signaling cascades, including NF-κB, PI3K or ERK (Wang et al. 2010). In the liver, the PDGF-B dimer (PDGF BB) is an important regulatory molecule for fibrogenesis. Together with TGF-β, it is secreted by activated hepatic stellate cells (HSCs). Therefore, it plays a crucial role in liver fibrosis and cirrhosis (Pinzani et al. 1998). Accordingly, chemical induction of HCC in a transgenic PDGF-B mouse showed increased tumor formation compared to control mice and led to enhanced levels of VEGF, fibroblast growth factor (FGF) and CD31 (Maass et al. 2011). Furthermore, overexpression of PDGF-C in mouse resembled

the etiology of alcohol abuse or NAFLD, leading to liver fibrosis and finally to HCC (Campbell et al. 2005).

Fibroblast Growth Factor. 23 Fibroblast Growth Factor (FGF) ligands are known. Upon processing in the extracellular matrix, they bind to the five known FGF-receptors (FGFR1-5). FGFR1-4 contain tyrosine kinase activity (Johnson and Williams 1993). Some FGFs are important pro-angiogenic factors during tumor development and show synergisms with VEGF and PDGF (Daniele et al. 2012). Since the FGF/FGFR axis participates in the development of liver fibrosis and cirrhosis, single components of this family are in the focus of further investigations regarding their role in HCC (Cheng et al. 2011). For example, it was shown that FGF19/FGFR4 levels are increased in HCC and acts in a pro-tumorigenic fashion (Miura et al. 2012). In line with this study, Sawey et al. explored the co-amplification of FGF19 and the *CCND1* gene (encoding cyclin D1) via screening of human HCC specimens. Interestingly, FGF19 exhibited an equal importance as cyclin D1 in driving tumor progression as suggested by gain- and loss-of-function studies (Sawey et al. 2011). The FGF8 subfamily, comprising of FGF8, 17 and 18, describes further important players in HCC due to its involvement in cell survival and neo-angiogenesis (Gauglhofer et al. 2011). Furthermore, screening of HCC samples indicated FGFR2 as a marker for poor prognosis and a promising target (Harimoto et al. 2010). However, another publication showed an anti-tumorigenic role of the FGFR2-IIIb isoform, demonstrating increased apoptosis and decreased proliferation upon re-expression in HCC (Amann et al. 2010). The latter examples strengthen the complexity of this signaling cascade.

Ras-Raf-MEK-ERK. Ras functions as a switch that governs various downstream effectors. Briefly, the member of the small GTPase family itself gets activated by guanosine exchange factors (GEFs), such as SOS (son of sevenless). In resting cells, SOS is stably bound to the adaptor protein Grb2 (growth factor receptor-bound 2). Upon receptor tyrosine kinase activation, SOS-Grb2 is recruited to Ras leading to its activation (Mitin et al. 2005). Ha-, K-, or N-Ras are active in their oncogenic versions on average in 30% of human cancers, with pancreatic cancer as the highest (90%; Malumbres and Barbacid 2003). However, this is not the case in HCC. Instead, Ras GTPase activating proteins (GAPs) that normally suppress wild-type Ras are downregulated. Re-introduction of these Ras-inhibitors reversed the pro-oncogenic phenotype in HCC cell lines (Calvisi et al. 2011). In a recent study, overexpression of N-Ras alone in the liver via hydrodynamic gene transfer showed no carcinogenic effect.

However, co-expression together with AKT induced dramatic tumor formation, indicating interactions between those pathways (Ho et al. 2012).

Ras signals via the Raf-MEK-ERK axis, which is one of the most important mediators of growth factor signaling that governs proliferation, differentiation and survival (Johnson and Lapadat 2002). The route of signaling is accomplished via 3 kinases, ultimately leading to activation of transcription factors. Beside the effector kinases of Raf (composed of A-, B-, and C-Raf), ERK1/2 (extracellular signal regulated Kinase), the p38 kinases, JNK1, 2, 3 (c-Jun amino-terminal kinases) and ERK5 complete the map of MAP kinases as depicted in Figure 1 (Roberts and Der 2007).

B-Raf leads the list of the most frequently mutated kinase in human malignancies following a screen of human cancer genomes comprising breast, lung, colorectal, gastric, testis, ovarian, renal, melanoma, glioma and acute lymphoblastic leukaemia (Greenman et al. 2007). The most frequent B-Raf mutation occurs on residual 600 (V600E), as shown in melanoma, colorectal and ovarian cancers. Several cancer models showed promotion of C-Raf-mediated signaling upon B-Raf depletion, thus compensating B-Raf inhibition. Since cells might also harbor mutated Ras, inhibitors targeting solely mutant B-Raf might be a leaky approach to attack this pathway (Osborne et al. 2012).

Enhanced levels of Ras, C-Raf and active MEK1 are predictive marker for poor prognosis in HCC (Chen et al. 2011). Notably, C-Raf, not B-Raf, was shown to be mostly overexpressed in liver cancers (Hwang et al. 2004). Several small molecule inhibitors targeting MAPK protagonists have been applied to HCC tissues. However, access is limited, since resistance was observed in some tumors, possibly triggered by hyperphoshorylation of MEK (Yip-Schneider et al. 2009).

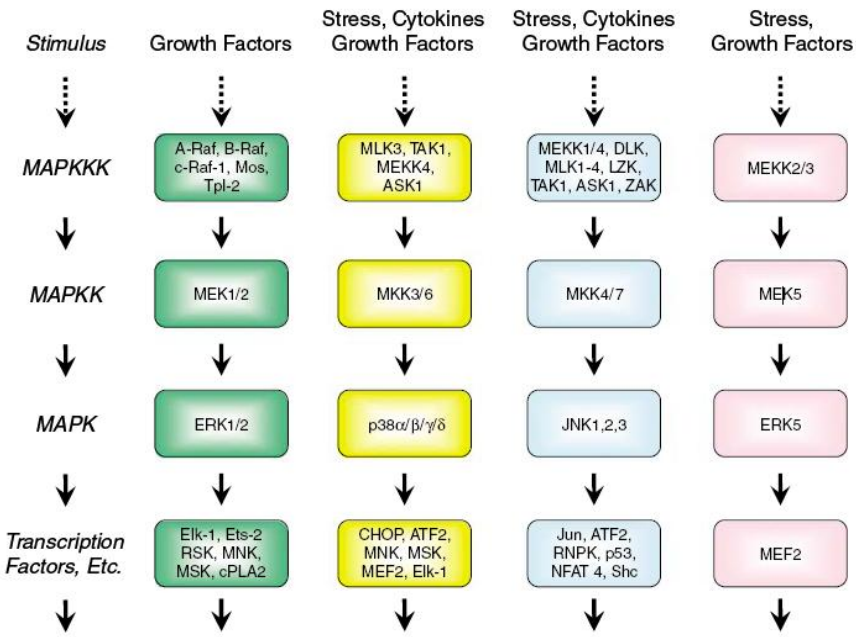

Fig. 1. MAP kinase pathway. The cascade contains three serine/threonine phosphorylation steps that predominantly activate transcription factors. Picture taken from Roberts et al. 2007.

PI3K/AKT/mTOR. Another crucial signal transduction pathway includes the PI3K/AKT/mTOR axis. To abstract it briefly, phosphoinositide 3-kinase (PI3K, comprising a catalytic and a regulatory subunit) transfers a phosphate group to phosphatidylinositol-4, 5-bisphosphate (PIP2), resulting in PIP3. In the next step, AKT and PDK1 (3-Phosphoinositide-dependent protein kinase-1) bind to PIP3 and PDK1 phosphorylates AKT (also known as protein kinase B, PKB). The latter represents a crucial hub with a plethora of downstream effectors, representing mTOR (mammalian target of rapamycin) as one of them (Willems et al. 2012). As depicted in Figure 2, the huge PI3K/AKT network is regulated by tyrosine kinase or G-protein coupled receptor, triggering class 1A or 1B PI3K signaling, respectively (Liu et al. 2009). An important negative regulator of this pathway is PTEN (phosphatase and tensin homolog deleted from chromosome 10), capable of reverting PIP3 back to PIP2 (Cully et al. 2006). PTEN is frequently lost in various cancers, both complete and mono-allelic. Accordingly, total loss of PTEN was shown to be responsible for directing tumor cells into senescence via interaction with p53, whereas haplo-sufficiency did not, explaining the benefit of partial deletion for the tumor. Furthermore, PTEN activity can be regulated by post-translational modifications. Depending on the site, phosphorylation causes either destruction or stabilization. Both acetylation and oxidation were shown to negatively regulate PTEN (Salmena et al. 2008).

MTOR appeared to be another important factor downstream of PI3K/AKT. It demonstrates an important sensor for cell homeostasis. Upon binding to raptor (regulatory associated protein of TOR) the complex switches on the translational machinery via phosphorylation of S6 kinase and eIF4EBP (eukaryotic translation-initiation factor 4E binding protein) that in turn releases eIF4E for cap-dependent translation initiation (Kim et al. 2002).

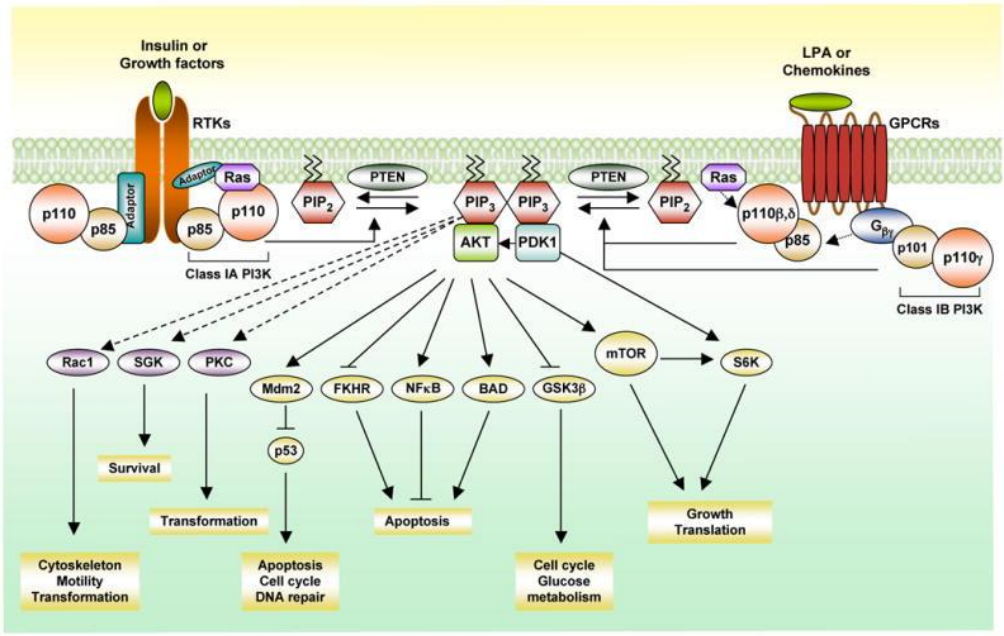

Fig. 2. Overview of PI3K/AKT signaling. Picture taken from Liu et al. 2009.

The mTOR inhibitor rapamycin exhibits anti-tumoral activity in several cancer models. However, also resistance represents a frequent observation, whereas limited literature regarding HCC exists (Huang and Houghton 2001). Recently it was shown that resistance was conducted via up-regulation of PDGFRβ. Co-treatment with Sorafenib achieved disruption of this feedback loop, resulting in enhanced anti-tumorigenic effect (Li et al. 2012). In another study, a small molecule inhibitor targeting PI3K revealed promising results via induction of apoptosis and disruption of neo-angiogenesis (Jung et al. 2012). Furthermore, an inhibitor acting on both PI3K and mTOR exhibited anti-oncogenic potential in human hepatoma cell lines and in murine *in vivo* experiments (Masuda et al. 2011). Knockout of PTEN yields to fatty liver and HCC as a result of PPARγ (peroxisome proliferator-activated receptor gamma) induction (Horie et al. 2004). Constitutively active expression of AKT upon PTEN loss has been recently reported in HCC. Importantly, a study investigating several AKT inhibitors on hepatoma cell lines revealed AKT inhibition in both moderate and hyperphosphorylated AKT expressing cells, respectively (Buontempo et al. 2011).

p53. More than 30 years ago, one of the still most important tumor suppressors was mentioned for the first time, as it has been found down-regulated in numerous cancers (Levine et al. 1983). In fact, the *TP53* gene encoding p53 is inactivated in half of human cancers by mutations, at which various grades of severity were identified (Petitjean et al. 2007). An overview of important up- and downstream factors of p53 is depicted in Figure 3. Upon DNA damage due to genotoxic or oncogenic stress, the cascade of checkpoint kinases (DNA-dependent protein kinase (DNA-PK)), ataxia telangectasia mutated (ATM), ATM and rad-3 related (ATR), checkpoint kinase 1 (CHK1), checkpoint kinase 2 (CHK2), MAPK activated protein kinase 2 (MK2) converge into p53. Activated p53 triggers downstream factors responsible for cell cycle arrest (via *CDKN1A* encoding p21 cyclin-dependent kinase inhibitor 1A, 14-3-3σ and growth arrest and DNA damage-inducible gene 45α (GADD45α)) and apoptosis (p53 upregulated modulator of apoptosis (PUMA), Bcl-2-associated protein X (BAX) and Bcl-2 antagonist/killer (BAK)). The balance of the respective outcomes is not fully elucidated, but might depend on cell type and severity of damage (Reinhardt and Schumacher 2012). Activation via ARF (p14 ^{ARF}/p19^{ARF}, right) will be discussed below in more detail.

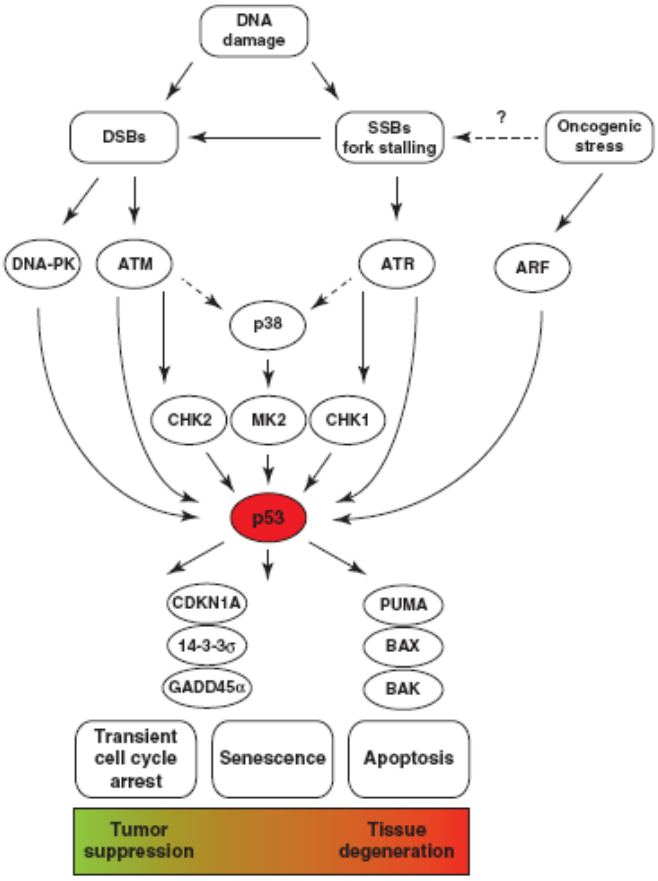

Fig. 3. Overview of the p53 network. Picture taken from Reinhardt et al. 2012.

p53 depletion is a frequent event in HCC. Its restoration caused senescence and activation of the innate immune system in a murine liver cancer model (Xue et al. 2007). 2 p53-related protein family members, p63 and p73, are also up-regulated in the liver, supporting quiescence of liver (Machado-Silva et al. 2010). Accordingly, transgenic mice harboring dysfunctional p73 in the liver developed HCC, following increased proliferation and inactivation of the tumor suppressor retinoblastoma (Rb), indicating interactions between these anti-tumorigenic pathways (Tannapfel et al. 2008). Another issue addresses the role of p53 in telomere shortening. Two publications observed increased tumor formation upon concomitant depletion of p53 and telomerase reverse transcriptase (mTERT), indicating their cooperation in HCC (Farazi et al. 2006; Lechel et al. 2007). Furthermore, a recent study showed that the pro- or anti-oncogenic direction of TGFβ depends on p53, as examined in a knockout mouse model (Morris et al. 2012), underlining the complexity of p53.

Transforming Growth Factor Beta (TGF-β). The TGF-β pathway exerts several important functions in cells under physiological conditions, among them tissue homeostasis and wound healing. TGF-β has a dual role in cancerogenesis, since these signals can either be pro- or anti-oncogenic (Calone and Souchelnytskyi 2012). Briefly, after binding of TGF-β to TGF-β receptor type II and subsequent heterodimerization and activation of TGF-β receptor type I, R-SMADs (regulatory-SMA Mothers against decapentaplegic; SMAD 2 or 3) are recruited and phosphorylated. Activated R-SMAD hetero-dimers interact with co-SMAD (SMAD 4; common SMAD) and translocate into the nucleus where they modulate transcription of target genes (Feng and Derynck 2005). Beside the canonical activation, TGF-β signaling is able to collaborate with other pathways relevant in tumorigenesis, such as Ras downstream effectors (MAPK, JNK, p38) and the PI3K/AKT/mTOR axis (Mu et al. 2012). These non-SMAD routes of activation are believed to be responsible for the pro-oncogenic fashion of TGF-β (Nagaraj and Datta 2010). For example, murine hepatocytes bearing Ha-Ras were shown to undergo an EMT upon TGF-β treatment (Gotzmann et al. 2002). In line with these findings, TGF-β induced EMT and concomitant enhancement of tumorigenic potential was also observed in various other epithelial tumors, such as pancreatic, prostate and breast cancer cells (Miyazono 2009). As shown by Tang and others, interaction between TGF-β and IL-6 (Interleukin 6) signaling drives stem cell derived HCC, disclosing therapeutic approaches targeting TGF-β in clonally derived liver cancer (Tang et al. 2008). Interestingly, CD44, an ECM (extracellular matrix) adhesion and stem cell marker, governs the outcome of EMT caused by TGF-β and shortens patient survival (Mima et al. 2012). The latter publication underlines the importance of TGF-β signaling in carcinogenesis and additionally corroborates

its role in the field of (cancer) stem cells. Dysfunctional TGF-β signaling was also shown to facilitate suppression of tumor growth upon inhibition of STAT3 (signal transducer and activator of transcription 3) activation (Lin et al. 2009). Accordingly, STAT3 overexpression desensitized TGF-β-mediated cytostasis in several tumor models (Jenkins et al. 2005, Luwor et al. 2012). Another study revealed TGF-β-induced STAT3 activation in a STAT5 knockout HCC model (Hosui et al. 2009). These findings indicate a significant crosstalk between TGF-β and STAT3 in tumorigenesis.

WNT/β-catenin. At first glance, the two main functions of β-catenin in the cell appeared to be rather distinct. On the one hand, it is a fundamental part of the cell adhesion complex by binding to E-cadherin and thereby providing epithelial integrity. On the other hand, β-catenin displays the central role of the canonical WNT/β-catenin pathway (Fig. 4). Without activation of WNT signals, β-catenin levels are kept low, executed by a complex that passes it into proteosomal degradation. This complex consists of Axin, adenomatous polyposis coli (APC) and glycogen synthase kinase 3β (GSK-3β). Activation upon WNT binding to Frizzled and its co-receptor LPR5/6 causes inactivation of GSK-3β and stabilization of β-catenin that is able to translocate into the nucleus (MacDonald et al. 2009). Subsequently, it forms a complex with LEF-1 (lymphoid enhancer factor 1) or TCF members (T-cell factor; TCF-1, -3, -4, respectively) and promotes expression of pro-oncogenic factors, such as e.g. cyclin D1, c-myc, fibronectin, urokinase plasmin activator (uPAR) or CD44. Of note, LEF-1 particularly serves as an important factor for nuclear retaining of β-catenin, competing with E-cadherin and APC (Jamieson et al. 2012). A simplified scheme is shown in Figure 4.

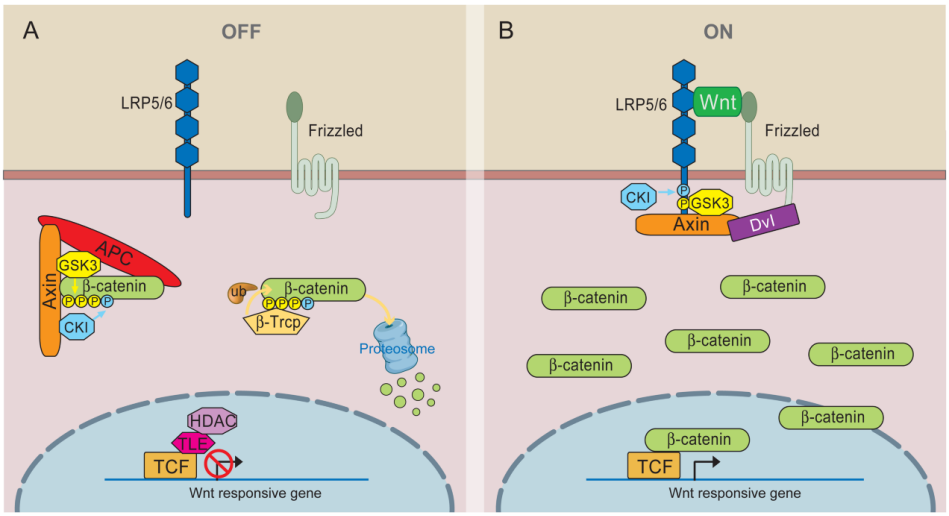

Fig 4. Overview of the WNT/β-catenin pathway. (A) Proteosomal degradation of β-catenin pathway in the absence of WNT ligands; (B) activated WNT- β-catenin signaling; taken from MacDonald et al. 2009.

Aberrant β-catenin signaling is common in solid tumors. Remarkably, T. Brabletz and colleagues observed increased nuclear localization at the invasive fronts of both primary tumors and metastases, suggesting a modulation via the microenviroment (Brabletz et al. 2001). In HCC, mutations in WNT- β-catenin signaling occur in about 25% of cases, predominantly by the gene encoding β-catenin itself (*CTNNB1*; Forner et al. 2012). Further, mutations of APC, Axin, constitutive activation via autocrine loops or crosstalks between other pathways, such as TGF-β, promotes dysregulated signaling (Dahmani et al. 2011). A recent study showed an unexpected role of c-Jun, a member of the AP-1 (activator protein 1) transcription factor family and putative target gene of β-catenin, in HCC. In contrast to earlier studies, c-Jun was shown to be hepatoprotective in this model (Trierweiler et al. 2012). Awuah and others demonstrated faster development of HCC upon loss of β-catenin following chemical induction via diethylnitrosamine/phenobarbital (DEN/PB). β-catenin negative mice were more susceptible to genotoxic stress and fibrosis and showed enhanced regeneration via PDGFRα activation (Awuah et al. 2012).

3.2 $p14^{ARF}$/$p19^{ARF}$

3.2.1 The ARF-p53 Pathway

The group of Charles Sherr identified an alternatively expressed protein encoded by the INK4a locus, designated as ARF (alternative reading frame) or $p19^{ARF}$ due to the size of 19 kDa. INK4a or CDKN2A (cell-dependent kinase inhibitor 2A) also encodes $p16^{INK4A}$ that is composed of exon1α, exon2 and exon3. In contrast, for transcription of $p19^{ARF}$, exon1β replaces exon1α (Fig. 5). Furthermore, translation is arranged in an alternative reading frame, thus exhibiting two unrelated proteins (Quelle et al. 1995). Increased susceptibility for tumor formation in INK4a null mice was observed. Furthermore, mouse embryonic fibroblasts demonstrated a higher escape rate from senescence. These observations confirmed $p16^{INK4A}$ as a tumor suppressor due to its known role in cell cycle inhibition. However, the specific contribution of $p19^{ARF}$ remained to be elucidated (Serrano et al. 1996). Strikingly, specific disruption of $p19^{ARF}$ via deletion of Exon1β could again show an oncogenic phenotype, suggesting $p19^{ARF}$ on its own acts as tumor suppressor. Concomitantly, an interaction with p53 was proposed for the first time (Kamijo et al. 1997). The human homologue to $p19^{ARF}$ was described by Francesca Stott and co-workers in 1998 and showed 132 amino acids of length and 13902 Dalton of size and has been therefore designated as $p14^{ARF}$. Additionally,

this study identified MDM2 (Murine Double Minute 2) as a mediator between $p14^{ARF}$ and p53 for the first time (Stott et al. 1998). Even though the human and the murine homologues harbors only 50 percent sequence homology, they share hydrophobicity and high alkalinity due to a large amount of arginine residues. $p19^{ARF}/p14^{ARF}$ resides in the nucleolus, whereas the first owns 1 and the latter owns 2 nucleolar localization signals (NLoS; Ozenne et al. 2010). $p19^{ARF}$ mutants bearing a deletion of this sequence (Δ26–37) failed to enter nucleoli and consequently did not succeed in disposing MDM2 into these compartments (Kamijo et al. 1998). In the human homologue, the NLoS located at the N-terminus provides both binding to HDM2 (the human homologue to MDM2) and is responsible for cell cycle arrest. The second one that is closer to the C-terminus binds to HDM2 and is required for degradation via sumoylation (Rizos et al. 2000; Xirodimas et al. 2002). $p19^{ARF}/p14^{ARF}$ is stabilized in the nucleolus upon binding to nucleophosmin (NPM, or B23), an endoribonuclease responsible for assembling ribosomal RNA. Furthermore, it owns chaperone potential and is involved in several homeostatic functions in the cell. Given its role in promoting mRNA translation, the finding that $p19^{ARF}/p14^{ARF}$ degrades NPM for counteracting cell growth was not surprising (Itahana et al. 2003). On the other hand, as mentioned above, $p19^{ARF}/p14^{ARF}$ retention and stabilization in the nucleolus failed in the absence of NPM. Interestingly, it was shown that specifically mutated NPM carrying extra nuclear export signals was capable to bind $p19^{ARF}/p14^{ARF}$, however, protection of p53 via MDM2 ubiquitination was not prevented in the cytoplasm (Colombo et al. 2006).

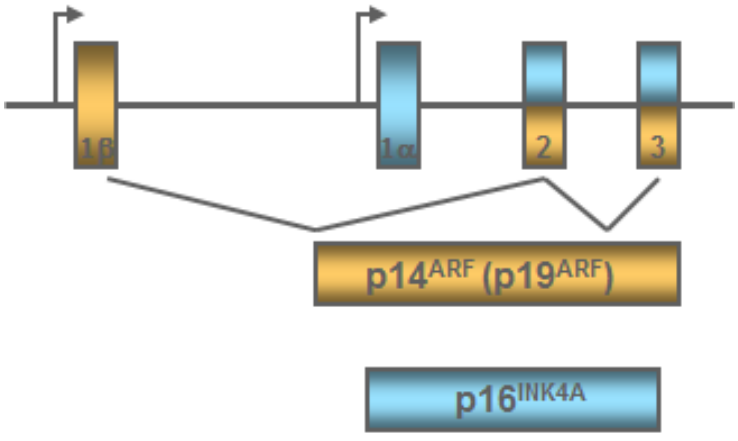

Fig. 5. Overview of the INK4a locus. $p16^{INK4a}$ (blue bars) and $p19^{ARF}$ (brown bars) differ in their exon composition. Figure by courtesy of Heidemarie Huber.

One of the first and most well-documented discoveries regarding the function of $p19^{ARF}/p14^{ARF}$ describes the indirect stabilization of p53, a key tumor suppressor (Fig. 6).

One of the main tasks of $p19^{ARF}/p14^{ARF}$ in this respect consists of deactivating MDM2, in particular its ubiquitin ligase activity that is mainly responsible for p53 degradation (Stott et al. 1998). Although binding of $p19^{ARF}/p14^{ARF}$ to MDM2 occurs in the nucleolus, several lines of evidence suggested that this localization is not essential. These results are strengthened by the fact that both p53 and MDM2 were generally attributed as rather nucleoplasmic proteins (Llanos et al. 2001). Besides MDM2, a second protein, ARF-BP1 (ARF-binding protein 1) capable for ubiquitination was found to mediate $p19^{ARF}/p14^{ARF}$-p53 regulation (Fig. 6). On the one hand, ARF-BP1 showed strong binding to $p19^{ARF}/p14^{ARF}$ following disruption of ubiquitin ligase activity. On the other hand, in cells bearing p53 knockout ARF-BP1 depletion resulted in growth arrest. These findings indicated both a MDM2 related activity and a p53 independent tumor suppressive activity of $p19^{ARF}/p14^{ARF}$, as discussed below (Chen et al. 2005).

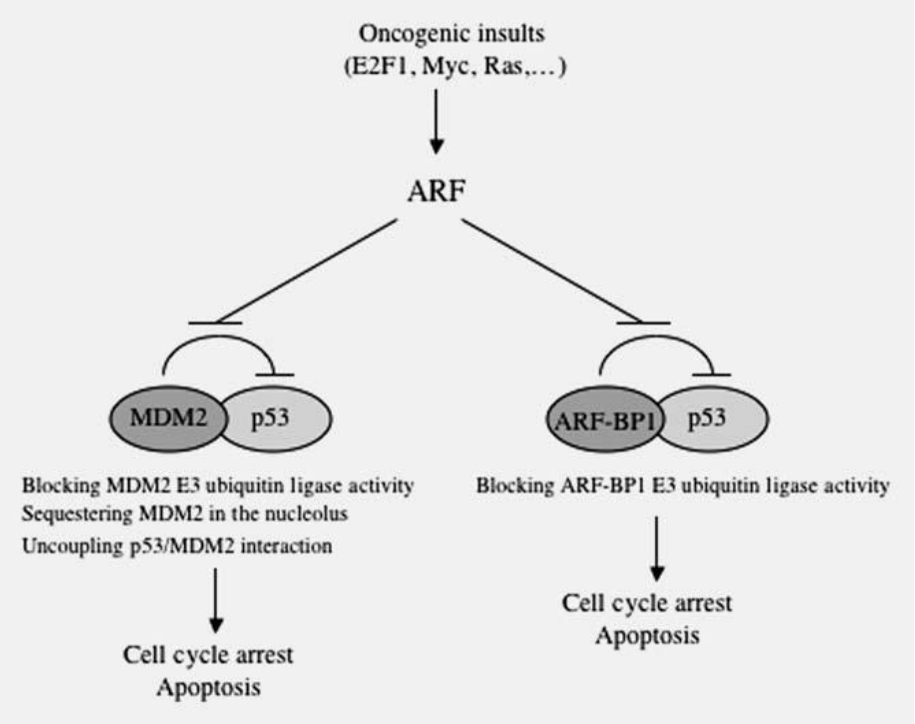

Fig 6. Schematic depiction of the $p19^{ARF}/p14^{ARF}$-p53 axis. Picture taken from Ozenne et al. 2010.

3.2.2 $p19^{ARF}/p14^{ARF}$ p53-Independent Tumor Suppression

An indication for p53 independent tumor suppressive actions of $p19^{ARF}/p14^{ARF}$ was achieved with a triple $p19^{ARF}$/MDM2/p53 knockout mouse model. In this setting, tumor development exceeded the tumor rate of single p53 or double p53/MDM2 mice, strongly suggested anti-oncogenic properties of $p19^{ARF}/p14^{ARF}$ apart from the p53 axis (Weber et al. 2000). In line

with these findings, an oncogenic Ras-transformed squamous cell carcinoma model also implied anti-tumorigenic features of $p19^{ARF}$ irrespective of p53 (Kelly-Spratt et al. 2004). Numerous investigations exploring $p19^{ARF}/p14^{ARF}$ actions apart from p53 has been performed. Figure 7 depicts a selection of binding partners and the respective consequences are color-coded. Some relevant candidates are considered in more detail in the text below. Transcription factor E2F1 is crucial for the transition of G1/S phase and gets activated via phosphorylated retinoblastoma (Rb) protein (Helin et al. 1993). A physical interaction of $p19^{ARF}/p14^{ARF}$ and E2F1 was detected and evidence for transcriptional repression of E2F1 genes was provided. Furthermore, it was shown that Exon1β sequence of $p19^{ARF}/p14^{ARF}$ is sufficient for inhibition (Eymin et al. 2001). Interestingly, another publication demonstrated the binding of $p19^{ARF}/p14^{ARF}$ to DP1 (DRTF1 polypeptide 1), a protein important for DNA binding and transcriptional activity of E2F1. Given the fact that $p19^{ARF}/p14^{ARF}$ physically affected the DP1 promoter following cell cycle arrest, DP1 exhibits a crucial target for an E2F1 related, anti-oncogenic feature of $p19^{ARF}/p14^{ARF}$ (Datta et al. 2005).

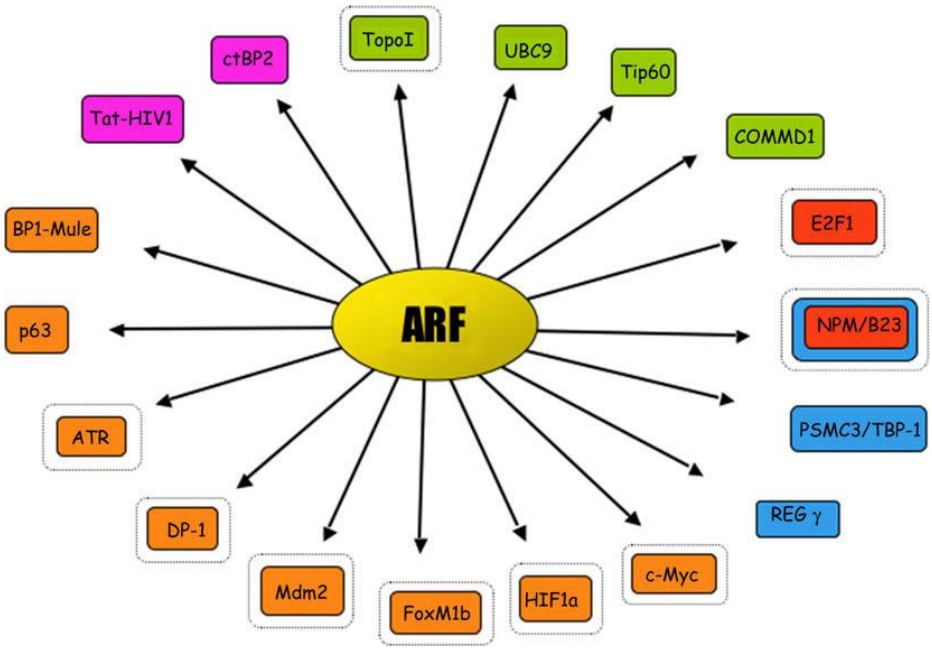

Fig. 7. "A schematic view of the ''ARF harem'' described in this review. Orange is for partners whose activities are blocked by ARF. Red is for partners that are induced to proteasome and ubiquitin-dependent degradation by ARF. Pink is for partners that are induced to proteasome and ubiquitin-independent degradation by ARF. Green is for partners whose activity or stability are positively regulated by ARF. Blue is for partners that regulate ARF protein turnover. A second black circle indicate nucleolar sequestration." Scheme and figure legend taken from Pollice et al. 2008.

Myc is another pro-oncogenic factor linked to $p19^{ARF}/p14^{ARF}$. This oncogene is up-regulated in many cancers, as such being downstream of e.g. Notch or WNT signaling. In general, Myc actions promote hallmarks of cancerogenesis, including proliferation, cell growth and stem cell capabilities. It is capable for both activation and repression of genes, depending on its binding partners. Furthermore, Myc governs a network of micro RNAs (miRNAs), thereby promoting pro-oncogenic pathways, such as activation of AKT via PTEN inhibition (Dang 2012). However, Myc also induces apoptosis, both in a p53 dependent and independent fashion. The latter includes binding of $p19^{ARF}/p14^{ARF}$ to Myc, following conversion of Myc actions from malignant to pro-apoptotic. However, the exact mechanisms remain to be elucidated. Whether the nucleolus or the nucleoplasm is the site of their interaction is still a matter of discussion (Li and Hann 2009).

As depicted in Figure 3, upon DNA strand breaks, ATM and ATR proteins activate p53, leading to p53-related responses such as cell cycle arrest (Abraham 2001). Although $p19^{ARF}/p14^{ARF}$ does not contribute directly to this pathway, several studies showed evidence for interaction between ATM/ATR and $p19^{ARF}/p14^{ARF}$. Interestingly, via this route, $p19^{ARF}/p14^{ARF}$ inhibits NFκB (nuclear factor kappa B), a pro-oncogenic transcription factor frequently up-regulated in cancers. More precisely, $p19^{ARF}/p14^{ARF}$ induces association of histone deacetylase 1 (HDAC1) to the NFκB subunit p65/RelA (Barnes and Karin 1997; Rocha et al. 2003) and promotes ATR and its downstream kinase Chk1 for RelA repression (Rocha et al. 2005). Another study confirmed the ATM/ATR/Chk1 upstream activities of $p19^{ARF}/p14^{ARF}$, additionally revealing Tat-interacting protein (Tip60) as a new binding partner and being crucial for proper $p19^{ARF}/p14^{ARF}$ mediated response to alkylating agents (Eymin et al. 2006). In this regard, $p19^{ARF}/p14^{ARF}$ implication was also found in nucleotide excision repair (NER) via xeroderma pigmentosum, complementation group C (XPC) regulation, suggesting a further role of $p19^{ARF}/p14^{ARF}$ in genomic integrity (Dominguez-Brauer et al. 2009).

Since $p19^{ARF}/p14^{ARF}$ is capable to strongly influence proliferation and cell growth, regulation of its turnover describes an important issue. In this respect, it was shown that proteasomes play a critical role, both in degradation and stabilization of $p19^{ARF}/p14^{ARF}$, dependent on the composition of the proteosomal apparatus. For instance, binding of 11S/Reg-γ to $p19^{ARF}/p14^{ARF}$ causes its degradation (Chen et al. 2007). On the other hand, tat binding protein-1 (TBP-1), an ATPase incorporated in the 19S proteasome, exerts stabilization of $p19^{ARF}/p14^{ARF}$. Given the localization of TBP-1 in the nucleoplasm, it was suggested that it

exhibits the main stabilizing partner of $p19^{ARF}/p14^{ARF}$ in this compartment, while nucleophosmin is the one in the nucleolus (Pollice et al. 2007).

Hypoxia induced factor-1 alpha (HIF-1α) has long been known to be a pro-oncogenic transcription factor, supplying tumors via neo-angiogenesis (Semenza 2000). Fatyol and colleagues showed that $p19^{ARF}/p14^{ARF}$ sequestered a subunit of HIF-1α into the nucleolus, thereby inhibiting its transcription activities (Fatyol and Szalay 2001). Interestingly, also the proteasome ATPase TBP-1 attenuates HIF-1α. Due to the interaction of TBP-1 and $p19^{ARF}/p14^{ARF}$, it was proposed that TBP-1 represents the link to the proteosomal activities of $p19^{ARF}/p14^{ARF}$ (Pollice et al. 2008).

Focusing on the role of $p19^{ARF}/p14^{ARF}$ in cancer, its loss, mutation or hypermethylation appears to be a crucial issue. Ink4a-ARF is a target of epigenetic regulation. For example, polycomb group (PcG) proteins repress this locus via histone methylation (Simboeck et al. 2011). Accordingly, the histone demethylase JMJD3 removes methyl groups and has been shown to be down-regulated in several cancers (Agger et al. 2009). Interestingly, also p53 together with HDAC1 and PcG proteins is involved in $p19^{ARF}$ repression, as shown in mouse cells, thus providing a regulatory feedback loop (Zeng et al. 2011). Besides, DNA methylation via maintenance and *de novo* DNA methyl transferases (DNMT1; DNMT3a, 3b, respectively) is frequently observed in binding to promoters of tumor suppressors (Simboeck et al. 2011). Hypermethylation is examined in several epithelial tumors, such as kidney, oral squamous cell and HCC. In line with this, knockdown of DNMT1 increased $p14^{ARF}$ (and p53) expression to undergo cell cycle arrest and circumvent aneuploidy (Barra et al. 2012).

The Ink4a-ARF locus is frequently deleted in neoplasms (Saporita et al. 2007). Notably, deletion of Exon1β is a very rare event and has been described in melanoma. An interaction of $p19^{ARF}/p14^{ARF}$ and pro-apoptotic STAT3 pathway has been identified in lung tumors bearing a specific EGFR mutation. In this scenario, phosphorylation of the tyrosine residue 705 and therefore activation of STAT3 occurred downstream of $p14^{ARF}$. $p14^{ARF}$ itself was depleted by the EGFR variant, disclosing an intriguing crosstalk between these regulatory components (Ozenne et al. 2012). Another study showed that $p19^{ARF}/p14^{ARF}$ inhibits angiogenesis via induction of tissue inhibitor of metalloproteinase-3 (TIMP3) in cooperation with transcription factor SP1 and HDM2. These finding underlines an exciting role of $p19^{ARF}/p14^{ARF}$ in angiogenesis (Zerrouqi et al. 2012). RUVBL2 (RuvB-like 2), a DNA helicase, has been shown to interfere with numerous cellular events, including migration, invasion, DNA repair and chromatin remodeling. Recently, one study reported that binding of

RUVBL2 to the distant site of the $p19^{ARF}/p14^{ARF}$ promoter induced transcriptional repression and consequent downregulation of p53 (Xie et al. 2012).

3.2.3 $p19^{ARF}/p14^{ARF}$ in HCC

Ambiguous data are available that describe how and to what extent $p19^{ARF}/p14^{ARF}$ is inactivated in HCC. In particular, a large number of HCC cases shows loss of $p19^{ARF}/p14^{ARF}$ due to DNA methylation (Randerson-Moor et al. 2001; Tannapfel et al. 2001; Anzola et al. 2004). Fukai and colleagues suggested a geographical reason for this phenomenon, however, further studies are needed for clarification (Fukai et al. 2005). Presumably, this tendency might be associated with hepatitis virus infections, since $p19^{ARF}/p14^{ARF}$ also exhibits antiviral activities (Garcia et al. 2006). A recent study in Chinese HCC samples (n=30) revealed that more than 50% of patients showed $p14^{ARF}$ promoter methylation. Interestingly, an inverse correlation to active telomerase and hTERT (human telomerase reverse transcriptase) expression was observed, indicating crosstalks between telomerase activity and cell cycle regulation (Zhang et al. 2008). One report described a low frequency of $p14^{ARF}$ alteration. Interestingly, this small proportion was associated with proper differentiation. Accordingly, an indirect correlation of $p14^{ARF}$ expression and differentiation status was suggested (Ito et al. 2004)

Besides epigenetic regulation, a novel regulator for $p19^{ARF}/p14^{ARF}$, termed CDK5 regulatory subunit associated protein 3 (CDK5RAP3) was shown to deplete $p19^{ARF}/p14^{ARF}$ expression. Its knockdown reduced invasion in HCC cells, suggesting a molecular target for re-establishing $p19^{ARF}/p14^{ARF}$ (Mak et al. 2012). As shown in Figure 7, forkhead box M1b (FoxM1b) represents a target for $p19^{ARF}/p14^{ARF}$. This transcription factor was described in several cancers as a strong oncogene, driving metastasis and correlating with poor prognosis. A recent study investigating the role of FoxM1b in a $p19^{ARF}$ negative HCC model revealed a significant impact during hepatocarcinogenesis, including metastasis. Given the mild effect of FoxM1b overexpression alone, these data underline $p19^{ARF}/p14^{ARF}$ as the major repressor of this oncogene (Park et al. 2011). Another role of $p19^{ARF}/p14^{ARF}$ in metastasis is triggered by C-terminal binding protein (CtBP), a pro-oncogenic transcription factor. By using $p19^{ARF}$ mutants, deletion of $p19^{ARF}$´s binding domain to CtBP displayed enhanced invasion, implying a central role of CtBP in the anti-oncogenic efforts of $p19^{ARF}/p14^{ARF}$ (Chen et al. 2008).

3.3 JAK-STAT Pathway and STAT3

3.3.1 JAK-STAT

More than 20 years ago, Wilks and co-workers designated newly explored tyrosine kinases as Janus kinases (JAKs; Wilks et al. 1991). Simultaneously, a transcription factor initially termed interferon-stimulated gene factor 3 (ISGF3) protein complex was identified downstream of interferon signaling (Schindler et al. 1992). Within this complex, the first so-called STAT (Signal Transducer and Activator of Transcription) proteins were isolated, namely STAT1 (STAT1α and STAT1β) and STAT2. Remarkably, both of them became phosphorylated on an exclusive tyrosine residue upon stimulation with interferon-alpha (IFN-α; Shuai et al. 1993). Darnell and colleagues finally discovered the JAK-STAT pathway as a fast and direct signaling from cell surface to nucleus. Generally, a phosphorylation cascade between ligand-activated receptors located at the cell membrane and JAKs leads to recruitment of STATs that in turn are phosphorylated. The latter forms dimers, translocate to the nucleus, bind to the DNA and act as transcription factors (Fig. 8; Darnell et al. 1994; Levy and Darnell 2002).

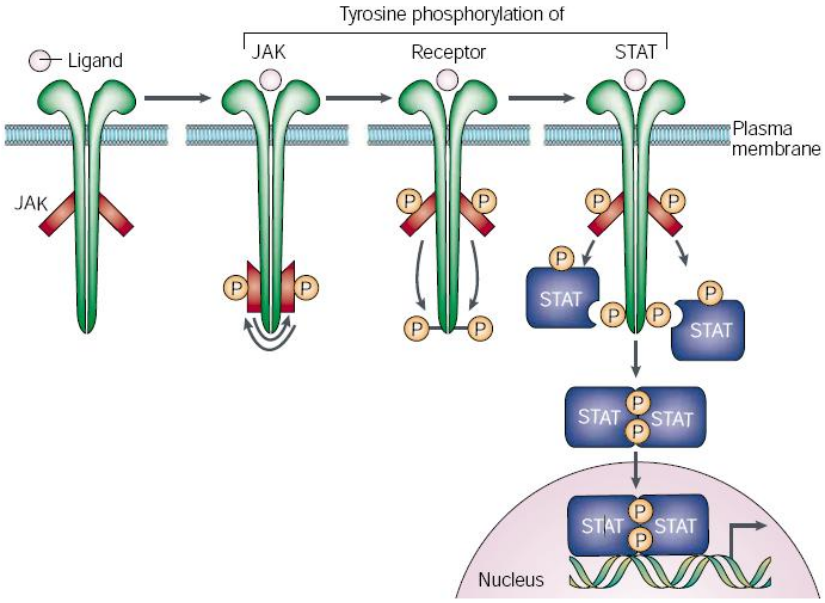

Fig. 8. The JAK-STAT pathway. Scheme taken from Levy and Darnell 2002.

Around the mid-1990ies, all members of JAK-STAT family were discovered. Tyk2, another tyrosine kinase was identified through screening of a human lymphoid cDNA library. As for the other JAKs known so far, no transmembrane domain was found in its structure (Firmbach-Kraft et al. 1990). Finally, Takahashi and co-workers were the first exploring the yet latest

Janus kinase JAK3, rounding up these group of enzymes to JAK1, JAK2, JAK3 and Tyk2 (Takahashi and Shirasawa 1994). The lab of Bruce Darnell had a leading role in identifying STAT3 and STAT4 and in describing hetero-dimerization of STAT1 and STAT3 (Zhong et al. 1994) Furthermore, the spectrum regarding activation of this pathway was broadened, since IL-6 and EGF were shown to enhance levels of STAT3 (Zhong et al. 1994). Interestingly, STAT3 appeared to be identical with the acute phase response factor (APRF), as it was demonstrated by two labs in parallel (Akira et al. 1994; Wegenka et al. 1994). In 1995, two STAT proteins, namely STAT5A and STAT5B were discovered in mammary and hematopoietic cells with a close homology (Liu et al. 1995; Mui et al. 1995). The last STAT was first mentioned in 1994 as IL-4 STAT and later on termed STAT6. As indicated, STAT6 acts predominantly in lymphocytes downstream of IL-4 signaling (Hou et al. 1994).

3.3.2 The Structure and Function of STAT Proteins

As depicted in Figure 9, STATs are structured in several domains. The N-terminus (NH2) of STATs has important functions for the so-called "dimer:dimer" interaction or "tetramerization" which plays a role in signal intensity (Vinkemeier et al. 1996). Furthermore, it has been shown that NH2-truncated STAT1 dimers failed to translocate into the nucleus and were unable for deactivation, suggesting a regulatory role of the N-terminus (Strehlow and Schindler 1998). A more recent study demonstrated this domain as crucial for the deacetylation and acetylation of STAT3 via HDAC1 and CREB-binding protein (CBP)/p300, respectively (Ray et al. 2008). Next to the NH2-domain resides the coiled-coil domain, composed of four alpha-helices. One of its functions was examined in STAT1, revealing a nuclear export signal (Begitt et al. 2000), which has also been found for STAT3 (Ma and Cao 2006). A recent publication showed an alternative STAT3 recruitment via binding of IL-22 receptor to the coiled-coil domain (Dumoutier et al. 2009). The DNA-binding domain is located downstream of the coiled coil domain and represents the beta-barrel shaped central region. Another nuclear export signal has been found in this domain and it is suggested that this signal is switched on and off by phosphorylation and dephosphorylation, respectively (O'Shea et al. 2002). This domain, identified by the group of Darnell in 1995 (Horvath et al. 1995), binds to STAT responsive DNA elements. The most important promoter sequences are ISRE (interferon-stimulated response elements) and GAS (gamma IFN-activated sequences). The ISRE element was isolated already in the year of 1987 and appeared to be the binding site for ISGF3 (Reich et al. 1987). Later on, T. Decker and colleagues identified GAS, another interferon specific promoter that turned out to be the second element being crucial for STAT

binding (Decker et al. 1991). Next to the DNA-binding domain is the most highly conserved domains among STAT proteins that contains of alpha-helices and is designated as linker region. Remarkably, canonical induction of STATs mutated in this domain showed all necessary steps of STAT activation, such as phosphorylation, dimerization and nuclear import, however transcriptional activation failed (Yang et al. 1999). Interestingly, the duration rate of DNA binding of STATs mutated in the linker region was observed to be drastically reduced, causing depletion of transcription (Yang et al. 2002). A further domain is profoundly responsible for the canonical activation of STAT molecules. At the SH2- (Src homology 2) domain, STATs are phosphorylated by activated receptors. Since this phosphorylation also demonstrates the prerequisite for dimerization and accompanied DNA binding, this domain is pivotal for bridging signal transduction and direct activation of transcription (Chen et al. 1998). Finally, the C-terminally located transactivation domain (TAD) completes STAT molecules. Early after the discovery of STATs it became clear that a second phosphorylation on Serine was necessary for efficient transcriptional activation. These amino acids to be phosphorylated are positioned in the TAD. Furthermore, it was suggested that this activation is promoted by MAP kinase signaling. Since the beta isoforms of (at least) STAT1 and STAT3 lacks this site, they were initially described as dominant negative effectors (Wen et al. 1995). Furthermore, as the N-terminal domain, CREB-binding protein (CBP)/p300 is capable to bind at the C-terminal end of STAT1 (Zhang et al. 1996).

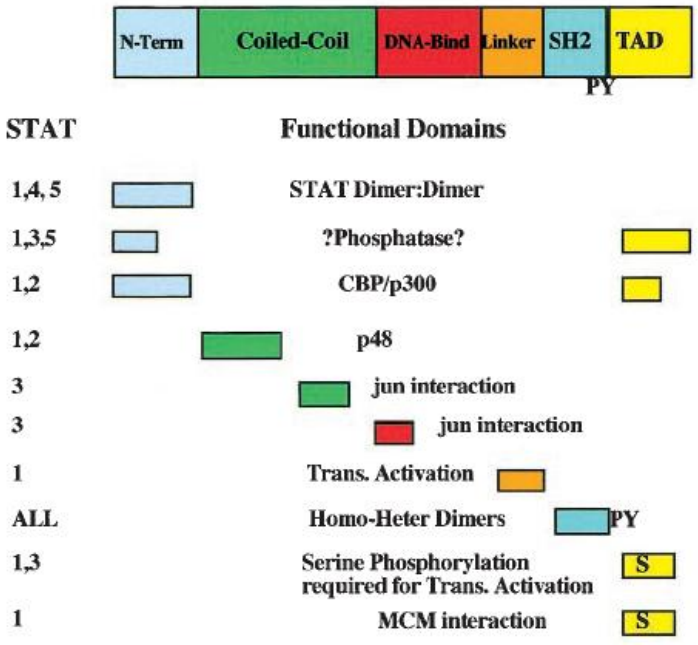

Fig. 9. Domains of the STAT protein. Numbers at left describe which STATs are concerned. Single domains are color-coded. Several interactions with the respective domains are listed. Graph taken from Bromberg and Darnell 2000.

3.3.3 STAT3

By intending to identify isoforms of STAT1 and STAT2, STAT3 (and STAT4) was isolated upon screening of murine cDNA libraries (Zhong et al. 1994). In contrast to STAT1 and STAT2, STAT3 could not be activated via interferon gamma (IFN-γ). Instead, epidermal growth factor (EGF) and interleukin-6 (IL-6) induced its activation. Given the fact that STAT1 could be induced also by EGF, and in addition, STAT1 and STAT3 are able to form heterodimers, the spectrum of signaling alternatives became greatly extended (Zhong et al. 1994). Several upstream activators are capable for STAT3 tyrosine phosphorylation (pY-705). The IL-6 cytokine family, also comprising e.g. IL-11, oncostatin M (OSM) and leukemia inhibitory factor (LIF), bind to their respective receptors and employ glycoprotein 130 (gp130), a protein harboring a transmembrane domain but does not bind to ligands. However, gp130 performs STAT3 phosphorylation upon binding to its SH2-domain (Kishimoto et al. 1995). Besides, activation upon tyrosine kinase receptors via EGF, PDGF and CSF-1 (colony stimulating factor-1), IL-2, -7, -10, -15 and IFN-α comprises the plethora of STAT3 upstream activators (Zhong et al. 1994). An alternative STAT3 activation is achieved by Src, a SH2-containing kinase involved in various cellular activities. For example, the G-protein coupled receptor pathway was shown to be upstream of Src (Ram and Iyengar 2001). Accordingly, Bromberg and colleagues identified STAT3 as the effector molecule for Src transformation (Bromberg et al. 1998).

STAT3 knockout causes early embryonic lethality (day 6.5-7.5 post coital). Given the presence of STAT3 in the visceral endoderm, lethality might be caused by nutrition deficiency (Akira 1999). The function of STAT3 under normal physiological conditions was sufficiently investigated both *in vitro* and *in vivo*, the latter via conditional knockout approaches. Cell culture experiments revealed surprising results, since STAT3 activation caused contrarian results depending on which cells type has been investigated. The spectrum encompasses proliferation and survival, but also differentiation and apoptosis (Huang 2007). Furthermore, upon constitutive STAT3 expression, embryonic stem cells maintained undifferentiated (Matsuda et al. 1999). In contrast to the large impact of the STAT3 total knockout, conditional deletion exhibited rather mild phenotypes. As observed *in vitro*, the effects caused by loss of STAT3 greatly varied *in vivo* (Table 2; Levy and Lee 2002).

Promoter used to drive Cre	Target cells	Phenotypes	Affected functions	Similar phenotypes[A]
K5	Keratinocytes	Impaired 2nd hair cycle, wound repair, and keratinocyte migration	Migration	*Egfr*$^{-/-}$, *Tgfr*$^{-/-}$, *hgf*$^{-/-}$
K5	Thymic epithelium	Age-dependent thymic hypoplasia, hypersensitivity to stress	Survival	CD3ε^{Tg}
Lck	T lymphocytes	Impaired IL-6–dependent survival, impaired IL-2Rα expression	Survival/proliferation	*Stat5a*$^{-/-}$
Mlys	Monocytes/Neutrophils	Enhanced inflammatory response, chronic colitis and Th1 differentiation	—	*Il10*$^{-/-}$
Blg	Mammary epithelium	Delayed mammary involution	Apoptosis	—
Mx	Liver	Impaired acute-phase response	Gene expression	*Il6*$^{-/-}$
Bal[B]	Sensory neurons	Enhanced neuronal apoptosis	Survival	*Lifrβ*$^{-/-}$, *Cntfrα*$^{-/-}$
Nfl	Motoneurons	Impaired survival after nerve damage	Survival (cytokine-stimulated)	*CT-1*

Table 2. Overview of conditional knockouts of STAT3. Table taken from Levy et al. 2002.

3.3.3.1 STAT3β

STAT3β was detected as an alternatively spliced isoform lacking 55 C-terminally located amino acids (AA) of wildtype STAT3 (or STAT3α). Instead, an alternative reading frame adds seven alternative AAs. Consequently, STAT3β lacks the TAD at Serine 727 (Caldenhoven et al. 1996). Furthermore, several experiments of this study showed evidence that STAT3β was capable of tyrosine phosphorylation, DNA binding and the ability to form hetero-dimers with STAT3α. They also examined stronger DNA binding and more pY-705 on STAT3β than on STAT3α. Yet, it was claimed that STAT3β represents a dominant negative factor of wildtype STAT3 following reporter assays (Caldenhoven et al. 1996). However, another independent investigation revealed transcriptional activating properties of STAT3β in cooperation with transcription factor c-Jun (Schaefer et al. 1995), which opened a discussion regarding STAT3β functions. In line with claims favoring repressive features, overexpression of STAT3β in murine melanoma cells promoted cell cycle arrest and apoptosis (Niu et al. 2001). Interestingly, C-terminal deletion of STAT3α prolongs DNA binding and dimer stability comparable with STAT3β, suggesting the C-terminus as decisive for stabilization (Park et al. 2000). A more previous study identified the seven alternative AAs of STAT3β being the cause of its prolonged nuclear retention time compared to STAT3α (Huang et al. 2007). A very recent investigation confirmed the different retention times. Additionally, it was shown that STAT3β increased the nuclear presence of STAT3α only when phosphorylated. Remarkably, transcriptome profiling revealed even more genes regulated by

STAT3β than by STAT3α under basal conditions (Ng et al. 2012). A possible explanation of prolonged STAT3β activation includes the fact that phosphorylation on serine^{727} within the TAD domain (lacking in STAT3β) exhibited a negative effect on tyrosine^{705} phosphorylation, as shown in several cell lines (Chung et al. 1997). Viability of mice lacking STAT3α but expressing STAT3β did not show embryonic lethality but exhibited prolonged lifetime until perinatal stage, implicating that STAT3β is sufficient to overcome STAT3 activities during embryogenesis, yet it is not capable to fully replace STAT3α (Maritano et al. 2004). Studying the literature regarding STAT3β yielding a puzzling view of its functions. The balance of claims suggesting a dominant negative and a transcriptionally active form is roughly equal (Dewilde et al. 2008). This discussion corroborates the huge variety of STAT3 actions.

3.3.3.2 Unphosphorylated STAT3 (U-STAT3) and its implication in cancer

Several studies raised the issue of latent, non-activated STATs residing in the cytoplasm. STAT1 was mentioned early being transcriptionally active without preceding phosphorylation by analyzing a STAT1 Y701F mutant (Chatterjee-Kishore et al. 2000). Regarding STAT3, first studies were limited to investigate its appearance in the cytoplasm. One study proposed that STAT3 monomers are located in two forms of bulk proteins (statosome I and II) rather than residing as a pool. Within these complexes, STAT3, STAT5a and STAT5b have been detected. Additionally, several other proteins, among them the chaperone GRP58 (glucose-regulated protein 58) have been identified (Ndubuisi et al. 1999). Further investigations indicated GRP58 as part of a shuttling complex for STAT proteins towards the nucleus, suggesting a regulatory function of GRP58 (Guo et al. 2002). STAT3 dimers were identified in the cytoplasm rather than as activated nuclear dimers (Schroder et al. 2004). U-STAT3 (homo-)dimerization has already been observed, however, crystal structure and mass spectrometry analysis revealed that, in contrast to U-STAT1, mutants harboring solely the core region of U-STAT3 (lacking N- and C-terminal domain) reside monomeric (Braunstein et al. 2003; Ren et al. 2008). In contrast to the active transport process required for the phosphorylated STAT3 dimer, U-STAT3 is able to enter the nucleus via nucleopores, independent of metabolic energy (Meyer and Vinkemeier 2004). Consistent with the findings above, mutations in nuclear localization and export signals (NLS and NES, respectively) did not influence shuttling of U-STAT3 and it was shown that translocation occurred as monomers or dimers. Importantly, the N-terminal domain appeared to be indispensable for U-STAT3 dimerization, in contrast to phosphorylated STAT3. However, N-terminally mutated

STAT3 were phosphorylated upon IL-6 stimulation, formed dimers but failed to translocate to the nucleus, implying the complex role of the N-terminal domain during STAT3 activation (Vogt et al. 2011). Further investigations on STAT3 translocation via cell imaging approaches revealed the need of the importin-α/β dimer for nuclear import (Cimica et al. 2011).

In 2005, the lab of George Stark proposed for the first time a transcriptional activity of U-STAT3. They group further stated that preceding canonical activation via IL-6 caused high levels of U-STAT3 that subsequently activate an alternative set of target genes after a time delay. By this second wave of induction, the constitutive activation of several genes is ensured. Among them, two oncogenes (*mras, met*) have been described as targets of U-STAT3 (Yang et al. 2005). In their succeeding work, they identified unphosphorylated NFκB (U-NFκB) as a further interaction partner of U-STAT3. U-NFκB utilizes the NLS of U-STAT3, explaining the expression of genes bearing κB elements upon U-STAT3 stimulation. Thereby, other interesting target genes, such as *rantes*, *IL-6* and *IL-8* have been discovered (Fig. 10; Yang et al. 2007). Given the capability also of STAT3β to drive *rantes* gene expression, the need of the TAD in this respect can be excluded (Yang and Stark 2008).

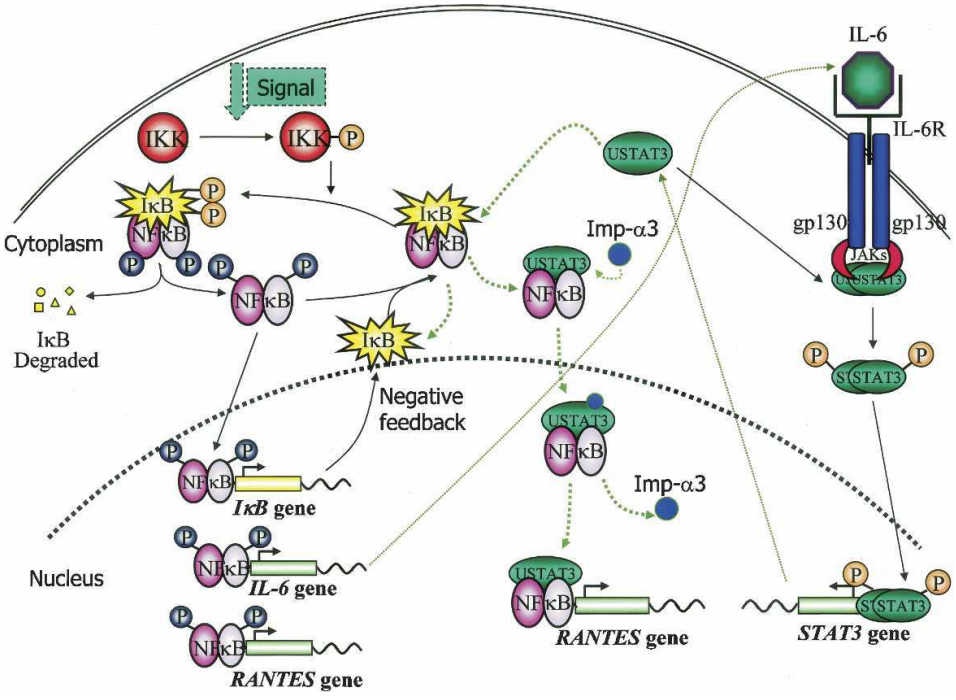

Fig. 10. Scheme of STAT3-NFκB interactions. Picture taken from Yang et al. 2007.

A correlation of U-STAT3 accumulation in the nucleus of myocytes in a transgenic mouse constitutively expressing Angiotensin II type-1 receptor (AT1R) and cardiac dysfunction has been examined. Additionally, an interaction of U-STAT3 with CBP/p300 was demonstrated.

This further emphasizes a crucial role of U-STATs in the maintenance of gene expression (Yue et al. 2010). U-STAT3 overexpression inhibited proliferation of vascular smooth muscle cells, suggesting an important role in vascular diseases (Yue et al. 2012). A further impact of U-STAT3 has been recently reported in diseases caused by infection and sepsis. U-STAT3, but not phosphorylated STAT3, exhibited anti-inflammatory effects via the alpha7 nicotinic receptor pathway. Furthermore, NFκB-mediated expression of pro-inflammatory TNF (tumor necrosis factor) was restricted upon binding of U-STAT3 to NFκB (Pena et al. 2010). U-STAT3 was identified to mediate the transition from acute to chronic kidney disease in a murine model of chronic nicotine exposed renal cells, highlighting the cell specificity of U-STAT3 responses (Arany et al. 2012). One study stated a role of U-STAT3 in effector T-cells via retaining phosphorylated (and thereby inactive) FoxO (Class O Forkhead transcription factors) proteins in the cytoplasm. Remarkably, phosphorylation of STAT3 ceased this interaction and FoxO proteins migrated into the nucleus to shut down T-cell expression. Therefore, U-STAT3/pTyr^{705}-STAT3 exhibited an antagonizing role in T-cell activation (Oh et al. 2012). A pro-oncogenic role of U-STAT3/NFκB has been described in chronic lymphocytic leukemia (CLL), which included a novel activation mechanism of NFκB without IκB degradation (Liu et al. 2011). High amounts of U-STAT3 have been also found in gastric cancer cells compared to adjacent tissue. Given the concomitant up-regulation of pro-metastatic factors, U-STAT3 was suggested as a candidate for poor prognosis in this malignancy (Cai et al. 2012).

A physical approach was recently applied to delineate DNA binding of U-STAT3. Via atomic force microscopy (AFM), binding to GAS elements was confirmed. Furthermore, binding to A-T rich elements, as frequently observed in chromatin organizing structures, were found, suggesting an epigenetic role of U-STAT3 (Timofeeva et al. 2012). So far, transcriptional activity specifically induced by a U-STAT3α/U-STAT3β heterodimer has not been identified. In general, although literature about U-STAT proteins is still moderately available, novel insights into U-STAT3 functions harbor a high potential in unraveling open questions in physiological and malignant situations.

3.3.3.3 STAT3 and cancer

More than 40 ligands are capable to activate STAT signaling. Given this high number and the numerous genes being regulated, a role in tumorigenesis is inevitable. Several mutations of JAKs, non-receptor kinases and aberrant STAT proteins (in particular STAT1, 3 and 5) have

been identified that promote malignancies (Bowman et al. 2000). Regarding STAT3, for example, it was shown that its constitutive activation represented the downstream effect of Src-mediated cell transformation (Garcia et al. 1997). Activated STAT3 has also been early observed in several lymphomas and in various cancers such as prostate, ovaries, kidney, pancreas, head and neck, lung and breast (Bowman et al. 2000). An important contribution to define STAT3 as an oncogene was the generation of a constitutive active STAT3 dimer upon modification of the SH2-domain (STAT3-C) that was capable to drive cell transformation (Bromberg et al. 1999). While the author proposed transcriptional activity of these mutants without prior phosphorylation, subsequent experiments employing STAT3-C revealed a basal phosphorylation level being responsible for their functional activity (Liddle et al. 2006).

The huge variability of STAT3 target genes that regulate several important hallmarks of cancer yielded early to the notification of being a classical oncogene (Fig. 11). Indeed, considering the "hallmarks of cancer" proposed by Weinberg and Hannahan, STAT3 can largely contribute to this register (Hanahan and Weinberg 2011). Some examples of STAT3 being implicated in these hallmarks are ascribed below.

Sustaining proliferative signaling: STAT3 has long been known to drive proliferation. Most importantly, up-regulation of genes encoding Cyclin D1 or c-myc upon constitutive STAT3 expression was examined in murine fibroblasts (Bromberg et al. 1999).

Resisting cell death: Catlett-Falcone et al. first showed that inhibition of the JAK-STAT pathway caused Bcl-X_L (Bcl-2-like 1) depletion and subsequent apoptosis induction, demonstrating Bcl-X_L as a STAT3 target gene (Catlett-Falcone et al. 1999). Mcl-1, another anti-apoptotic member of the Bcl-2 family, has also been found downstream of STAT3 in large granular lymphocytes (Epling-Burnette et al. 2001). STAT3 also contributes to FasL-mediated apoptosis, as shown in several malignant tissues (Ivanov et al. 2001; Lin et al. 2012).

Evading growth suppressors: STAT3 has been identified as the effector molecule of PDGF-Src-mediated suppression of p53 (Niu et al. 2005). In line with these findings, a recent publication implied Piwil2, a member of the Argonaut family, as an upstream regulator of the Src-STAT3-p53 axis (Cai et al. 2012).

Inducing angiogenesis: STAT3 activation has been identified in both directly bound to VEGF promoter and indirectly promoted VEGF expression vie the PI3-AKT-HIF1α axis, suggesting STAT3 as a crucial mediator for angiogenesis (Xu et al. 2005).

Activating invasion and metastasis: Matrix-metalloproteinases (MMPs) are important modifiers of extracellular matrix and their expression therefore often provide cell invasion

and metastasis. In breast cancer cells that had been transformed with STAT3-C constructs, up-regulation of MMP-9 was observed. Inhibition of MMP-9 did not reduce proliferation but was required for anchorage-independent growth (Dechow et al. 2004). A more recent study revealed STAT3 dependent expression of MMP-9 in monocytes located in the tumor stroma of cervical cancer (Schroer et al. 2011). The promoter of MMP-1 exhibits binding sites for a STAT3/c-Jun complex, as shown in colorectal cancer tissues (Zugowski et al. 2011). Further STAT3 dependent regulations of MMPs, such as MMP-2 and MMP-10 have been reported in melanoma and bladder cancer cells (Huang 2007). STAT3 has also been implicated in EMT, nowadays widely accepted as a program that transformed cells undergo to acquire capabilities for dissemination and invasion (Hanahan and Weinberg 2011). For example, inhibition of activated STAT3 reversed EGFR- and IL-6R-induced EMT in high-grade ovarian cancer (Colomiere et al. 2009). In this respect, STAT3 binding sites in the promoter of TWIST, a known EMT-inducer, have been found that responds to EGF signaling (Lo et al. 2007).

Enabling replicative immortality: Several studies suggest an inhibitory role of STAT3 in senescence. For example, a previous study showed that ablation of the IL-6/STAT3 pathway diminished senescence upon DNA damage (Yun et al. 2012). Furthermore, STAT3 depletion caused senescence in breast cancer cells, underlining a pivotal role of STAT3 in immortalization (Tkach et al. 2012).

Deregulating cellular energetics: It has long been known that the metabolism of tumor cells undergo an alteration to the so-called aerobic glycolysis, designated as “Warburg-effect”. Ras protein, HIF1α and HIF2α have been implicated in favoring glycolysis (Hanahan and Weinberg 2011). The lab of David Levy detected mitochondrial STAT3 and exclusive localization of STAT3 in these organelles was sufficient for Ras mediated transformation. Moreover, STAT3 also appeared under normal physiological conditions and showed specific mitochondrial functions (Gough et al. 2009). A recent publication employing constitutive active STAT3 in mouse fibroblasts confirmed these results, revealing STAT3 dependent enhanced levels of HIF1α and suppression of mitochondrial genes (Demaria et al. 2010). The findings mentioned above opens a new feature of STAT3 in oncogenic metabolism that is partly transcriptionally independent.

Evading immune destruction: A functional immune surveillance is proposed to destroy the majority of potentially aberrant growing cells. Both innate and adaptive immune reactions are capable to achieve recognition and ablation of neoplasms (Hanahan and Weinberg 2011). STAT3 was shown to inhibit precursors of an innate immune response and dendritic cell maturation in tumor cells, thereby preventing tumor-specific T-cell activation (Wang et al.

2004). Accordingly, STAT3 deletion in hematopoietic cells elicited significant increase of functional natural killer cells, neutrophils, T-cells and dendritic cells, suggesting STAT3 as a crucial mediator for antitumoral immune surveillance (Kortylewski et al. 2005).

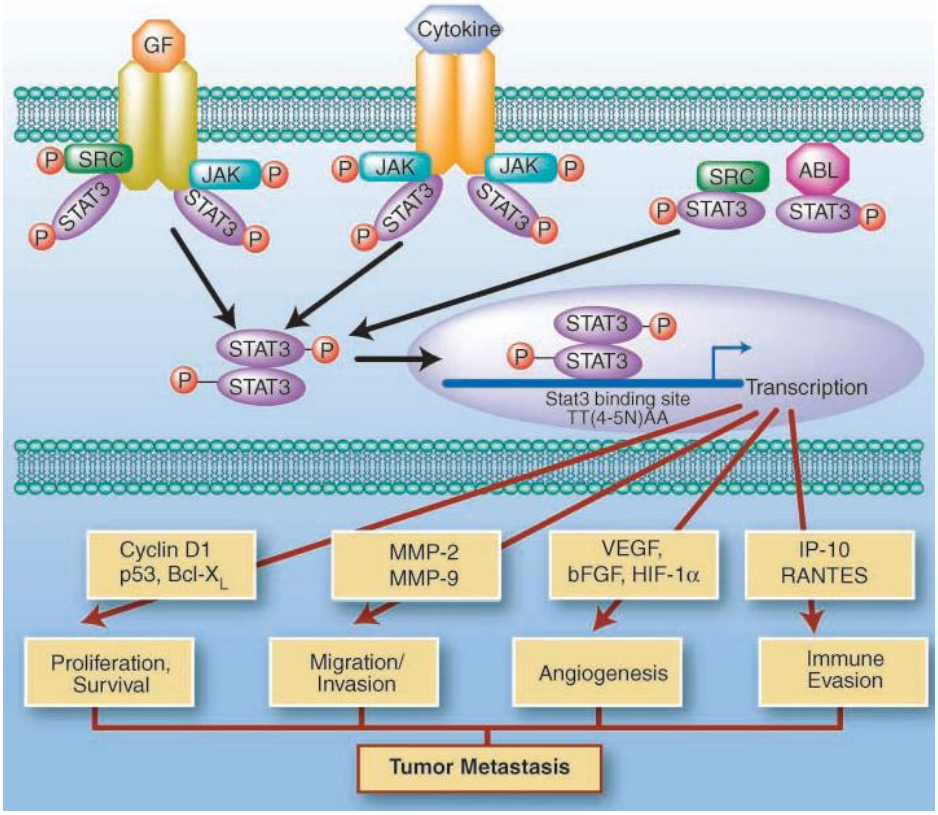

Fig. 11. Scheme of pro-metastatic features of the STAT3 pathway. Abbreviations: P, phosphorylated tyrosine residue; bFGF, basic fibroblast growth factor; IP-10, IFN-γ inducible protein-10. Picture taken from Huang et al. 2007.

3.3.3.4 STAT3 and HCC

Constitutive activation of STAT3 in human HCC specimen is a common finding in several studies (Calvisi et al. 2006; He et al. 2010). Mice bearing a conditional knockout of STAT3 showed significantly reduced tumor growth upon DEN (diethylnitrosamine) administration and DEN induced hepatoma cells silenced with shRNA against STAT3 were incompetent to generate subcutaneous tumors (He et al. 2010). A previous publication found a direct correlation of SOCS-1 (suppressor of cytokine signaling-1) methylation and constitutive activation of JAK2/STAT3 pathway in hepatoma cells, since SOCS proteins bear a SH2-domain and act as pseudo-substrates for JAKs. Reconstitution of SOCS-1 in these cells attenuated tumor growth. Furthermore, SOCS methylation in human HCC samples appeared

comparably high as constitutive STAT3 activation (Yoshikawa et al. 2001). Accordingly, analysis of microdissected tissue of HCC and normal liver tissue revealed up-regulation of STAT3 and down-regulation of SOCS-1 in HCC samples. Cyclin D1, a known target gene of STAT3, has also been found up-regulated (Tannapfel et al. 2003). Another screening of paraffin-embedded HCC linked phosphorylated STAT3 to microvessel density, a prognostic value for angiogenesis (Yang et al. 2007). Several studies showed anti-tumoral effects, including down-regulation of VEGF, survivin, MMP-2, MMP-9, cyclin D1 and c-myc upon blocking STAT3 with antisense oligonucleotide targeting (Li et al. 2006; Sun et al. 2008). Noteworthy, activated STAT3 has been also implicated as a marker of stem/progenitor cell phenotype. As mentioned above, inactivated TGF-β signaling has been frequently observed in this respect (Tang et al. 2008). Consistently, STAT3 inactivation via small molecule inhibitor targeting the SH2-domain exhibited significant larger anti-oncogenic effects in hepatoma cell lines harboring a dysfunctional TGFβ pathway (Lin et al. 2009). Obesity and ensuing nonalcoholic fatty liver disease (NAFLD) often precedes HCC. As examined in obese mice, the IL-6/STAT3 axis largely contributed to this connection (Park et al. 2010). Accordingly, antagonizing leptin (that is up-regulated in obese individuals and a known inducer of STAT3 via leptin receptor) with adiponectin depleted STAT3 activation and increased SOCS-3 expression (Sharma et al. 2010). Furthermore, STAT3 facilitates hepatitis C (HCV) mediated hepatocarcinogenesis together with c-Jun. C-Jun was found being upstream of STAT3 via IL-6 induction, suggesting co-treatment of these transcription factors as promising in HCV infections (Machida et al. 2010). One mechanism of Sorafenib efficacy appeared the depletion of STAT3 activation, presumably via SHP-1 (SH2 domain–containing tyrosine phosphatase-1) activation. As a result, TRAIL (tumor necrosis factor-related apoptosis-inducing ligand) resistant hepatoma cells were sensitized for apoptosis (Chen et al. 2010). An ensuing study referring features of Sorafenib confirmed up-regulation of SHP-1 as a kinase-independent mechanism (Tai et al. 2011). Similar results have been obtained utilizing Dovitinib, another multikinase inhibitor, also showing SHP-1 dependent STAT3 inactivation (Chen et al. 2012). SHP-2, another phosphatase that revealed pro-oncogenic features in leukemia, exhibited tumor-suppressive properties in HCC via disruption of the STAT3 pathway and ensuing inflammation (Bard-Chapeau et al. 2011). Cetuximab effectively antagonizes ligand binding to EGFR. Chen and co-workers identified a direct correlation of STAT3 activation and resistance to Cetuximab in hepatoma cell lines, further emphasizing therapies including STAT3 inhibition (Chen et al. 2012). A recent publication conceded IL-22 as a potent HCC inducer via STAT3 activation, given the large amount of IL-22 in tumor stroma of liver

cancers. The mechanism might be a pro-survival effect on damaged liver cells (Jiang et al. 2011). Consistently, phosphorylated STAT3 has been also detected in monocytes located in the tumor microenvironment, accompanied with poor prognosis (Wu et al. 2011). A role in HCC progression was previously related to IL-17 through triggering IL-6 and subsequent STAT3 activation via onset of the AKT pathway, supporting tumor invasion upon vessel formation and neutrophil infiltration (Gu et al. 2011).

$CD24^+$ expressing cells were identified as tumor-initiating cells (TICs), exhibiting stemness properties and high chemoresistence. Remarkably, it was shown that CD24 induces expression of the stemness factor NANOG via Src and STAT3 that binds to the *nanog* promoter. This finding underlines the pivotal role of STAT3 in clonal HCC development (Lee et al. 2011). Several microRNAs (miRs) are playing both anti- and pro-oncogenic roles in HCC. MiR-637 was recently observed to be down-regulated in hepatoma cell lines and human HCC tissues. Indeed, miR-637 depleted STAT3 phosphorylation via the IL-6 family cytokine LIF, which had been found as a target of this miR (Zhang et al. 2011). MiR-23a was identified as a crucial regulator in altering glucose metabolism in HCC. Particularly, miR-23a repressed genes encoding enzymes responsible for gluconeogenesis, such as glucose-6-phosphatase and fructose-1, 6-phosphatase, therefore favoring aerobic glycolysis. STAT3 was found to bind the miR-23a promoter region, thus regulating miR-23a expression (Wang et al. 2012). A recent publication addressed the higher incidence of HCC in males. Estrogen receptor alpha (ERα) promoted protein tyrosine phosphatase receptor type O (PTPRO) expression, which had been found acting as a tumor suppressor via its phosphatase domain. The authors showed deactivation of STAT3 via PTPRO-dependent dephosporylation of JAK2 and PI3K. These results suggested an ERα related gender-specific bias in HCC (Hou et al. 2012).

3.3.3.5 Tumor-suppressive roles of STAT3

Even though literature regarding an oncogenic fashion prevails, studies considering a tumor suppressive STAT3 are emerging. For example, STAT3 exhibited a hepatoprotective effect in liver cancer upon long-term carbon tetrachloride (CCl(4)) treatment. In this study, mice harboring a liver-specific STAT3 knockout exhibited increased inflammation and oxidative stress, suggesting STAT3 to protect hepatocytes against DNA damage in early stages of HCC In contrast, the same authors reported decreased tumorigenesis in hepatocyte-specific STAT3 knockout mice applying DEN injection (Wang et al. 2011). An elegant approach identifying a

possible role of STAT3β in anti-tumorigenicity was achieved using so-called morpholino oligomers that engage forced alternative splicing from STAT3α to STAT3β (Zammarchi et al. 2011). Surprisingly, subcutaneous tumor formation of breast cancer cells harboring STAT3β was decreased, in contrast to both STAT3α and full knockdown cells. Among down-regulated genes, p300/CBP-associated factor (PCAF) appeared to be responsible for viability, confirming previous suggestions that STAT3β exhibited transcriptional activity rather than dominant negative wildtype STAT3 features. However, even total STAT3 elicits anti-oncogenic properties, depending on the cell type. In the case of papillary thyroid carcinoma (PTC), an inverse correlation between activated STAT3 and metastasis has been evaluated. Moreover, STAT3 depletion enhanced tumor growth in thyroid cancer cells and was shown to be downstream of B-RAFV600E, a commonly mutated form of B-RAF in PTC (Couto et al. 2012). Tumor suppressor IGFBP7 (IGF-binding protein 7) has been found down-regulated upon STAT3 ablation. Importantly, the anti-tumorigenic phenotype has been exclusively observed *in vivo*. Another example demonstrating the importance of the molecular background regarding STAT3 actions has been described in glioblastoma. In a subclass of PTEN-deficient tumors, STAT3 is not expressed. Remarkably, exogenous re-expression of STAT3 in this scenario exhibited tumor suppressive properties. Finally, IL-8 has been demonstrated as a key player in this axis (de la Iglesia et al. 2008). Recently, a mechanism of STAT3 suppressing EMT in colorectal carcinoma has been reported. Via regulation of GSK-β (glycogen synthase kinase-β), EMT-inducer SNAI (Snail-1) was degraded. Interestingly, in this connection, STAT3 acted as an adaptor protein rather than as a transcription factor (Lee et al. 2012). Ambiguous roles of STAT3 were recently shown in the Apc(Min) mouse model for intestinal cancer. While deletion of STAT3 in intestinal epithelial cells provoked decreased early adenoma formation, lack of STAT3 caused enhanced tumor growth at later stages, possibly due to downregulation of the CEACAM adhesion protein (Musteanu et al. 2010). The issue of STAT3 and cancer outcome has been also stressed in head and neck squamous cell cancer (HNSCC). Nuclear localization was correlated with better prognosis in HNSCC. Notably, possible transcriptional activity of U-STAT3 had not been taken into account (Pectasides et al. 2010). Screening of total and phosphorylated STAT3 with respect to its localization has been also conducted in human breast cancer tissues. Activated STAT3, both nuclear and cytoplasmic, has been associated with better overall survival (Dolled-Filhart et al. 2003). Moreover, the tumor-suppressive role of STAT3 in the absence of $p14^{ARF}$/$p19^{ARF}$ in HCC must be mentioned, which is part of this PHD thesis (Schneller et al. 2011). In this study (see section 4), other interesting reports regarding the still unusual role of tumor-

suppressive STAT3 will be presented, which were published partly by collaborating laboratories. Certainly, the list of unexpected features of STAT3 is not completed and will be an intriguing subject of discussion.

3.4. Aims of the study

Aberrant signaling pathways play an important role in carcinogenesis. Several lines of evidence suggested STAT3 to be pro-oncogenic in cancer development. However, recent observations described a more ambiguous role of the canonical STAT3 signaling in tumor formation. Unphosphorylated STAT3 (U-STAT3) was also shown to be transcriptionally active and NFκB was identified as a binding partner. In this study, the role of STAT3 was addressed in Ras-transformed HCC, depending on the availability of $p14^{ARF}/19^{ARF}$.

The aims of the study included to

(i) investigate the role of STAT3 in hepatocellular tumorigenesis dependent on the presence or absence of $p19^{ARF}$ in a murine HCC model

(ii) discriminate the functions of the STAT3α and STAT3β isoforms lacking the phosphorylation site on Tyr^{705} in $p19^{ARF}$-deficient, Ras-transformed hepatoma cells

(iii) analyze the ability of U-STAT3 for transactivation in HCC cells

(iv) examine NFκB as a putative binding partner of U-STAT3

(v) study the interaction of STAT3 with other crucial signaling pathways, such as TGF-β and PTEN

(vi) determine the crosstalk of STAT3 and $p14^{ARF}$ in human hepatoma cell lines

(vii) correlate $p14^{ARF}$ and STAT3 expression in human HCC samples for estimation of the clinical relevance

4 Manuscript

$p19^{ARF}/p14^{ARF}$ controls oncogenic functions of Stat3 in hepatocellular carcinoma

Doris Schneller[1*], Georg Machat[1*], Alexandra Sousek[1*], Verena Proell[2], Franziska van Zijl[1], Gudrun Zulehner[1], Heidemarie Huber[1], Markus Mair[3], Markus K. Muellner[4], Sebastian M.B. Nijman[4], Robert Eferl[3], Richard Moriggl[3] and Wolfgang Mikulits[1]

[1]Department of Medicine I, Division: Institute of Cancer Research, Comprehensive Cancer Center, Medical University of Vienna, Vienna, [2]Department of Natural Sciences, University of Veterinary Medicine, Vienna, [3]Ludwig Boltzmann Institute for Cancer Resarch, Vienna, and the [4]Research Center of Molecular Medicine of the Austrian Academy of Sciences, Vienna, Austria

[*]These authors contributed equally to this work.

Keywords: Stat3, HCC, Ras, $p19^{ARF}/p14^{ARF}$, oncogene

Corresponding author: Wolfgang Mikulits, Department of Medicine I, Division: Institute of Cancer Research, Medical University of Vienna, Borschke-Gasse 8a, A-1090 Vienna, Austria.
Tel: +43 1 4277 65250; Fax: +43 1 4277 65239;
E-mail: wolfgang.mikulits@meduniwien.ac.at

Abbreviations: Ca, constitutive active; DEN, diethylnitrosamine; H&E, hematoxylin and eosin; HCC, hepatocellular carcinoma; HNF, hepatocyte nuclear factor; IL, interleukin; Jak, Janus kinase; pY-Stat3, Tyr^{705} phosphorylated Stat3; RT-PCR, reverse transcription polymerase chain reaction; Stat, signal transducer and activator of transcription; SCID, severe combined immunodeficient; SD, standard deviation; U-Stat3, unphosphorylated Stat3.

Financial Support: This work was supported by the Austrian Science Fund, FWF, grant numbers SFB F28 (RE, RM, WM), P19598 (WM) and P20905 (WM), and the **European Union, FP7** Health Research, project number HEALTH-F4-2008-202047 (WM).

4.1 Contribution to this study

The author of this doctoral thesis mainly contributed to the setup of human models in the study of Schneller et al. In detail, the experiments performed by the author involved the evaluation of Hep3B cells harboring a knockdown of $p14^{ARF}$ (Hep4B-shp14) by immunofluorescence assays (Supporting Fig. 3). It also contained the analysis of tumor kinetics of Hep3B cells harboring a knockdown of $p14^{ARF}$ (Fig. 5D). Furthermore, biochemical detection of active STAT3 (pY705-STAT3) in respective tumor tissues was performed (Fig. 5C). The author further established PLC/PRF/5 cells overexpressing $p14^{ARF}$ that were used as an alternative cell line for STAT3 *de novo* synthesis and JAK-inhibitor assays (Fig. 6 and data not shown). Together with Alexandra Sousek, the author developed the model depicted in Fig. 7 of the publication by Schneller et al. Accordingly, the putative interactions of STAT3 and $p14^{ARF}$ has been discussed and several approaches to dissect the pro- and anti-oncogenic phenotype of STAT3 have been considered. In particular, STAT3 variants, such as constitutive active STAT3 or variants lacking the activation sites have been taken into account. Based on these considerations, the experiments performed by the author of the PhD thesis are presented in section 5.

4.2 Abstract

Signal transducer and activator of transcription 3 (Stat3) is activated in a variety of malignancies including hepatocellular carcinoma (HCC). Activation of Ras occurs frequently at advanced stages of HCC by aberrant signaling through growth factor receptors or inactivation of effectors negatively regulating Ras signaling. Here, we addressed the role of Stat3 in Ras-dependent HCC progression in the presence and absence of $p19^{ARF}$/$p14^{ARF}$. We show that constitutive active (ca) Stat3 is tumor-suppressive in Ras-transformed $p19^{ARF-/-}$ hepatocytes, while expression of Stat3 lacking Tyr^{705} phosphorylation (U-Stat3) enhances tumor formation. Accordingly, Ras-transformed $Stat3^{\Delta hc}$/$p19^{ARF-/-}$ hepatocytes (lacking Stat3 and $p19^{ARF}$) showed increased tumor growth compared to those expressing Stat3, demonstrating a tumor suppressor activity of Stat3 in cells lacking $p19^{ARF}$. Notably, endogenous expression of $p19^{ARF}$ in Ras-transformed hepatocytes conveyed oncogenic Stat3 functions, resulting in augmented or reduced HCC progression after expression of caStat3 or U-Stat3, respectively. In accordance with these data, the knock-down of $p14^{ARF}$ (the human homologue of $p19^{ARF}$) in Hep3B cells was associated with reduced pY-Stat3 levels during tumor growth in order to circumvent the tumor-suppressive effect of Stat3. Inhibition of Janus kinases (Jaks) revealed that Jak causes pY-Stat3 activation independently of $p14^{ARF}$ levels, indicating that $p14^{ARF}$ controls the oncogenic function of pY-Stat3 downstream of Jak. *Conclusion:* These data show evidence that $p19^{ARF}$/$p14^{ARF}$ determines the pro- or anti-oncogenic activity of U-Stat3 and pY-Stat3 in Ras-dependent HCC progression.

4.3 Introduction

Constitutive activation of signal transducer and activator of transcription 3 (Stat3) is frequent in solid cancers and contributes to oncogenesis (Levy and Lee 2002; Yu and Jove 2004). Stat3 is considered as an oncogene because (i) Stat3 that constitutively activates transcription (ca Stat3) provides cellular transformation of NIH3T3 fibroblasts, (ii) Stat3 is stimulated by growth-promoting signals such as activated growth factor receptors via several Janus kinases (Jaks) or Src, (iii) both non-phosphorylated and phosphorylated Stat3 accumulate in many human cancers, and (iv) Stat3 contributes to abrogated immune surveillance leading to enhanced tumor cell growth (Bromberg et al. 1999; Levy and Inghirami 2006; Yu et al. 2007; Dewilde et al. 2008). However, recent findings in glioblastoma and intestinal tumors support the idea that Stat3 can also act as a tumor suppressor (de la Iglesia et al. 2008; Ecker et al. 2009; Musteanu et al. 2010).

In the liver, Stat3 is important for liver regeneration by stimulating hepatic cell proliferation and survival (Taub 2004). Stat3 is upregulated and activated in the vast majority of human hepatocellular carcinoma (HCC) specimens (Zhang et al. 2010; He and Karin 2011) and is essential for cell growth, survival, tumor dedifferentiation, intratumoral microvessel density and metastasis of HCC (Li et al. 2006; Yang et al. 2007). Deactivation of Stat3 by low molecular compounds or inhibition of Stat3 expression employing RNA interference approaches enhanced the chemo-sensitivity of HCC cells and suppressed growth and metastasis of human HCC in xenografted mice (Lau et al. 2007; Lin et al. 2009). Recent findings demonstrate that Stat3 is a critical regulator of liver cancer development and progression through a negative crosstalk with NF-κB (He et al. 2010).

Notably, constitutive activation of Stat3 is accompanied by high levels of unphosphorylated Stat3 (U-Stat3), which differs from Tyr^{705} phosphorylated Stat3 (pY-Stat3)-mediated gene expression in both, its binding partners and mechanism to activate transcription. The formation of U-Stat3 complexes occurs either in the cytoplasm or in the nuclear compartment. Its transcriptional targets also differ from those of pY-Stat3 dimers as other promoters can be modulated by e.g. U-Stat3/NF-κB heterodimers (Yang and Stark 2008).

The Ras cascade mainly transduces extracellular signals via activated growth factor receptors resulting in proliferative and anti-apoptotic signals (Zender et al. 2010). In HCC, the expression of oncogenic Ras, which is locked in its active form due to the insensitivity against GTPase activating proteins (GAPs), is rare (Zender et al. 2010; Calvisi et al. 2011). Yet, aberrant activation of Ras signaling is frequently observed by overexpression of Ras,

epigenetic silencing of GAPs by promoter hypermethylation, or by mutations of upstream inducers or downstream effectors (Zender et al. 2010; Calvisi et al. 2011).

The tumor suppressor $p14^{ARF}$ (the human homologue of $p19^{ARF}$) is an important sensor of hyperproliferative stimuli that restricts cell proliferation through both, p53-dependent and independent pathways when activated by sustained mitogenic or oncogenic signals like Ras (Tannapfel et al. 2001; Sherr 2006; Pollice et al. 2008). Disruption of the $p14^{ARF}$-Mdm2-p53-pathway is a very common feature in cancer (Tannapfel et al. 2001). Remarkably, $p14^{ARF}$ is inactivated by promoter hypermethylation in up to 40 % of HCC cases (Tannapfel et al. 2001; Anzola et al. 2004).

In this study, we found that caStat3 acts tumor-suppressive in Ras-transformed $p19^{ARF-/-}$ hepatocytes, whereas expression of U-Stat3 or loss of Stat3 increased tumor growth. Reciprocal effects of caStat3 and U-Stat3 were observed in Ras-transformed hepatocytes endogenously expressing $p19^{ARF}$. In human HCC cells, knock-down of $p14^{ARF}$ resulted in reduced pY-Stat3 levels upon tumor formation, thus impeding the tumor-suppressive function of Stat3. Activation of pY-Stat3 by Jak was not affected by $p14^{ARF}$ levels, suggesting that $p14^{ARF}$ modulates the oncogenic function of Stat3 downstream of Jak in Ras-transformed hepatocytes.

4.4 Materials and Methods

Cell culture

Mouse hepatocyte cell lines were generated by stable retroviral transmission of immortalized $p19^{ARF-/-}$ hepatocytes (MIM-1-4), $Stat3^{\Delta hc}/p19^{ARF-/-}$ or MMH-D3 cells with a construct expressing oncogenic v-Ha-Ras or Stat3 variants (wtStat3, caStat3α, caStat3β, U-Stat3; Supporting Information Fig. 1; Ecker et al. 2009) and cultured on collagen-coated dishes (Gotzmann et al. 2002; Mikula et al. 2004). Ras-transformed mouse hepatocytes, human Hep3B, PLC/PRF/5, SW480 and $p14^{ARF}$-deficient MCM1 melanoma cells (Paulitschke et al. 2010; a kind gift of Dr. Mario Mikula, Medical University of Vienna) were cultivated at 37°C and 5% CO_2. All cells were routinely screened for absence of mycoplasma. Details for treatment of HCC cells with cytokines and Jak inhibitors as well as for lentiviral-mediated knock-down of $p14^{ARF}$ are provided in Supporting Information.

Gene targeted mice

Stat3Δhc mice harboring the liver-specific Stat3 null allele were generated as described recently.(Mair et al. 2010) Stat3Δhc mice were crossed to p19ARF-/- mice to obtain Stat3Δhc/p19ARF-/- mice (Kamijo et al. 1997).

Isolation and immortalization of hepatocytes from $Stat3^{\Delta hc}/p19^{ARF-/-}$ mice

Hepatocytes of four-week-old $Stat3^{\Delta hc}/p19^{ARF-/-}$ mice were isolated by liver perfusion and propagated as described (Mikula et al. 2004). MIM-$Stat3^{\Delta hc}$-1 and MIM-$Stat3^{\Delta hc}$-2 cells were obtained by single cell cloning and employed for retroviral expression of oncogenic v-Ha-Ras. MIM-R-$Stat3^{\Delta hc}$-2 hepatocytes were used for stable co-expression of wtStat3, termed MIM-R-$Stat3^{\Delta hc}$-2-wtStat3.

Tumor formation and recultivation of tumor cells

Briefly, $1x10^6$ murine or $5x10^6$ human cells in 100 µl Ringer solution were subcutaneously injected into severe combined immunodeficient (SCID) mice (Harlan Laboratories, San Pietro, Italy). Tumor volume was determined as described (Fischer et al. 2007). Pulmonary metastatic colonization was analyzed after injection of $1x10^5$ cells/100 µl Ringer solution into the tail vein of SCID mice. Orthotopic liver transplantation was performed by injection of $1x10^6$ cells/20 µl Ringer solution into the spleen of SCID mice (Mikula et al. 2004). The

recovery of tumor cells is provided in Supporting Information. All experiments were performed according to the Austrian guidelines for animal care and protection.

HCC induction

To initiate tumor development in the liver, 14-day-old $Stat3^{fl/fl}$ and $Stat3^{\Delta hc}$ animals were intraperitoneally injected with a single dose of diethylnitrosamine (DEN, 25 mg/kg). After 12 months of age, mice were sacrificed and livers were processed for PCR analysis or fixed in 4% formaldehyde for immunohistochemistry.

Immunohistochemistry

Mice were sacrificed and tumors and lungs were fixed as described.(Mikula et al. 2004) 4 μm thick, paraffin-embedded sections were stained with hematoxylin and eosin (H&E). For immunohistochemistry, sections were stained with anti-phospho-Stat3 (Tyr^{705}, Cell Signaling, Beverly, USA) and anti-Stat3 antibodies (Cell Signaling).

Immunoblotting

Immunoblotting was performed as described (Gotzmann et al. 2002). The primary anti-phospho-Stat3 (Tyr^{705}), anti-Stat3 (both Cell Signaling, Beverly, USA), anti-$p14^{ARF}$ and anti-Actin antibodies (both Sigma, St Louis, USA) were used at dilutions of 1:1.000.

Reverse transcription polymerase chain reaction (RT-PCR)

Semi-quantitative RT-PCR was performed as described (Mikula et al. 2004). Quantitative PCR was performed with Fast SYBR Green Master Mix (Applied Biosystems, Foster city, CA, USA) according to the recommendations of the manufacturer and quantified with the 7500 Fast Real Time PCR System (Applied Biosystems, CA, USA). Arbitrary units were calculated by the dCT method. Primer sequences are provided in Supporting Information.

Statistical analysis

Data are expressed as means ± standard deviation (SD). The statistical significance of differences was evaluated using an unpaired, non-parametric Student's t-test. Significant differences between experimental groups were * $p<0.05$, ** $p<0.01$ or *** $p<0.005$.

4.5 Results

4.5.1 Stat3 represses tumor growth of Ras-transformed p19$^{ARF-/-}$ hepatocytes

We employed an established mouse tumor transplantation model to assess the role of Stat3 during HCC progression. This model is based on the lack of p19^{ARF} in hepatocytes which allows immortalization (Mikula et al. 2004). Non-tumorigenic p19$^{ARF-/-}$ hepatocytes (MIM-1-4) have been transformed with oncogenic Ras (MIM-R; Fischer et al. 2007). To study the effect of Stat3 on Ras-dependent tumor growth, caStat3 variants of Stat3α and the natural splice variant Stat3β lacking the Ser^{727} phosphorylation site (Dewilde et al. 2008) and U-Stat3 (lacking both Tyr^{705} and Ser^{727} phosphorylation sites) were stably expressed in MIM-R hepatocytes (Supporting Information Fig. 1A, B).

Proliferation kinetics showed no changes between MIM-R hepatocytes and those expressing Stat3 mutants (data not shown). To investigate the tumorigenicity, Stat3 mutant hepatocytes were subcutaneously injected into SCID mice. MIM-R-caStat3α- and MIM-R-wtStat3-derived tumors displayed 2-fold reduced volumes compared to those generated by MIM-R hepatocytes. An even 5-fold suppression of tumor growth was observed upon injection of MIM-R-caStat3β hepatocytes. On the contrary, MIM-R-U-Stat3 cells caused a 2-fold increased tumor volume compared to MIM-R hepatocytes (Fig. 1A). Orthotopic transplantation of MIM-R-wtStat3, MIM-R-caStat3α and MIM-R-caStat3β hepatocytes led to a strong reduction of HCC formation, whereas MIM-R-U-Stat3 cells exhibited enhanced HCC generation compared to MIM-R-derived liver tumors (Fig. 1B). Notably, both frequency and size of lung metastases were significantly reduced after tail vein injection of MIM-R-wtStat3, MIM-R-caStat3α or MIM-R-caStat3β cells. In contrast, MIM-R-U-Stat3 cells showed pulmonary metastasis comparable to MIM-R hepatocytes (Fig. 1C, D).

These data show that exogenous expression of caStat3 or U-Stat3 causes anti- or pro-oncogenic effects in p19$^{ARF-/-}$ MIM-R hepatocytes, respectively.

4.5.2 Loss of Stat3 promotes tumor formation in p19$^{ARF-/-}$ MIM-R hepatocytes

To verify a tumor-suppressive role of Stat3, we performed a conditional Stat3 knock-out in hepatocytes of p19$^{ARF-/-}$ mice. Hepatocytes were isolated from Stat3$^{\Delta hc}$/p19$^{ARF-/-}$ mice and deletion of Stat3 was confirmed by PCR and immunoblot analysis (Supporting Information Fig. 2A, B; Mair et al. 2010). Two randomly isolated clones of the hepatocyte pool, designated MIM-Stat3$^{\Delta hc}$-1 and MIM-Stat3$^{\Delta hc}$-2, expressed several hepatocyte-specific

markers such as keratin 18, hepatocyte nuclear factor (HNF)-1α and HNF-4α (Supporting Information Fig. 2C).

We next analyzed the tumorigenic potential after subcutaneous injection into SCID mice. Both, MIM-R-Stat3$^{\Delta hc}$-1 and MIM-R-Stat3$^{\Delta hc}$-2 hepatocytes showed increased tumor development compared to MIM-R cells, while re-expression of wtStat3 in MIM-R-Stat3$^{\Delta hc}$ hepatocytes abolished faster tumor kinetics (Fig. 2). In summary, these results confirm that Stat3 has tumor-suppressive functions in Ras-transformed p19$^{ARF-/-}$ hepatocytes.

4.5.3 Stat3 acts pro-oncogenic in p19^{ARF}-positive Ras-transformed hepatocytes

To investigate a possible impact of p19^{ARF} deficiency on Stat3 functions, we employed murine MMH-D3 hepatocytes that express endogenous p19^{ARF} (Fig. 3A; Amicone et al. 1997). MMH-D3 cells transformed with oncogenic Ras (MMH-R) were further analyzed after expression of either caStat3β or U-Stat3 since these variants showed strongest tumor-suppressive or tumor-promoting activities in p19$^{ARF-/-}$ MIM-R hepatocytes, respectively (Fig. 1). Subcutaneous injection of p19^{ARF}-positive MMH-R cells expressing caStat3β into mice showed an 8-fold increased tumor formation compared to MMH-R, whereas expression of U-Stat3 lowered tumor generation about 1.5-fold (Fig. 3B). After tail vein injection of cells, MMH-R-caStat3β cells exhibited enhanced lung colonization, while MMH-R-U-Stat3 hepatocytes showed lower numbers and a reduced size of lung metastasis (Fig. 3C, D). From these data we conclude that p19^{ARF} modulates the pro- and anti-oncogenic activities of Stat3 during HCC progression.

4.5.4 Upregulation of p19^{ARF} is associated with DEN-induced tumor formation in *Stat3$^{fl/fl}$ mice*

Stat3 was recently shown to be required for diethylnitrosamine (DEN)-induced HCC development (He et al. 2011). In accordance with these data, we observed a reduction in number and size of liver tumors in Stat3$^{\Delta hc}$ relative to Stat3$^{fl/fl}$ mice after DEN treatment (unpublished data). To confirm that the pro-oncogenic role of Stat3 in this background correlates with p19^{ARF}, we analyzed samples of DEN-induced liver tumors. Indeed, p19^{ARF} was remarkably high during HCC development in Stat3$^{fl/fl}$ mice, whereas DEN-induced liver tumors of Stat3$^{\Delta hc}$ mice showed strongly reduced levels of p19^{ARF} (Fig. 4A). As expected, activation of pY-Stat3 was observed in tumor sections from DEN-treated Stat3$^{fl/fl}$ mice (Fig. 4B). These data show that pY-Stat3 activation is linked to the presence of p19^{ARF} during

DEN-induced tumor formation (Fig. 4A), underlining the functional interaction of $p19^{ARF}$ and pY-Stat3 in tumor growth.

4.5.5 $p14^{ARF}$ modulates Stat3 activation during human HCC development

To bridge mouse to human hepatocarcinogenesis, we analyzed an established human HCC cell line for expression of $p14^{ARF}$, the human homologue of $p19^{ARF}$. Real-time PCR analysis showed that human Hep3B cells express $p14^{ARF}$ (Supporting Information Fig. 3A) and activate Ras/MAPK signaling effectors as described (Yip-Schneider et al. 2009). To investigate the effects of Stat3 in the presence or absence of $p14^{ARF}$, we introduced short hairpin (sh)RNAs targeted against $p14^{ARF}$ (sh-p14-1 and sh-p14-2) as well as a mixture of both shRNAs (sh-p14-3) into Hep3B cells. Expression of $p14^{ARF}$ was almost eliminated after shRNA expression (Supporting Information Fig. 3B, C). Hep3B and corresponding shRNA cell lines were subcutaneously injected into SCID mice to examine tumorigenesis. Knock-down of $p14^{ARF}$ by expression of sh-p14-3 was accompanied by a significant downregulation of pY-Stat3 *in vivo* as observed by immunohistochemistry and immunoblotting of tumors (Fig. 5A-C). Notably, tumor volumes of Hep3B cells expressing sh-p14 were comparable to control cells (Fig. 5C). A persistent downregulation of $p14^{ARF}$ was confirmed after re-cultivation of cells from subcutaneous tumors (Fig. 5D). From these data we conclude that the tumor-suppressive function of Stat3 in the absence of $p14^{ARF}$ is circumvented by inhibition of pY-Stat3 *in vivo*.

4.5.6 $p14^{ARF}$ acts downstream of Jak-mediated Stat3 phosphorylation

Next we analyzed whether *de novo* RNA and protein synthesis affects pY-Stat3 activation and whether it depends on the presence of $p14^{ARF}$. Interestingly, inhibition of either transcription or translation using actinomycin D or cycloheximide, respectively, reduced pY-Stat3 levels in both Hep3B as well as in Hep3B-sh-p14_3 cells while keeping total Stat3 levels unaffected (Fig. 6A, B). Comparable results were obtained by employing human PLC/PRF/5 hepatoma cells (data not shown). These data suggest that *de novo* synthesis of an upstream mediator is essential for pY-Stat3 activation in Hep3B hepatoma cells. However, pY-Stat3 activation occurs in a mode independent of $p14^{ARF}$ expression.

In order to study the impact of $p14^{ARF}$ on the canonical Jak-Stat signaling, Hep3B cells and those showing a knock-down of $p14^{ARF}$ were treated with a pan-Jak inhibitor (blocking Jak1, Jak 2, Jak3 and Tyk2 activity). The pan-Jak inhibitor efficiently blunted pY-Stat3 activation

upon IL-6 treatment independently of $p14^{ARF}$ expression (Fig. 6C). PLC/PRF/5 hepatoma cells revealed comparable results (data not shown). These findings suggest that Jak activity mainly causes pY-Stat3 activation irrespectively of $p14^{ARF}$ levels, implicating that the control of oncogenic Stat3 function by $p14^{ARF}$ occurs downstream of Stat3 phosphorylation.

4.6 Discussion

This study shows that Stat3 is able to execute both, pro- and anti-oncogenic functions depending on $p19^{ARF}$/$p14^{ARF}$ expression during Ras-mediated HCC development. CaStat3 acts tumor-suppressive in Ras-transformed $p19^{ARF-/-}$ hepatocytes as well as tumor-promoting in hepatocytes expressing $p19^{ARF}$. Strikingly, the Y705F mutant (U-Stat3) shows the opposite effect. In line with these findings, tumors derived from the human HCC cell line Hep3B show reduced pY-Stat3 upon $p14^{ARF}$ silencing. In this scenario, human HCC cells counteract the tumor-suppressive effects of Stat3 as observed in the murine $p19^{ARF-/-}$ model and prevent diminished tumor growth. $p14^{ARF}$ levels in HCC cells affect pY-Stat3 activation *in vivo*, whereas pY-Stat3 activation mainly induced by Jak seems to be independent of $p14^{ARF}$ expression *in vitro*.

$p14^{ARF}$ is a potential target for inactivation in HCC due to its positive role in p53 stabilization by promoting MDM2 degradation (Sherr 2001). In accordance with our results, the $p14^{ARF}$-negative HCC cell lines HepG2 and PLC/PRF/5 are less sensitive to the Stat3 inhibitor NSC 74859 treatment, while $p14^{ARF}$ expressing Huh-7 and SNU-398 cells show reduced cell proliferation after administration of NSC 74859 (Lin et al. 2009). Our observations in murine hepatocytes suggest that a tumor-suppressive Stat3 function depends on $p19^{ARF}$ deficiency but might be independent of both $p16^{INK4B}$ and p53 inactivation, since $p19^{ARF-/-}$ hepatocytes express $p16^{INK4A}$ and show p53 response (Fischer et al. 2007). In line with this, the human hepatoma Hep3B cells used in this study harbor a p53 mutation that is not affecting the response of reduced pY-Stat3 activation in $p14^{ARF}$ knocked-down cells (Lin et al. 1996).

Furthermore, pro-oncogenic Stat3 functions are observed in hepatitis B virus-positive HCC cell lines such as SNU-182 or SNU-387 which express mutated and inactivated p53 (Kang et al. 1996; Fuchs et al. 2008), indicating tumor-promoting Stat3 functions independent of p53.

Modulation of pro- or anti-oncogenic Stat3 functions through tumor suppressors has been described in different cancers. In glioblastoma, deficiency in PTEN induces malignant transformation of astrocytes upon Stat3 knock-out, arguing for anti-oncogenic functions of Stat3 (de la Iglesia et al. 2008). Recently, we also described a dual role of Stat3 in $Apc^{Min/+}$ mice, where Stat3 promotes early microadenoma formation, whereas Stat3 deficiency in intestinal epithelial cells increased later stage carcinoma progression associating with nuclear β-catenin and impaired Ceacam1 expression (Musteanu et al. 2010). In addition, we showed that caStat3 blocked c-myc-induced transformation of $p53^{-/-}$ mouse fibroblasts (Ecker et al.

2009). These findings indicate that Stat3 functions are modulated by various tumor suppressors.

Despite the inability of oncogenic Ras to drive Stat3 tyrosine phosphorylation or nuclear translocation, Ras transformation was found impaired in the absence of Stat3 (Gough et al. 2009). Similar results were obtained upon mouse mammary tumor progression showing that Stat3 is indispensable for the metastasis of ErbB2-activated cancer cells to the lung (Ranger et al. 2009). In contrast, our data suggest that Stat3 is not required for Ras transformation of hepatocytes in the absence of $p19^{ARF}$ (Fig. 2). Furthermore, Stat3 regulates metabolic functions in mitochondria requiring Ser^{727} phosphorylation that supports Ras-dependent malignant transformation (Gough et al. 2009). Our data exclude an involvement of Ser^{727} phospho-Stat3 in the dual role of Stat3 in Ras-transformed hepatocytes since expression of the C-terminally truncated Stat3β either suppressed or promoted tumor growth dependent on $p19^{ARF}$ expression similar to gain-of-function studies using full-length Stat3α (Fig. 1 and Fig. 3B-D).

U-Stat3 harboring the Y705F mutation abrogated tumor suppression and even enhanced tumor formation (Fig. 1), probably driven by expression of a gene set specific for U-Stat3 and its putative interaction partners. Since $p14^{ARF}$/$p19^{ARF}$ is known to interact with a multitude of proteins from different functional classes (Pollice et al. 2008), it is conceivable that a putative factor, designated ARF-X, is involved in the U-Stat3 driven transcriptional control as hypothesized in Fig. 7. The occupation of ARF-X by $p14^{ARF}$/$p19^{ARF}$ could be responsible for the different outcome in the presence of $p14^{ARF}$/$p19^{ARF}$ (Fig. 1 versus Fig. 3B-D). Jak activity, which might be crucially involved in pY-Stat3 activation of HCC cells (Xie et al. 2009), is not altered by $p14^{ARF}$ in human HCC cells *in vitro* (Fig. 6). However, pY-Stat3 is affected in tumors generated by $p14^{ARF}$ knocked-down Hep3B cells in order to overcome tumor-suppressive actions (Fig. 5A, B). Presumably, the *in vivo* environment including tumor-stroma interactions allows the tumor to act distinctive from malignant cells *in vitro*. In this scenario, the identification of ARF-X is the matter of future experiments with highest priority.

The activation of Stat3 occurring in the majority of HCC patients suggests a critical role in liver cancer (Zhang et al. 2010; He and Karin 2011). Stat3 is considered as a potential target for therapeutic intervention, since Stat3 inhibition represses experimental tumors but shows little side effects (Germain and Frank 2007). We provide first evidence that $p14^{ARF}$ determines whether Stat3 acts pro- or anti-oncogenic in HCC cells. The link of Stat3 with $p14^{ARF}$ might be of prognostic value for HCC therapy. Treatment of pY-Stat3-positive HCC

patients showing loss of $p14^{ARF}$ with Stat3 inhibitors could have adverse effects on cancer progression, thus opening new aspects for individualized medicine.

4.7 References

Amicone, L., F. M. Spagnoli, G. Spath, S. Giordano, C. Tommasini, S. Bernardini, V. De Luca, C. Della Rocca, M. C. Weiss, P. M. Comoglio and M. Tripodi (1997). "Transgenic expression in the liver of truncated Met blocks apoptosis and permits immortalization of hepatocytes." EMBO J **16**(3): 495-503.

Anzola, M., N. Cuevas, M. Lopez-Martinez, A. Saiz, J. J. Burgos and M. Martinez de Pancorboa (2004). "P14ARF gene alterations in human hepatocellular carcinoma." Eur J Gastroenterol Hepatol **16**(1): 19-26.

Bromberg, J. F., M. H. Wrzeszczynska, G. Devgan, Y. Zhao, R. G. Pestell, C. Albanese and J. E. Darnell, Jr. (1999). "Stat3 as an oncogene." Cell **98**(3): 295-303.

Calvisi, D. F., S. Ladu, E. A. Conner, D. Seo, J. T. Hsieh, V. M. Factor and S. S. Thorgeirsson (2011). "Inactivation of Ras GTPase-activating proteins promotes unrestrained activity of wild-type Ras in human liver cancer." J Hepatol **54**(2): 311-319.

de la Iglesia, N., G. Konopka, K. L. Lim, C. L. Nutt, J. F. Bromberg, D. A. Frank, P. S. Mischel, D. N. Louis and A. Bonni (2008). "Deregulation of a STAT3-interleukin 8 signaling pathway promotes human glioblastoma cell proliferation and invasiveness." J Neurosci **28**(23): 5870-5878.

de la Iglesia, N., G. Konopka, S. V. Puram, J. A. Chan, R. M. Bachoo, M. J. You, D. E. Levy, R. A. Depinho and A. Bonni (2008). "Identification of a PTEN-regulated STAT3 brain tumor suppressor pathway." Genes Dev **22**(4): 449-462.

Dewilde, S., A. Vercelli, R. Chiarle and V. Poli (2008). "Of alphas and betas: distinct and overlapping functions of STAT3 isoforms." Front Biosci **13**: 6501-6514.

Ecker, A., O. Simma, A. Hoelbl, L. Kenner, H. Beug, R. Moriggl and V. Sexl (2009). "The dark and the bright side of Stat3: proto-oncogene and tumor-suppressor." Front Biosci **14**: 2944-2958.

Fischer, A. N., E. Fuchs, M. Mikula, H. Huber, H. Beug and W. Mikulits (2007). "PDGF essentially links TGF-beta signaling to nuclear beta-catenin accumulation in hepatocellular carcinoma progression." Oncogene **26**(23): 3395-3405.

Fuchs, B. C., T. Fujii, J. D. Dorfman, J. M. Goodwin, A. X. Zhu, M. Lanuti and K. K. Tanabe (2008). "Epithelial-to-mesenchymal transition and integrin-linked kinase mediate sensitivity to epidermal growth factor receptor inhibition in human hepatoma cells." Cancer Res **68**(7): 2391-2399.

Germain, D. and D. A. Frank (2007). "Targeting the cytoplasmic and nuclear functions of signal transducers and activators of transcription 3 for cancer therapy." Clin Cancer Res **13**(19): 5665-5669.

Gotzmann, J., H. Huber, C. Thallinger, M. Wolschek, B. Jansen, R. Schulte-Hermann, H. Beug and W. Mikulits (2002). "Hepatocytes convert to a fibroblastoid phenotype through the cooperation of TGF-beta1 and Ha-Ras: steps towards invasiveness." J Cell Sci **115**(Pt 6): 1189-1202.

Gough, D. J., A. Corlett, K. Schlessinger, J. Wegrzyn, A. C. Larner and D. E. Levy (2009). "Mitochondrial STAT3 supports Ras-dependent oncogenic transformation." Science **324**(5935): 1713-1716.

He, G. and M. Karin (2011). "NF-kappaB and STAT3 - key players in liver inflammation and cancer." Cell Res **21**(1): 159-168.

Kamijo, T., F. Zindy, M. F. Roussel, D. E. Quelle, J. R. Downing, R. A. Ashmun, G. Grosveld and C. J. Sherr (1997). "Tumor suppression at the mouse INK4a locus mediated by the alternative reading frame product p19ARF." Cell **91**(5): 649-659.

Kang, M. S., H. J. Lee, J. H. Lee, J. L. Ku, K. P. Lee, M. J. Kelley, Y. J. Won, S. T. Kim and J. G. Park (1996). "Mutation of p53 gene in hepatocellular carcinoma cell lines with HBX DNA." Int J Cancer **67**(6): 898-902.

Lau, C. K., Z. F. Yang, S. P. Lam, C. T. Lam, P. Ngai, K. H. Tam, R. T. Poon and S. T. Fan (2007). "Inhibition of Stat3 activity by YC-1 enhances chemo-sensitivity in hepatocellular carcinoma." Cancer Biol Ther **6**(12): 1900-1907.

Levy, D. E. and G. Inghirami (2006). "STAT3: a multifaceted oncogene." Proc Natl Acad Sci U S A **103**(27): 10151-10152.

Levy, D. E. and C. K. Lee (2002). "What does Stat3 do?" J Clin Invest **109**(9): 1143-1148.

Li, W. C., S. L. Ye, R. X. Sun, Y. K. Liu, Z. Y. Tang, Y. Kim, J. G. Karras and H. Zhang (2006). "Inhibition of growth and metastasis of human hepatocellular carcinoma by antisense oligonucleotide targeting signal transducer and activator of transcription 3." Clin Cancer Res **12**(23): 7140-7148.

Lin, L., R. Amin, G. I. Gallicano, E. Glasgow, W. Jogunoori, J. M. Jessup, M. Zasloff, J. L. Marshall, K. Shetty, L. Johnson, L. Mishra and A. R. He (2009). "The STAT3 inhibitor NSC 74859 is effective in hepatocellular cancers with disrupted TGF-beta signaling." Oncogene **28**(7): 961-972.

Lin, Y., C. Y. Shi, B. Li, B. H. Soo, S. Mohammed-Ali, A. Wee, C. J. Oon, P. O. Mack and S. H. Chan (1996). "Tumour suppressor p53 and Rb genes in human hepatocellular carcinoma." Ann Acad Med Singapore **25**(1): 22-30.

Mair, M., G. Zollner, D. Schneller, M. Musteanu, P. Fickert, J. Gumhold, C. Schuster, A. Fuchsbichler, M. Bilban, S. Tauber, H. Esterbauer, L. Kenner, V. Poli, L. Blaas, J. W. Kornfeld, E. Casanova, W. Mikulits, M. Trauner and R. Eferl (2010). "Signal transducer and activator of transcription 3 protects from liver injury and fibrosis in a mouse model of sclerosing cholangitis." Gastroenterology **138**(7): 2499-2508.

Mikula, M., E. Fuchs, H. Huber, H. Beug, R. Schulte-Hermann and W. Mikulits (2004). "Immortalized p19ARF null hepatocytes restore liver injury and generate hepatic progenitors after transplantation." Hepatology **39**(3): 628-634.

Musteanu, M., L. Blaas, M. Mair, M. Schlederer, M. Bilban, S. Tauber, H. Esterbauer, M. Mueller, E. Casanova, L. Kenner, V. Poli and R. Eferl (2010). "Stat3 is a negative regulator of intestinal tumor progression in Apc(Min) mice." Gastroenterology **138**(3): 1003-1011 e1001-1005.

Paulitschke, V., N. Schicher, T. Szekeres, W. Jager, L. Elbling, A. B. Riemer, O. Scheiner, G. Trimurtulu, S. Venkateswarlu, M. Mikula, A. Swoboda, E. Fiebiger, C. Gerner, H. Pehamberger and R. Kunstfeld (2010). "3,3',4,4',5,5'-hexahydroxystilbene impairs melanoma progression in a metastatic mouse model." J Invest Dermatol **130**(6): 1668-1679.

Pollice, A., M. Vivo and G. La Mantia (2008). "The promiscuity of ARF interactions with the proteasome." FEBS Lett **582**(23-24): 3257-3262.

Ranger, J. J., D. E. Levy, S. Shahalizadeh, M. Hallett and W. J. Muller (2009). "Identification of a Stat3-dependent transcription regulatory network involved in metastatic progression." Cancer Res **69**(17): 6823-6830.

Sherr, C. J. (2001). "The INK4a/ARF network in tumour suppression." Nat Rev Mol Cell Biol **2**(10): 731-737.

Sherr, C. J. (2006). "Divorcing ARF and p53: an unsettled case." Nat Rev Cancer **6**(9): 663-673.

Tannapfel, A., C. Busse, L. Weinans, M. Benicke, A. Katalinic, F. Geissler, J. Hauss and C. Wittekind (2001). "INK4a-ARF alterations and p53 mutations in hepatocellular carcinomas." Oncogene **20**(48): 7104-7109.

Taub, R. (2004). "Liver regeneration: from myth to mechanism." Nat Rev Mol Cell Biol **5**(10): 836-847.

Xie, H. J., H. J. Bae, J. H. Noh, J. W. Eun, J. K. Kim, K. H. Jung, J. C. Ryu, Y. M. Ahn, S. Y. Kim, S. H. Lee, N. J. Yoo, J. Y. Lee, W. S. Park and S. W. Nam (2009). "Mutational analysis of JAK1 gene in human hepatocellular carcinoma." Neoplasma **56**(2): 136-140.

Yang, J. and G. R. Stark (2008). "Roles of unphosphorylated STATs in signaling." Cell Res **18**(4): 443-451.

Yang, S. F., S. N. Wang, C. F. Wu, Y. T. Yeh, C. Y. Chai, S. C. Chunag, M. C. Sheen and K. T. Lee (2007). "Altered p-STAT3 (tyr705) expression is associated with histological grading and intratumour microvessel density in hepatocellular carcinoma." J Clin Pathol **60**(6): 642-648.

Yip-Schneider, M. T., P. J. Klein, S. C. Wentz, A. Zeni, A. Menze and C. M. Schmidt (2009). "Resistance to mitogen-activated protein kinase kinase (MEK) inhibitors correlates with up-regulation of the MEK/extracellular signal-regulated kinase pathway in hepatocellular carcinoma cells." J Pharmacol Exp Ther **329**(3): 1063-1070.

Yu, H. and R. Jove (2004). "The STATs of cancer--new molecular targets come of age." Nat Rev Cancer **4**(2): 97-105.

Yu, H., M. Kortylewski and D. Pardoll (2007). "Crosstalk between cancer and immune cells: role of STAT3 in the tumour microenvironment." Nat Rev Immunol **7**(1): 41-51.

Zender, L., A. Villanueva, V. Tovar, D. Sia, D. Y. Chiang and J. M. Llovet (2010). "Cancer gene discovery in hepatocellular carcinoma." J Hepatol **52**(6): 921-929.

Zhang, C. H., G. L. Xu, W. D. Jia, J. S. Li, J. L. Ma, W. H. Ren, Y. S. Ge, J. H. Yu, W. B. Liu and W. Wang (2010). "Activation of STAT3 Signal Pathway Correlates with Twist and E-Cadherin Expression in Hepatocellular Carcinoma and Their Clinical Significance." J Surg Res: [Epub ahead of print].

4.8 Figures

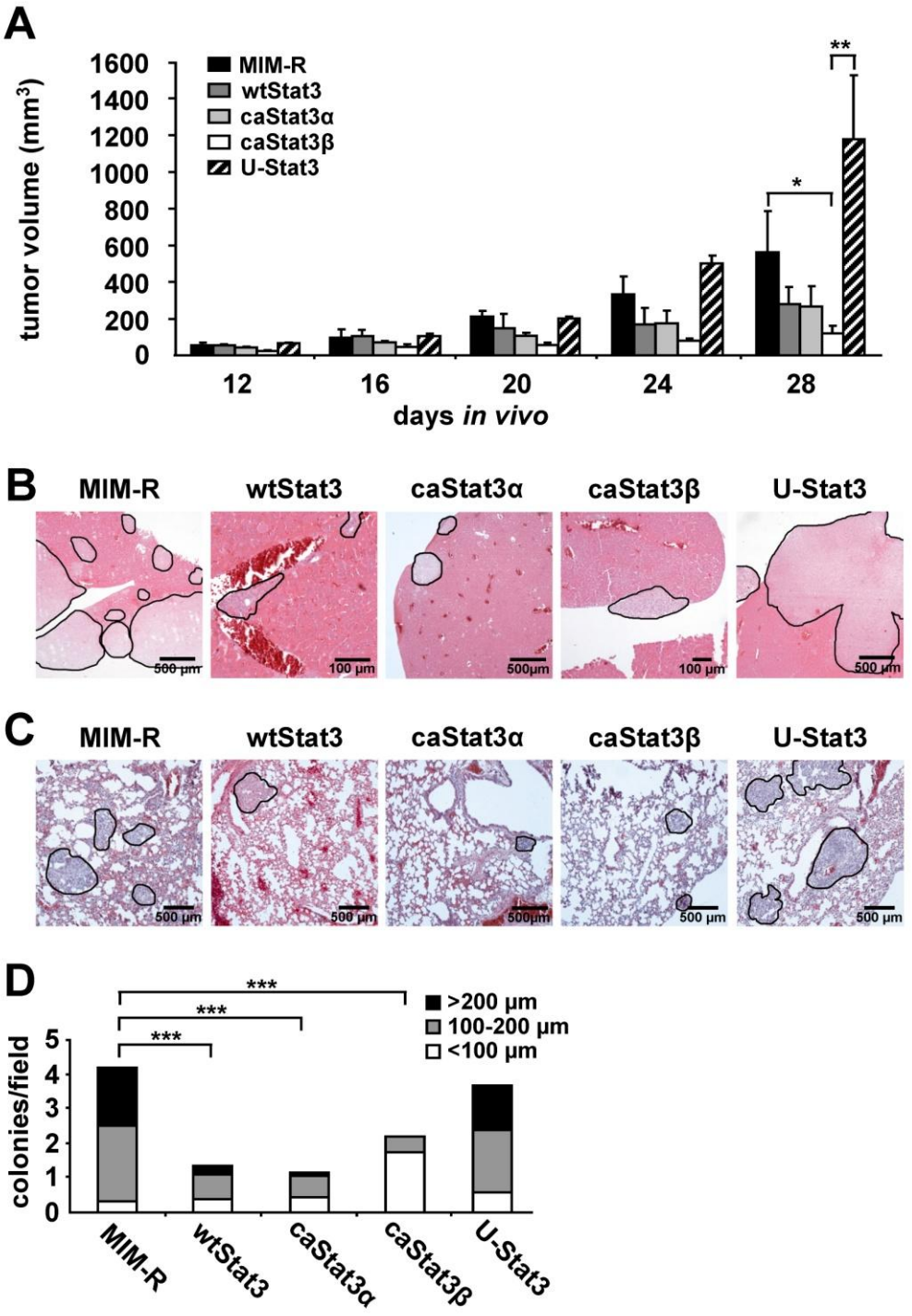

Fig. 1. Expression of caStat3 in Ras-transformed p19$^{ARF-/-}$ hepatocytes leads to reduced tumor formation and metastatic colonization. (A) Tumor volumes after subcutaneous injection into SCID mice. (B, C) Cells were either orthotopically transplanted or injected into tail vein, respectively. Resulting liver tumors and lung metastases were stained with H&E. (D) Quantification of metastatic colonies according to size after tail vein injection. Statistical significance is indicated with asterisks (*, p<0,05; **, p<0,01; ***, p<0,005). Error bars depict SD from at least three individual experiments.

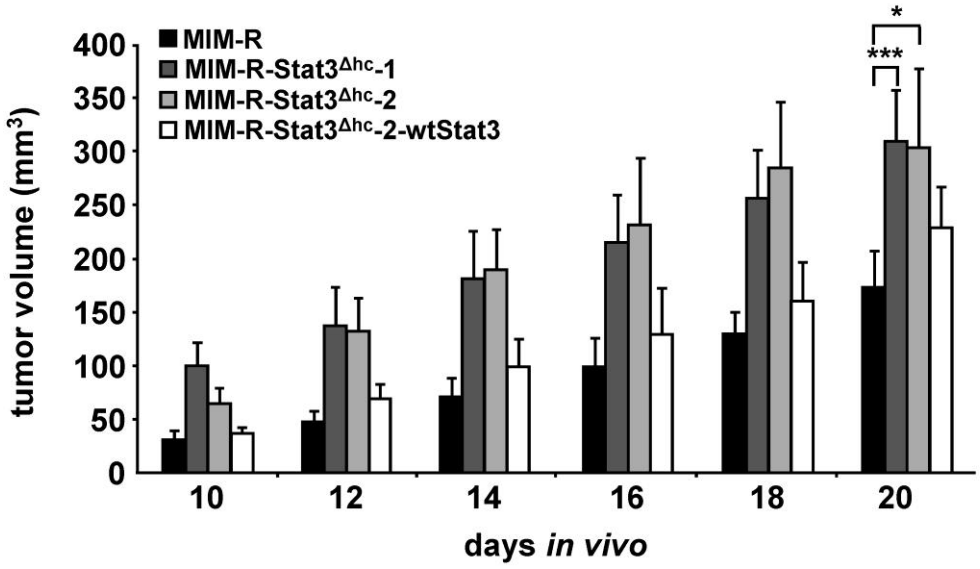

Fig. 2. Ras-transformed Stat3$^{\Delta hc}$ hepatocytes show increased tumor formation. Tumor volumes after subcutaneous injection of MIM-R, MIM-R Stat3$^{\Delta hc}$-1, MIM-R Stat3$^{\Delta hc}$-2 and MIM-R Stat3$^{\Delta hc}$-2-wtStat3 cells into SCID mice. Statistical significance is indicated with asterisks (*, $p<0,05$; ***, $p<0,005$). Error bars depict SD from at least five individual experiments.

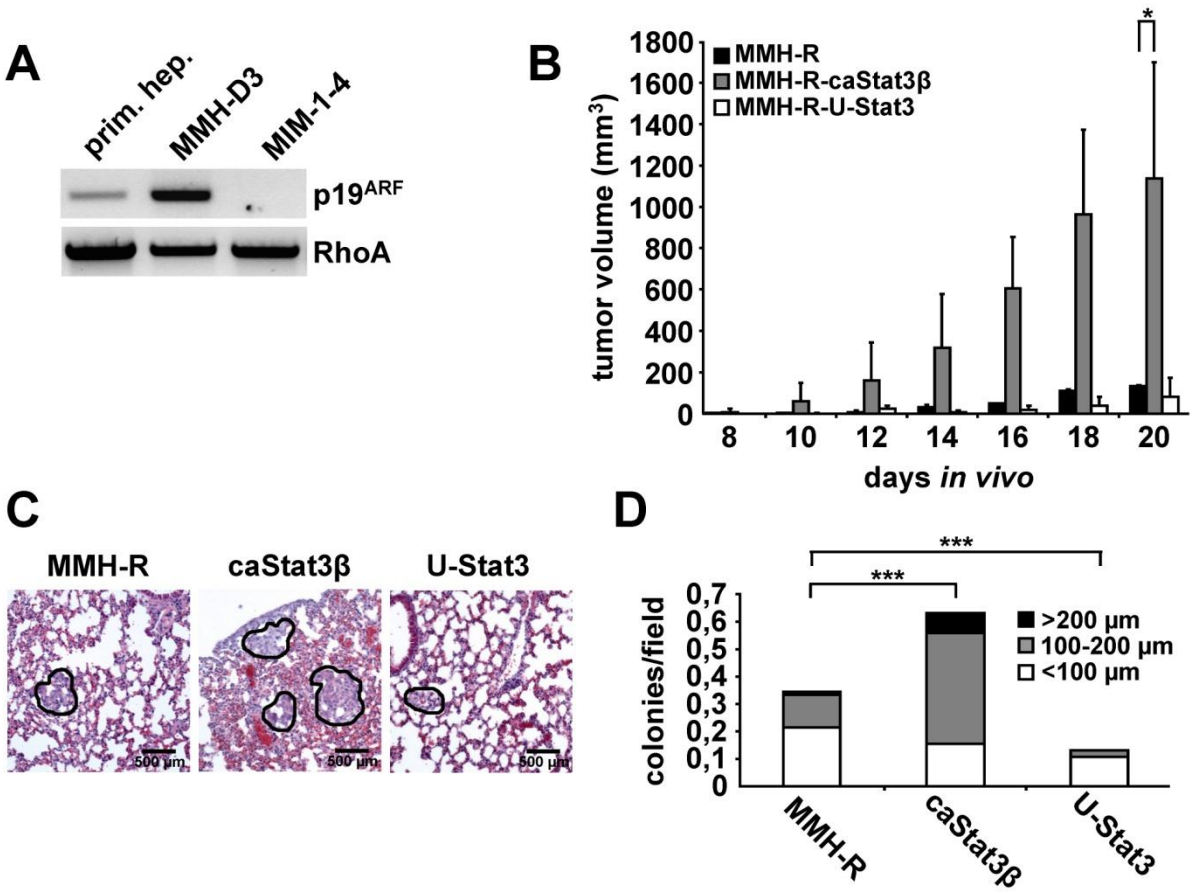

Fig. 3. Expression of caStat3 is pro-oncogenic in $p19^{ARF}$-expressing hepatocytes transformed with oncogenic Ras (MMH-R). (A) Expression of $p19^{ARF}$ in primary hepatocytes (prim. hep.), MMH-D3 and MIM-1-4 hepatocytes was analyzed by linear semi-quantitative RT-PCR. RhoA is shown as loading control. (B) Tumor formation after subcutaneous injection of MMH-R and MMH-R-Stat3 mutants into SCID mice. (C) H&E stainings of lung sections after tail vein injection of cells. (D) Quantification of metastatic colonies according to size. Statistical significance is indicated with asterisks (*, $p<0,05$; **, $p<0,01$; ***, $p<0,005$). Error bars depict SD from at least three individual experiments.

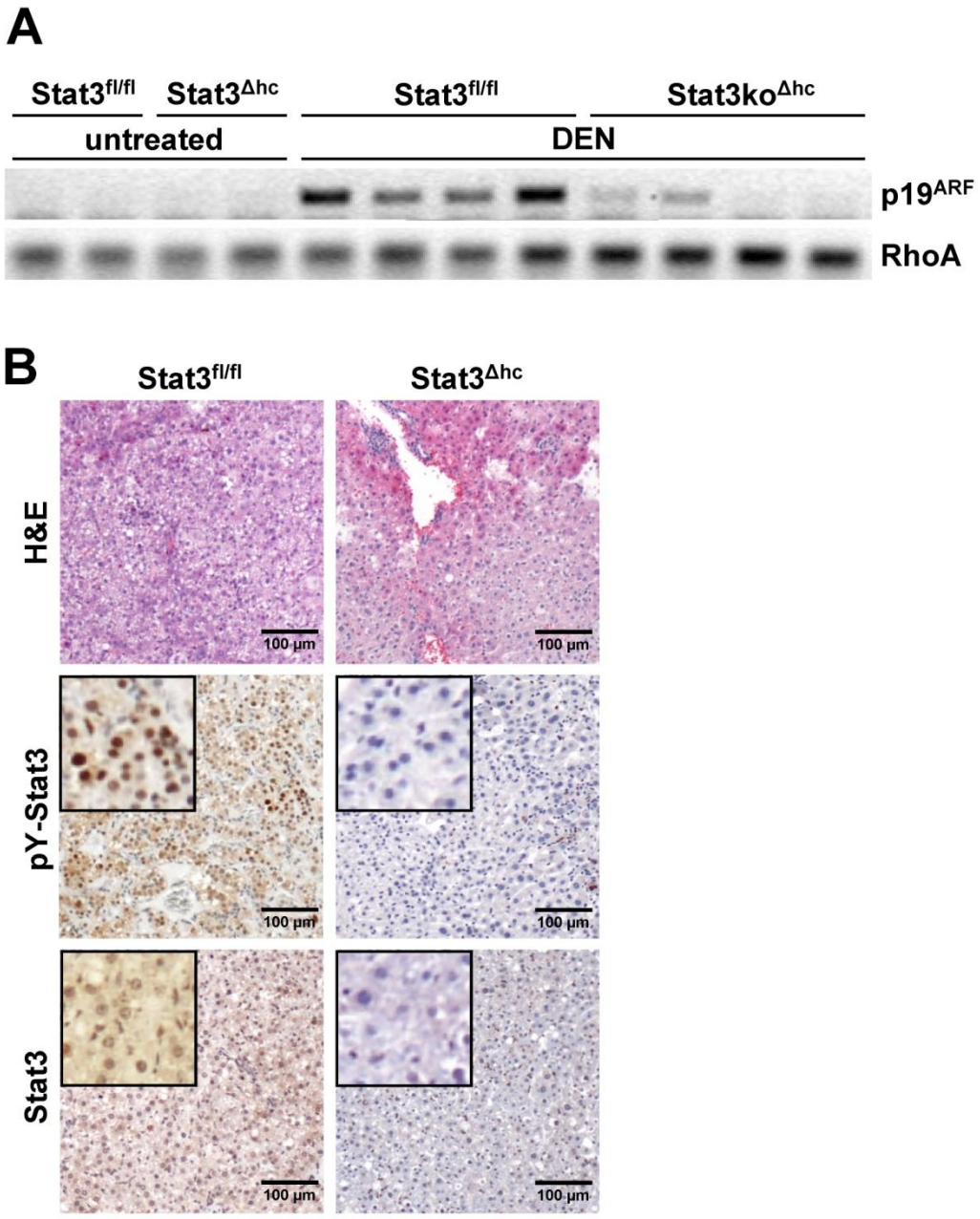

Fig. 4. Upregulation of $p19^{ARF}$ in DEN-induced HCC of $Stat3^{fl/fl}$ mice. (A) $p19^{ARF}$ expression analyzed by linear semi-quantitative RT-PCR in untreated liver samples as well as in DEN-induced tumors of $Stat3^{fl/fl}$ and $Stat3^{\Delta hc}$ mice. The constitutive expression of RhoA is shown as loading control. (B) Sections of DEN-induced liver tumors were stained with H&E or with anti-Stat3 or anti-phospho-Stat3 antibodies. Insets show magnification of tumor sections.

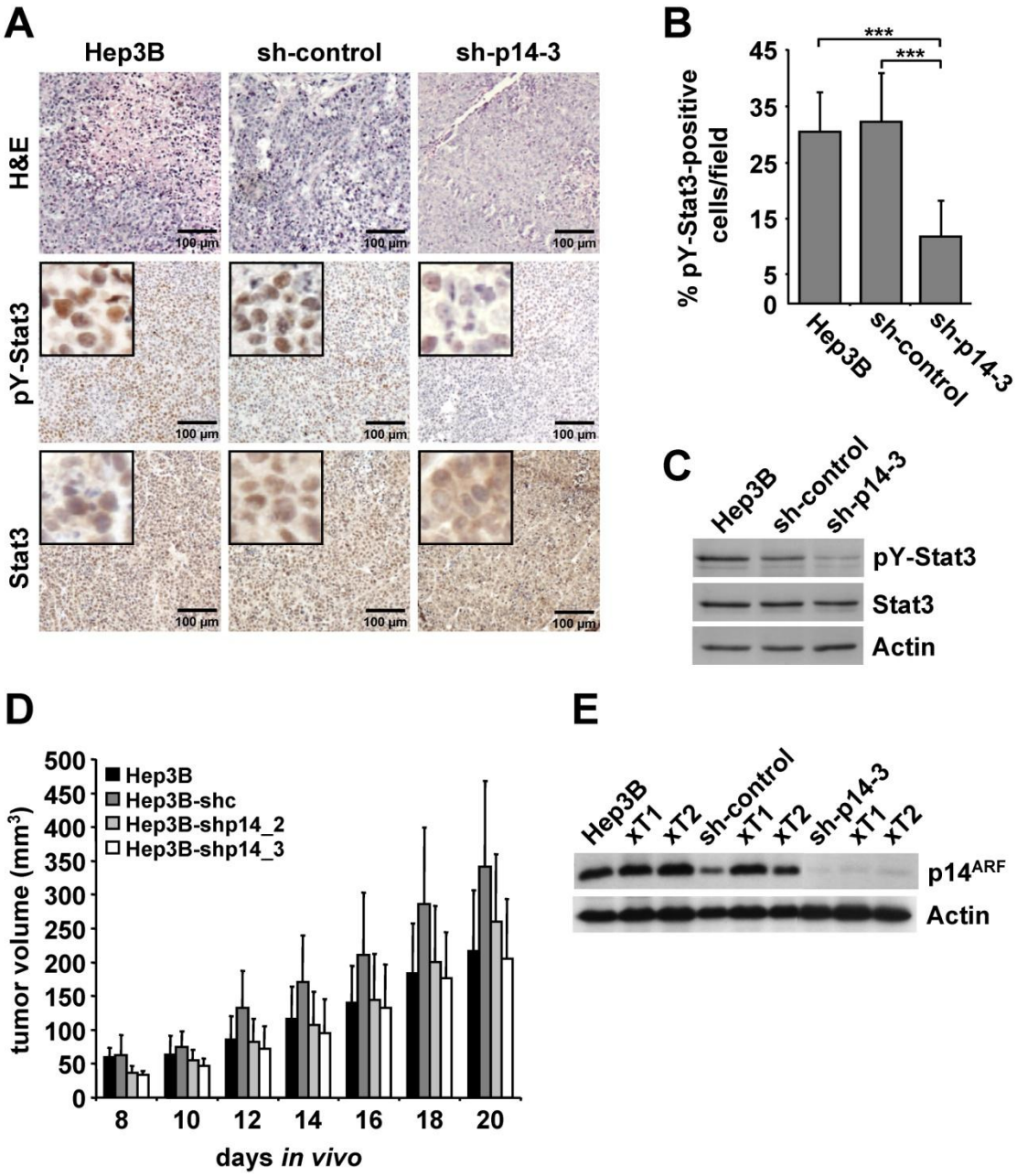

Fig. 5. Knock-down of $p14^{ARF}$ in Hep3B-derived tumors suppresses Stat3 phosphorylation. (A) Sections from tumors generated after injection of Hep3B, sh-control and sh-p14-3 were stained with H&E or with anti-Stat3 or anti-phospho-Stat3 antibodies. Insets show magnification of tumor sections. (B) Quantitative evaluation of pY-Stat3-positive nuclei. Statistical significance is indicated with asterisks (***, p<0,005). Error bars depict SD from at least five xenografts. (C) Immunoblotting analyzing pY-Stat3 levels in tumor tissues. (D) Tumors generated by subcutaneous injection of Hep3B cells expressing either control shRNA (sh-control) or shRNA against $p14^{ARF}$ (sh-p14-2, sh-p14-3). (E) Expression of $p14^{ARF}$ in Hep3B cells and those harboring shRNAs after re-cultivation from two tumors (xT1, xT2) was determined by immunoblot analysis. Actin was used as loading control.

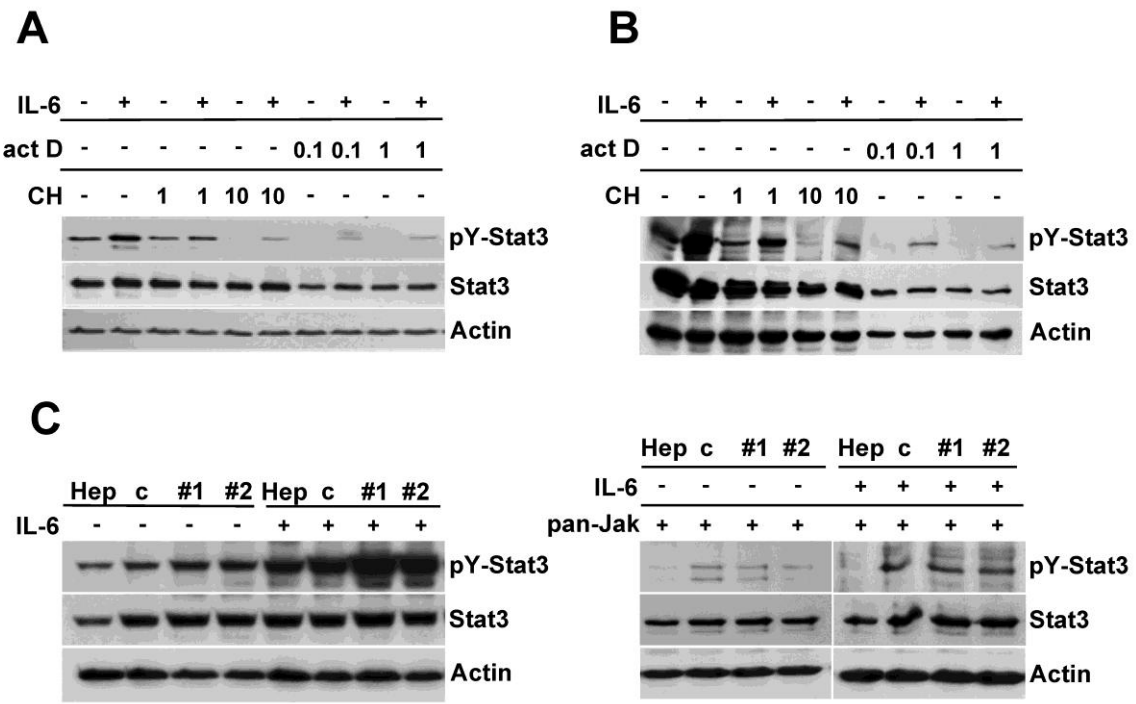

Fig. 6. *De novo* RNA and protein synthesis as well as Jak activity are required for pY-Stat3 activation independently of $p14^{ARF}$. Inhibition of transcription, translation or Jak activity diminishes IL-6 induced pY-Stat3. (A) Hep3B and (B) sh-p14-3 cells were treated with actinomycin D (act D) or cycloheximide (CH) for 24 hours at the indicated concentrations (µg/ml). 20 ng/ml IL-6 were added 20 minutes before harvesting of cells. (C) Hep3B cells, sh-control (c), sh-p14-2 (#1) and sh-p14-3 (#2) were treated with IL-6 (20 ng/ml) alone for 20 minutes or pretreated with a pan-Jak inhibitor (Jak-Inhibitor I, 10 ng/ml) for 24 hours. Protein extracts were probed with anti-phospho-Stat3 and anti-Stat3 antibodies. Actin was used as loading control.

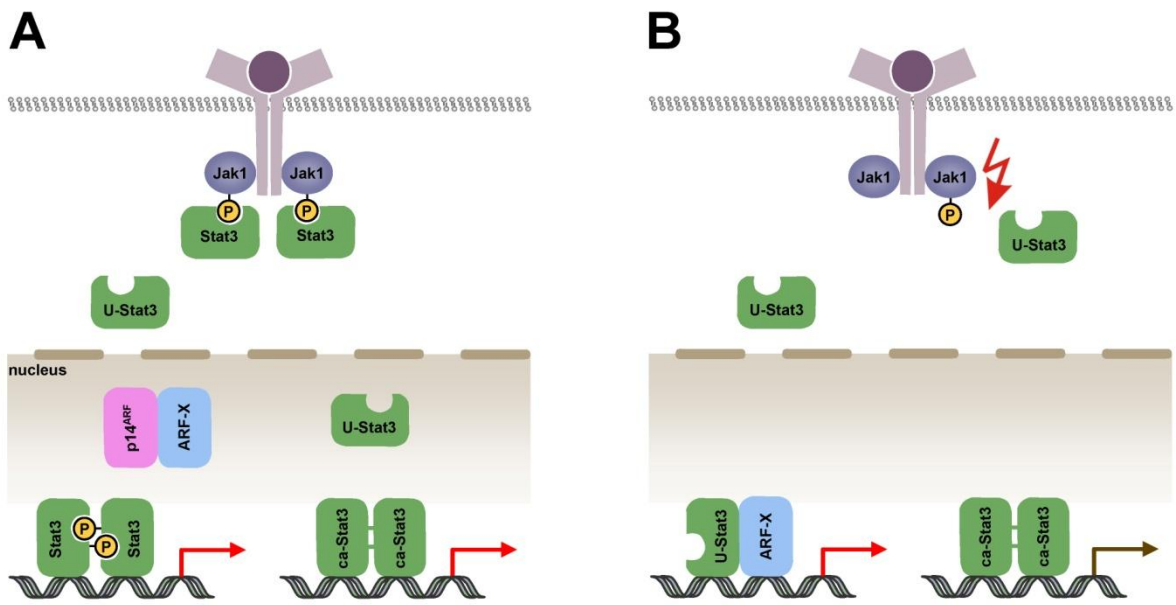

Fig. 7. A model depicting (anti)-oncogenic Stat3 actions dependent on $p14^{ARF}$ in HCC cells. (A) In the presence of $p14^{ARF}$, active Stat3 either caused by Jak phosphorylation or by constitutive activation (ca) via dimerization modulates target genes and promotes tumorigenesis (red arrows). $p14^{ARF}$ sequesters an unknown factor termed ARF-X. (B) In the absence of $p14^{ARF}$, U-Stat3 interacts with ARF-X to drive an oncogenic program (red arrow). U-Stat3 is generated by suppression of Jak-mediated Stat3 activation. CaStat3 causes tumor suppression (brown-colored arrow) by modulating an alternative set of Stat3-specific target genes.

4.9 Supplemetary data

4.9.1 Supporting Figures

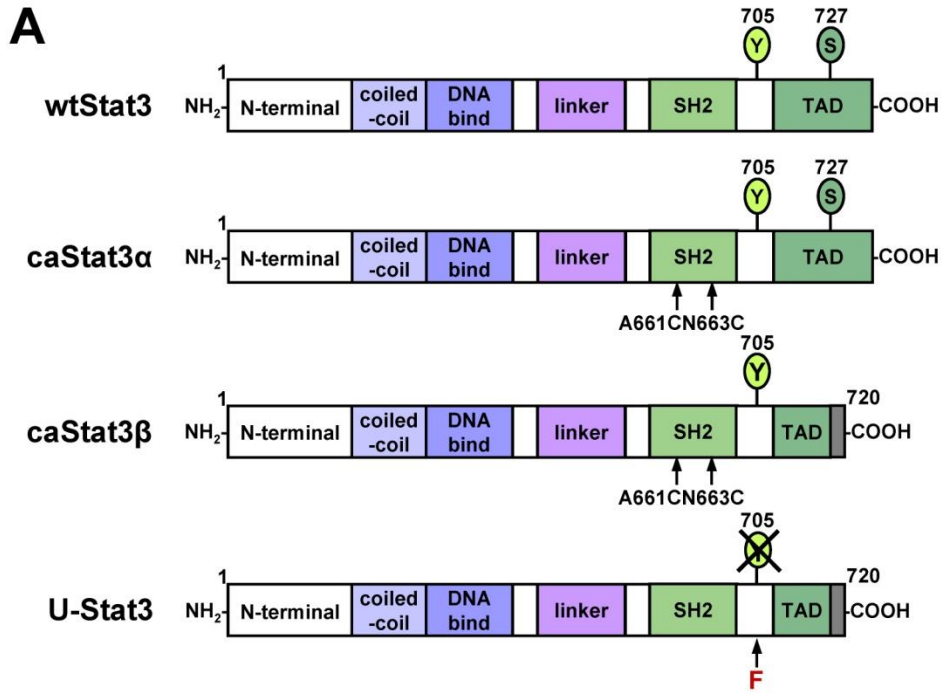

Supporting Fig. 1. Expression of constitutively active (ca) Stat3 versions and U-Stat3 in Ras-transformed hepatocytes. (A) Schematic representation of wtStat3 and Stat3 mutants. Stat3 is composed of the N-terminal domain, the coiled-coil, DNA-binding, linker, Src homology 2 (SH2) and transcriptional activation domain (TAD). (B) Overexpression of Stat3 as shown by immunoblotting using anti-Stat3 and anti-Actin antibodies. Actin was used as loading control.

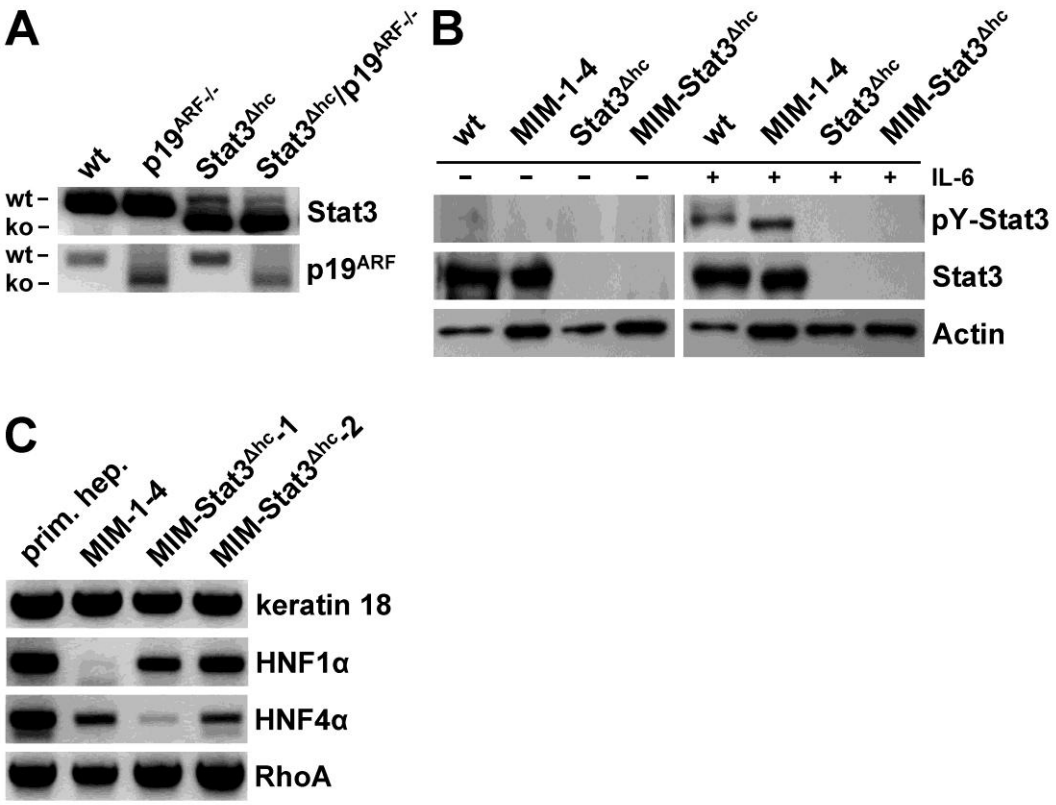

Supporting Fig. 2. Characteristics of Stat3$^{\Delta hc}$/p19$^{ARF-/-}$ hepatocytes. (A) The loss of Stat3 and p19^{ARF} in single and double knocked-out hepatocytes was analyzed by linear semi-quantitative RT-PCR (wt, wild type; ko, knock-out). (B) pY-Stat3 levels were analyzed by immunoblotting after stimulation with IL-6 (20 ng/ml). Actin was used as loading control. (C) Hepatocellular marker expression analyzed by linear semi-quantitative RT-PCR in primary hepatocytes (prim. hep.), parental MIM-1-4 hepatocytes (MIM-1-4) and the two single cell clones MIM-Stat3$^{\Delta hc}$-1 and MIM-Stat3$^{\Delta hc}$-2. The constitutive expression of RhoA is shown as loading control. One representative out of three experiments is shown. HNF, hepatocyte nuclear factor.

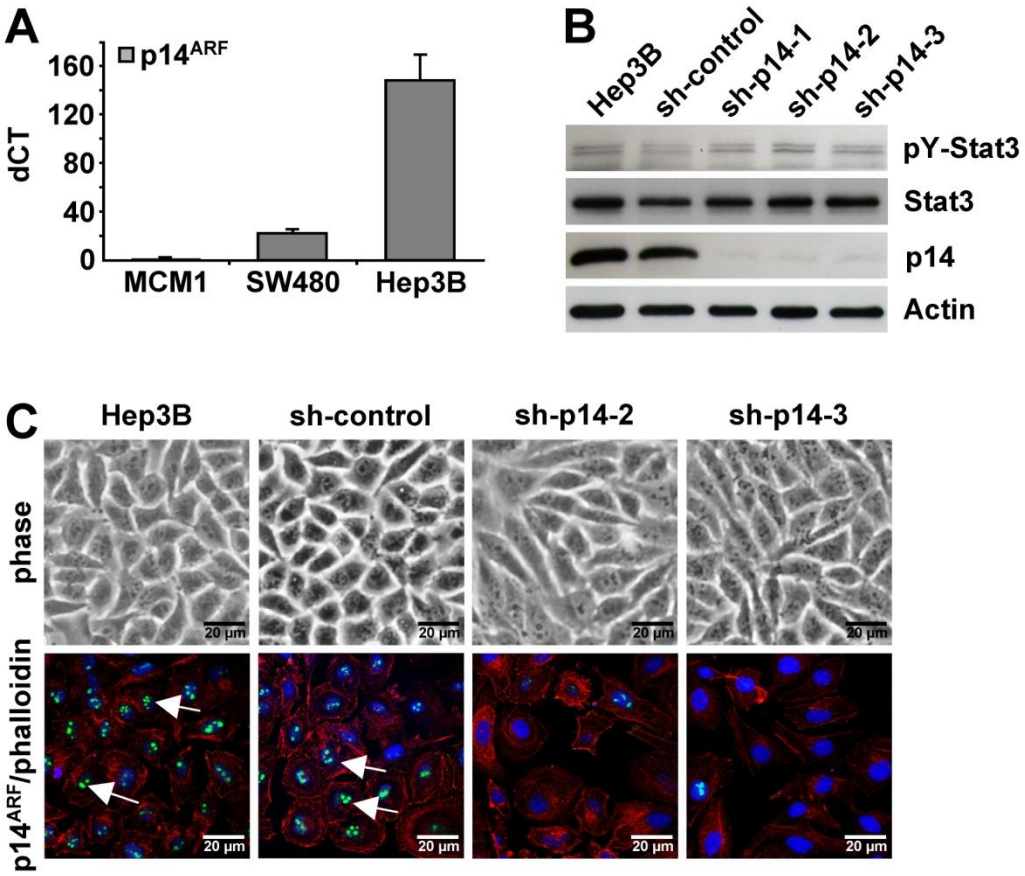

Supporting Fig. 3. Knock-down of $p14^{ARF}$ in human Hep3B cells. (A) Real-time PCR analysis of $p14^{ARF}$ in $p14^{ARF}$-deficient MCM-1, $p14^{ARF}$-positive SW480 and Hep3B cells. (B) Levels of $p14^{ARF}$ and pY-Stat3 in Hep3B cells after expression of either scrambled control shRNA (sh-control) or shRNAs against $p14^{ARF}$ (sh-p14-1, sh-p14-2, sh-p14-3) as determined by immunoblot analysis. Actin was used as loading control. (C) Phase contrast and confocal immunofluorescence images after staining of Hep3B cells and those expressing sh-control or sh-p14 with anti-$p14^{ARF}$ antibody. Red, phalloidin; green, $p14^{ARF}$; blue, DNA. Arrows indicate $p14^{ARF}$ localization in cell nucleoli. Error bars depict SD from at least three individual experiments.

4.9.2 Supporting Material and Methods

Cell culture

Cells were treated with 20 ng/ml interleukin (IL)-6 (R&D Systems, Minneapolis, USA) to activate Stat3. Hep3B cells were treated with Jak-Inhibitor I (pan-Jak; 10 ng/ml, Calbiochem Merck, Darmstadt, Germany) for 24 hours. Actinomycin D and cycloheximide (both Sigma) were used for 24 hours at the indicated concentrations.

Stable knock-down $p14^{ARF}$

For lentiviral-mediated knock-down of $p14^{ARF}$ in human cell lines, shRNA sequences targeting $p14^{ARF}$ (ARF-1: 5'-CCGGGAACATGGTGCGCAGGTTCTTCAAGAGAGAACC-TGCGCACCATGTTCTTTTTT-3'; ARF-2: 5'-CCGGCATGGTGCGCAGGTTCTTGTTCA-AGAGACAAGAACCTGCGCACCATGTTTTTT-3'; Voorhoeve,P.M. and Agami,R. 2003) and scrambled control (5´-CCGGAGGCTGCTTGCACGATCTATTCAAGAGATAGATCG-TGCAAGCACCTTTTT-3´) were cloned into the pLKO.1 lentiviral vector. Lentiviral VSV-G pseudotyped virus was produced as described (Naldini et al. 1996). Hep3B cells were infected by spin infection (800 g, 40 minutes, 32°C) and subsequently selected with 2.0 µg/ml puromycin.

Recovery of tumor cells

To recover tumor cells for cultivation, small pieces of tumor tissue were put on culture plates and attached cells were sub-cultured at a ratio of 1:3 twice a week in RPMI 1640 plus 10% FCS and antibiotics.

Reverse transcription polymerase chain reaction (RT-PCR)

PCR for genotyping of wild-type and deleted Stat3 alleles was performed with primers APRF_11_up, 5´-CACCAACACATGCTATTTGTAGG-3´; APRF_11_do, 5´-CCTGTCTC-TGACAGGCCATC-3´; APRF_14_do, 5´-GCAGCAGAATACTCTACAGCT-3´. Wild-type and $p19^{ARF}$-knockout alleles were detected with primers C018, 5´-AGTACAGCA-GCGGGAGCATGG-3´; C019, 5´-TTGAGGAGGACCGTGAAGCCG-3´; C020, 5´-ACCA-CACTGCTCGACATTGGG-3´.The sequences of the forward and reverse primers for semi-quantitative RT-PCR: hepatocyte nuclear factor (HNF)-1α, 5´-GGTGGCCCAGTAC-ACGCACA-3´ and 5´-GGTGGCATGGCAG-GCTCAGA-3´; HNF-4α, 5´-CCTGGTCGAG-TGGGCCAAGT-3´ and 5´-TGGCAGACC-CTCCGAGAAGC-3´; keratin 18, 5´-AGAG-

CCTGGAAACTGAGAAC-3´ and 5´-AGACTTGGTGGTGACA ACTG-3´; RhoA, 5´-GTGGAATTCGCCTTGCATCTGAGAAGT-3´ and 5´-CACGAATTCAATTAACGCAT-GAGGCT-3´. Primer sequences for quantitative Real-time PCR analysis: $p14^{ARF}$, 5´-TGATGCTACTGAGGAGCCAGC-3´ and 5´-AGGGCCTTTCCTAC CTGGTC-3´; RhoA, 5´-CCATCATCCTGGTTGGGAAT-3´ and 5´-CCATGTACCCAAAA GCGC-3´.

Confocal immunofluorescence microscopy

Cells grown on slides were processed for immunological detection as described(Gotzmann et al. 2002). Anti-$p14^{ARF}$ (Sigma, St Louis, USA) and Phalloidin-TexasRed (Invitrogen, Carlsbad, CA, USA) were used at dilutions of 1:100. Cells were imaged with a TCS-SP confocal microscope (Leica, Heidelberg, Germany).

References

1. Voorhoeve,P.M. and Agami,R. (2003). The tumor-suppressive functions of the human INK4A locus. *Cancer Cell* 4: 311-319.

2. Naldini,L., Blomer,U., Gallay,P., Ory,D., Mulligan,R., and Gage,F.H. (1996). In vivo gene delivery and stable transduction of nondividing cells by a lentiviral vector. *Science* 272: 263-267.

3. Gotzmann J, Huber H, Thallinger C, Wolschek M, Jansen B, Schulte-Hermann R, et al. Hepatocytes convert to a fibroblastoid phenotype through the cooperation of TGF-beta1 and Ha-Ras: steps towards invasiveness. J Cell Sci 2002;115:1189-1202.

5 Results

5.1 Microarray analysis of murine STAT3-deficient HCC cells expressing STAT3 isoforms

Gene expression profiling of cells stably expressing a single isoform of STAT3 (STAT3α and STAT3β) was performed to identify their respective target genes. With this analysis, we expected to gain deeper insights into their particular functions in Ras-transformed HCC progression. Therefore, we employed oncogenic Ras-expressing murine hepatocytes lacking both $p19^{ARF}$ and STAT3 (MIM-R-$STAT3^{\Delta hc}$) to exogenously expressing constitutive active (ca)STAT3α, caSTAT3β or wildtype (wt)STAT3, respectively. Total RNA was isolated and Affymetrix™ whole genome GeneChip analysis was performed. MIM-R-$STAT3^{\Delta hc}$ cells were used as reference. Unfortunately, statistical evaluation revealed no regulation of target genes in neither of the cells under investigation. This finding is in line with a study of Liddle et al. suggesting that stimulation with IL-6 is required prior to analysis of caSTAT3 expression (Liddle et al. 2006). Furthermore, exogenous expression of wtSTAT3 without IL-6 stimulation might be also insufficient for transactivation.

5.2 Murine HCC cells show functional p53 pathway

$p19^{ARF}$ represents an important upstream regulator of the tumor suppressor p53. By antagonizing the ubiquitin ligases MDM2 and ARF-BP1, $p19^{ARF}$ indirectly stabilizes p53 (Ozenne et al. 2010). Alterations of p53, such as homozygous deletion or inactivating mutations could have an impact on the tumorigenic phenotype of cells under investigation. In this respect, we have previously shown that U-STAT3 expression caused enhanced tumor formation in $p19^{ARF-/-}$ hepatocytes, while expression of caSTAT3 produced smaller tumors in these cells. Endogenous expression of $p19^{ARF}$ showed the reversed phenotype (Schneller et al. 2011) .To rule out the fact that the functionality of the p53 pathway governs the outcome of our tumor kinetics, we challenged our murine HCC cells with Etoposide, a DNA breaking agent and known inducer of p53. Western blot analysis showed upregulation of p53 in all cell types (Fig. 12). Importantly, a concomitant up-regulation of $p21^{WAF1}$, a target of p53, was observed. This observation provides evidence for a functional p53 pathway in $p19^{ARF-/-}$ (MIM-R) hepatocytes and those expressing wild-type $p19^{ARF}$ (MMH-R). Therefore, loss or functional alterations of p53 might not influence oncogenic or anti-oncogenic STAT3

functions of Ras-transformed p19^{ARF}-positive (MMH-R) and p19^{ARF}-negative (MIM-R) murine HCC cells.

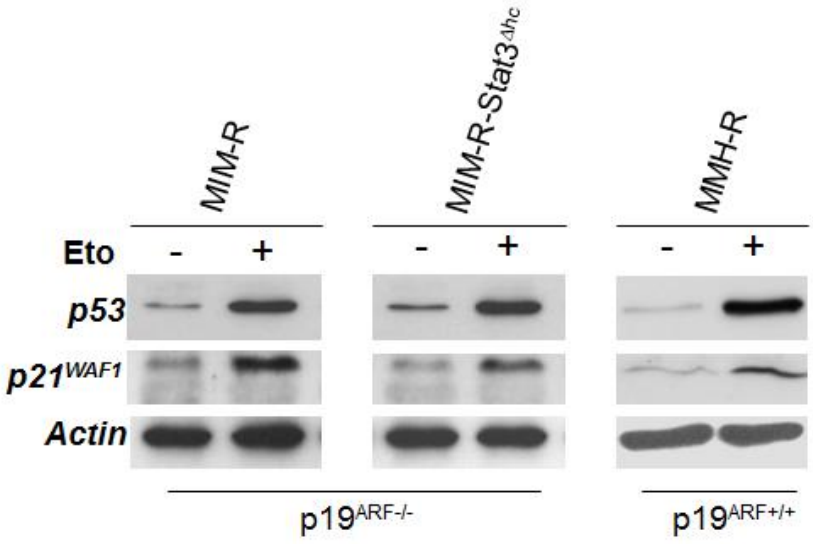

Figure 12. p19^{ARF}-negative (MIM-R) and p19^{ARF}-positive (MMH-R) mouse hepatoma cells show functional p53 activity. Protein extracts of cells that had been treated with Etoposide (Eto, 200 μM; 2.5 hours) were analyzed for p53 and p21^{WAF1} expression. Actin was used as loading control.

5.3 Unphosphorylated STAT3 (U-STAT3) translocates to the nucleus and is transcriptionally active

Schneller et al. suggested nuclear translocation and transcriptional activity of U-STAT3 for oncogenic STAT3 functions in the absence of p19^{ARF}. Thereby, active STAT3 signaling without Tyr^{705} phosphorylation had been stated (Fig. 7; Schneller et al. 2011). To provide evidence for this hypothesis, several experiments have been performed. We focused on STAT3/p19^{ARF} deficient hepatocytes expressing the U-STAT3β-isoform, since they were predominantly employed in the manuscript of Schneller et al. (Schneller et al. 2011) Analysis of MIM-R-STAT3$^{\Delta hc}$-U-STAT3β cells revealed localization of U-STAT3β in both cytoplasmic and nuclear compartments (Fig. 13A, red box). Endogenously expressing STAT3 cells (MIM-Ras) which predominately express STAT3α and non-transfected STAT3/p19^{ARF} deficient hepatocytes (MIM-R-STAT3$^{\Delta hc}$) were used as controls (Fig. 13A, left and middle). Next, a reporter assay using a minimal STAT3 promoter was performed in order to examine the ability of U-STAT3β to show transcriptional transactivation. As shown in Fig. 13B, MIM-R-STAT3$^{\Delta hc}$ cells expressing U-STAT3β exhibit increased luciferase activity. However, no statistical significance has been observed. Cells overexpressing a wild-type construct of STAT3 (MIM-R-STAT3$^{\Delta hc}$-wtSTAT3) did not show elevated levels of reporter activity.

Finally, immunofluorescence staining of MIM-R-STAT3$^{\Delta hc}$ cells expressing U-STAT3α or U-STAT3β indicated localization of the respective U-STAT3 in both cytoplasm and nucleus (Fig. 13C). Altogether, these data demonstrate U-STAT3 as a potent molecule capable for nuclear translocation and transcriptional activity.

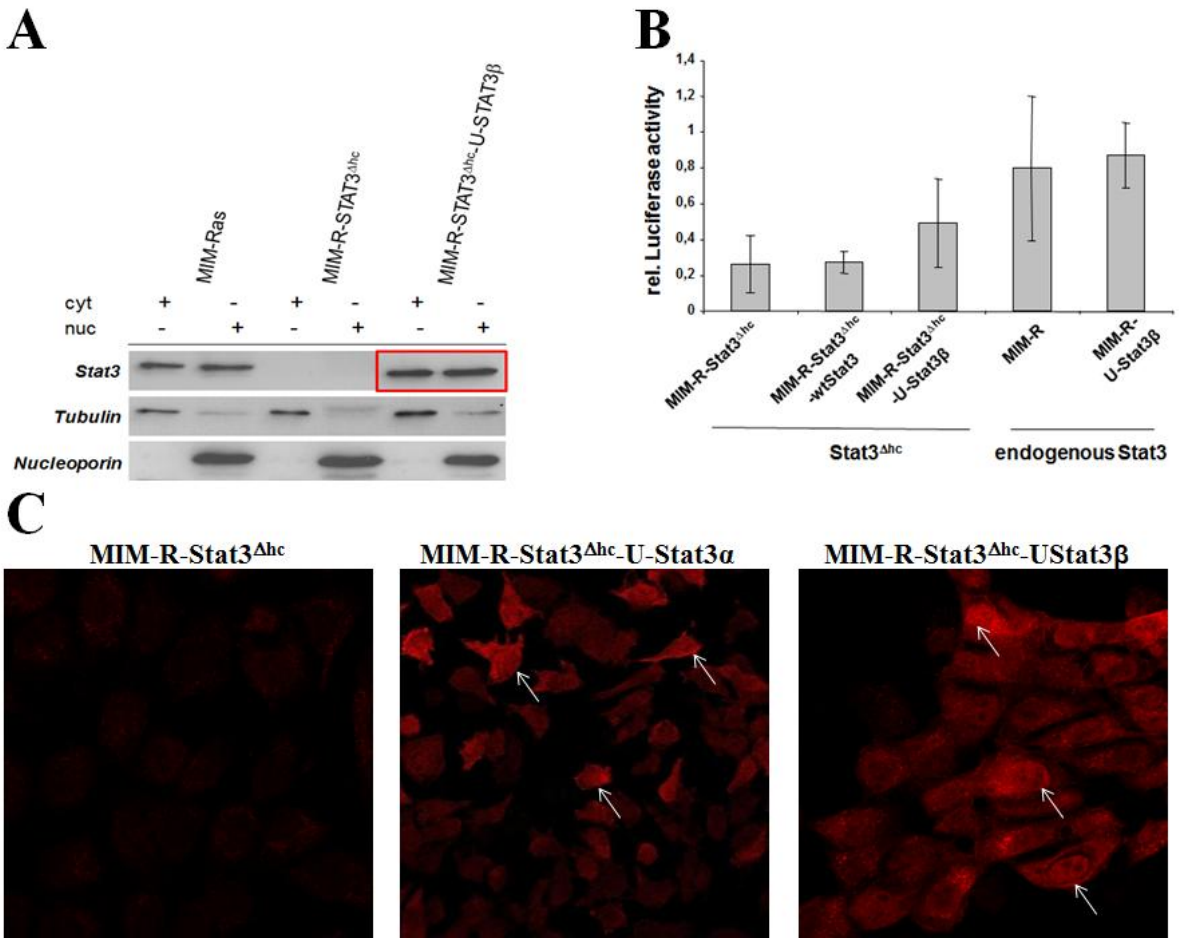

Figure 13. U-STAT3 is localized in the nucleus and is able to transactivate reporter gene expression. (A) Cytoplasmic fraction (cyt) and nuclear fraction (nuc) of MIM-Ras, MIM-R-STAT3$^{\Delta hc}$, and MIM-R-STAT3$^{\Delta hc}$-U-STAT3β cells were analyzed by immunoblotting. Antibodies against tubulin and nucleoporin were used to confirm the integrity of fractionation. (B) STAT3-dependent reporter assay of MIM-R cells in the STAT3$^{\Delta hc}$ background (STAT3$^{\Delta hc}$, STAT3$^{\Delta hc}$-wtSTAT3, -U-STAT3β) and in the endogenous STAT3 background (MIM-R, MIM-R-U-STAT3β). (C) Immunofluorescence analysis staining of MIM-R-U-Stat3α and MIM-R-U-STAT3β cells with STAT3 antibody (red). Representative cytoplasmic and nuclear staining is indicated with arrows. MIM-R-STAT3$^{\Delta hc}$ cells were used as a negative control.

5.4 NFkB translocates to the nucleus irrespective of U-STAT3

Since NFκB has been shown to interact with unphosphorylated STAT3 (Yang et al. 2007), we next investigated the role of NFκB in the nuclear accumulation of U-STAT3. For this purpose, MIM-R-STAT3$^{\Delta hc}$ cells and MIM-R-STAT3$^{\Delta hc}$-U-STAT3β cells were treated with

tumor necrosis factor alpha (TNF-α), a known inducer of NFκB (Pena et al. 2010). First, translocation of NFκB into the nucleus was analyzed. As shown in Fig. 14A by immunofluorescence staining, a nuclear localization of NFκB was observed upon TNF-α treatment. In the next step, we investigated a possible interaction of U-STAT3 and NFκB in more detail, employing cellular fractionation into cytoplasmic and nuclear compartments. Immunoblotting of the respective fractions of MIM-R-STAT3$^{\Delta hc}$ and MIM-R-STAT3$^{\Delta hc}$-U-STAT3β cells revealed an increased signal of NFκB in the nuclear fraction of both cell lines (Fig. 14B, bottom). Remarkably, the levels of U-STAT3 in MIM-R-STAT3$^{\Delta hc}$-U-STAT3β cells remained constant with or without TNF-α treatment in each fraction (Fig.14B, top right). In conclusion, these results indicate that U-STAT3 and NFκB act in an independent manner.

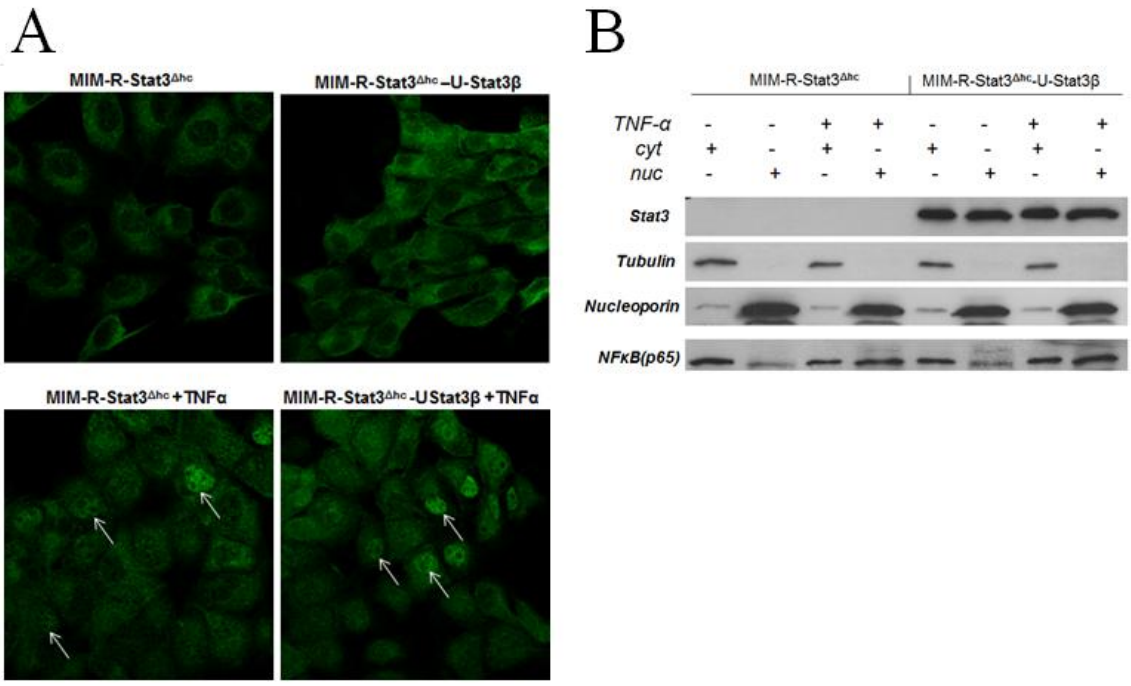

Figure 14. Nuclear localization of NFκB occurs independent of U-STAT3. (A) Immunofluorescence staining of NFκB (green) in MIM-R-STAT3$^{\Delta hc}$ and MIM-R-STAT3$^{\Delta hc}$-U-STAT3β cells, either untreated (top) or treated with 20 ng/ml TNF-α for 30 minutes (bottom); (B) Western blot analysis of MIM-R-STAT3$^{\Delta hc}$ and MIM-R-STAT3$^{\Delta hc}$-U-STAT3β cells after nuclear and cytoplasmic fractionation. Representative nuclei are indicated with arrows. Antibodies against tubulin and nucleoporin were used as cytoplasmic and nuclear markers, respectively.

5.5 Suppression of STAT3 phosphorylation in p14^{ARF} knockdown Hep3B cells occurs early in tumor development

We have shown that the level of pY705-STAT3 was significantly decreased in subcutaneous tumors derived from Hep3B cells bearing a p14^{ARF} knockdown (Fig. 5A-C; Schneller et al.

2011). We described this phenomenon as a tumor-mediated action to circumvent an anti-oncogenic effect of pY705-STAT3. To find out at which point the down-regulation took place in tumor development, we performed a tumor kinetic experiment exploring early time points of tumor growth. A tumor weight of approximately 100 mg was determined as "early". For this reason, parental Hep3B, Hep3B-sh-control (bearing a scrambled shRNA) and Hep3B cells carrying two combinations of shRNAs against $p14^{ARF}$ (sh-p14-2, sh-p14-3) were injected subcutaneously into SCID mice. By measuring and subsequent calculation of the tumor volume, the weight was estimated and the tumors were employed for immunohistochemical processing. Representative pictures are depicted in Fig. 15A. After staining with pY-STAT3 antibody, positive cells were counted. As shown in Fig. 15B, the percentage of positive nuclei in Hep3B cells with shRNAs targeted against $p14^{ARF}$ was clearly reduced as compared to parental and Hep3B-sh-control cells, respectively. These results demonstrate an early interference on the canonical STAT3 activation in $p14^{ARF}$ depleted hepatoma cells.

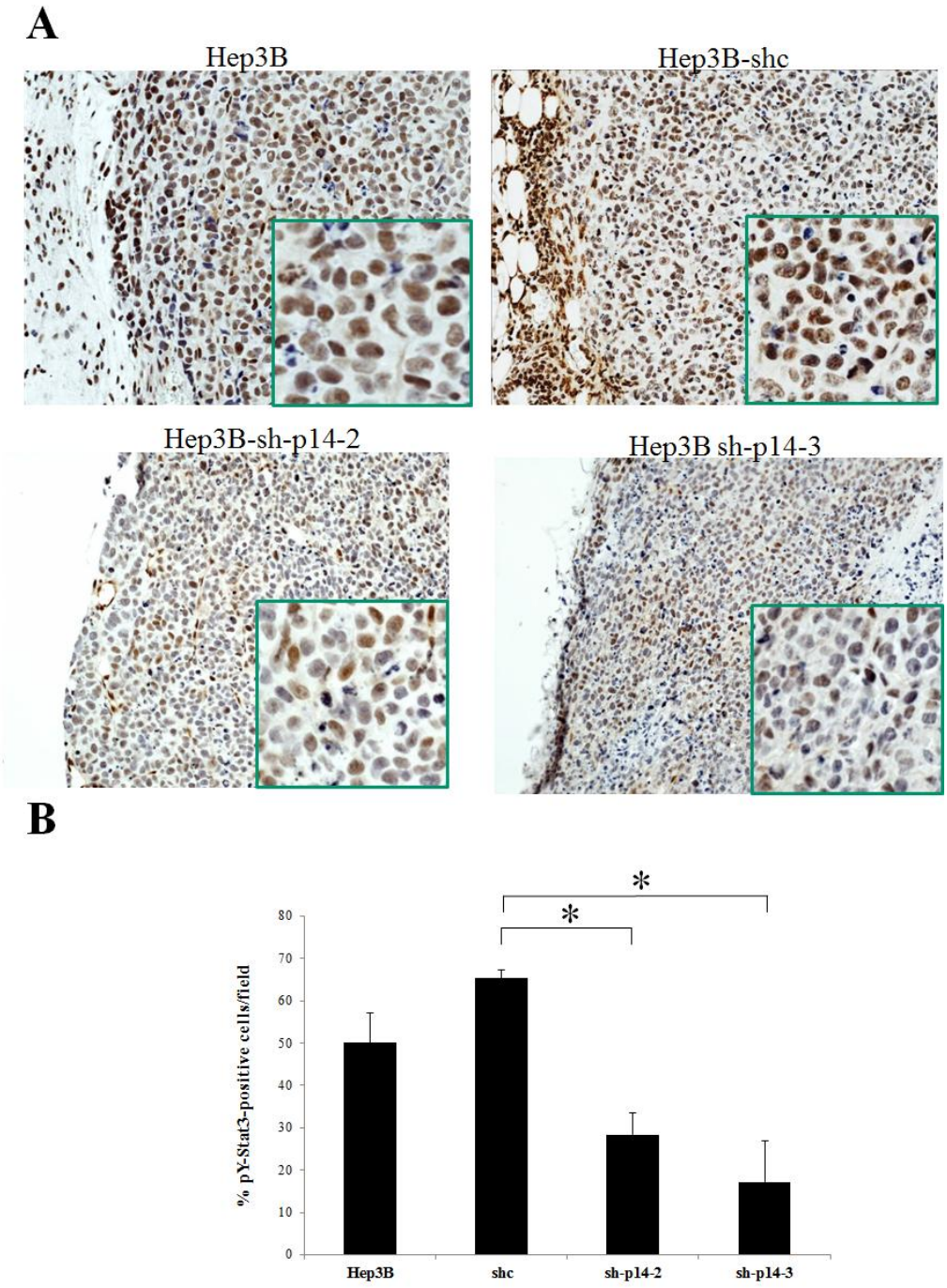

Fig. 15. Decreased levels of pY705-STAT3 in early stages of tumor progression. (A) Immunohistochemical staining using anti-pY-STAT3 of Hep3B, Hep3B-sh-control, Hep3B-shp14-2 and Hep3B-shp14-3 tumors that have developed after subcutaneous cell injection. Inserts are showing magnifications. (B) Diagram depicting the percentage of pY-STAT3 positive nuclei. Error bars reflect SD of three individual experiments. *P-value <0,05.

5.6 *Proliferation of Hep3B cells lacking p14^{ARF} in vitro is independent of STAT3 activation*

The tumor size of subcutaneously injected Hep3B cells bearing a p14^{ARF} knockdown is not affected (Fig. 5D; Schneller et al. 2011). To elucidate whether pY705-STAT3 phosphorylation influences proliferation in a p14^{ARF} negative background *in vitro*, Hep3B-sh-p14 cells were treated with IL-6, a known inducer of STAT3 activation. Analysis of proliferation via dense curve assays revealed that both control and treated cells showed a slight increase in growth upon IL-6 stimulation, however, overall proliferation capacity was comparable (Fig. 16). This experiment confirms that proliferation is independent of pY705-STAT3 in this cellular model.

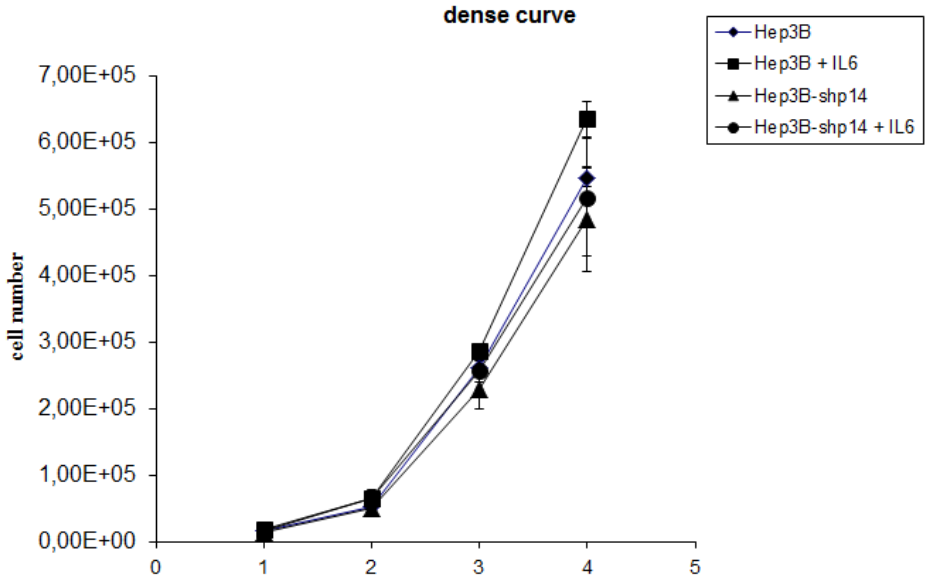

Fig. 16. Activation of pY705-STAT3 has no effect on proliferation *in vitro*. Diagram depicting parental and p14^{ARF} knockdown cells (Hep3B, Hep3B-sh-p14) with or without treatment with 20 ng IL-6. Cell numbers of triplicates were measured every second day.

5.7 *Exogenous expression of p14^{ARF} leads to decreased tumor formation and vascularization*

Knockdown of p14^{ARF} in Hep3B cells caused a decline of pY705-STAT3 levels *in vivo*, however, the decrease of p14^{ARF} did not result in lower tumor growth, as it had been shown in murine hepatoma cells lacking p19^{ARF} (Fig. 1A and Fig. 5A-C, Schneller et al.). To figure out whether this observation is cell line specific, we employed another human HCC cell line, termed PLC/PRF/5 (PLC), to investigate the role of p14^{ARF}. Since these cells display no

$p14^{ARF}$ expression, we exogenously expressed $p14^{ARF}$ via retroviral transmission, thereafter designated as PLC-p14. Subcutaneous injection of PLC-p14 cells into SCID mice showed no difference in tumor growth compared to parental cells (data not shown). Therefore, we generated single cell clones to select for cells with high-level $p14^{ARF}$ expression. Clone number 4, referred to as PLC-p14 scc#4, exhibited the most promising expression (Fig. 17A). In the next step, we injected these cells subcutaneously into SCID mice. As controls, parental PLC and $p14^{ARF}$ low expressing clone number 3 (PLC-p14 scc#3) were used. Macroscopic observation and evaluation of tumor weights revealed high variability in tumors of PLC and PLC-p14 scc#3 cells, whereby in a similar range. However, all tumors generated of PLC-p14 scc#4 cells showed clearly attenuated growth. Due to the large difference in tumor weights within the control groups, no statistical significance was achieved (Fig. 17B, C). Interestingly, pY705-STAT3 levels of all cells that were recultivated of several tumors appeared to be similar (Fig. 17D).

As shown in Fig. 17B, tumors developed from PLC-p14 scc#4 cells were colored in a brighter red, compared to tumors gained form parental and PLC-p14 scc#3 cells. To identify a possible effect on vascularization, H&E staining were performed. Indeed, tumors of PLC-p14 scc#4 cells showed lower amount of blood vessels (Fig. 17E). In conclusion, expression of $p14^{ARF}$ in these cells caused decreased tumor development, probably by attenuated blood supply. Accordingly, PLC cell show different characteristics as the human Hep3B cells. Furthermore, these data are in contrast to the murine hepatoma model (MIM-R and MMH-R hepatocytes).

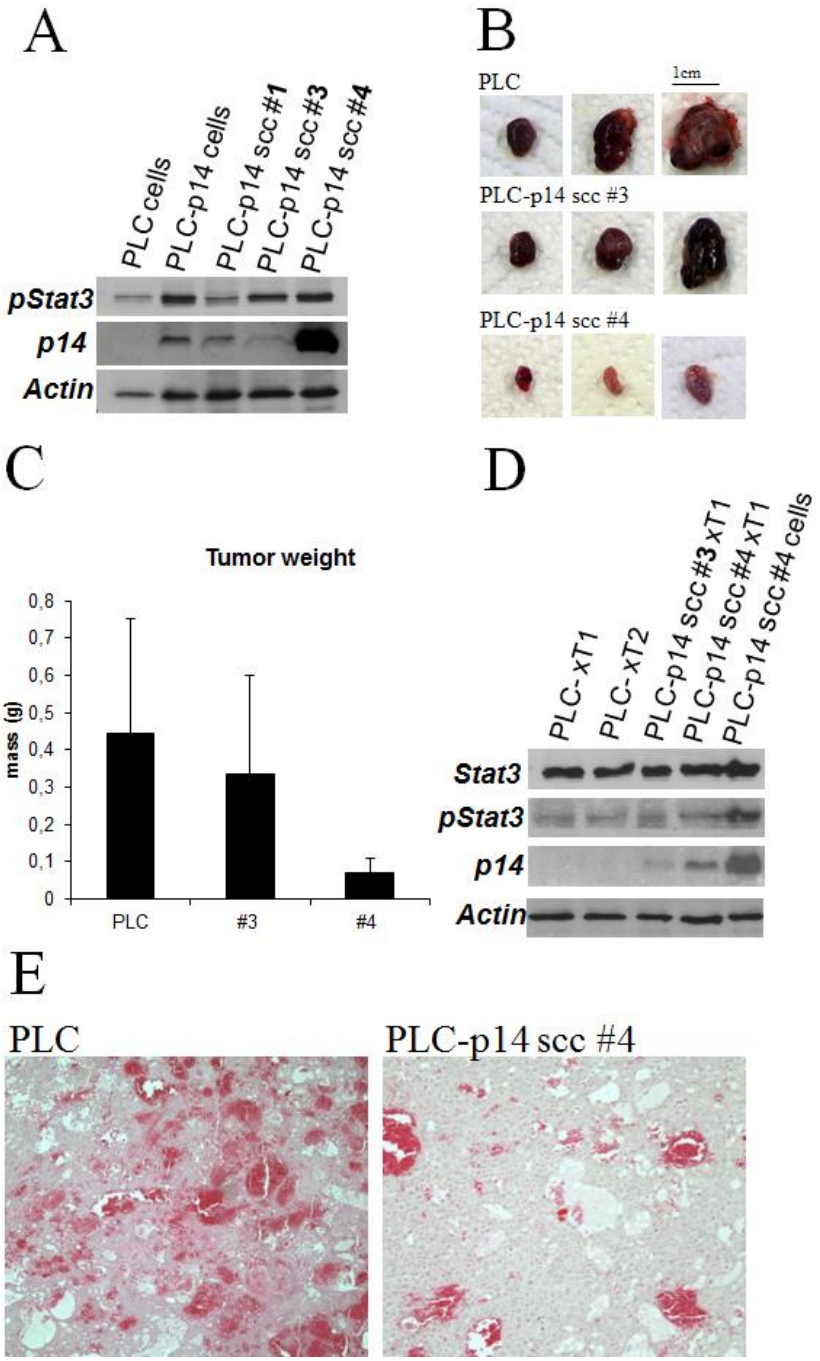

Fig. 17. Decreased tumor growth and vascularization upon introduction of $p14^{ARF}$. (A) PLC cells were retrovirally transmitted with a $p14^{ARF}$ construct (PLC-p14 cells) and analyzed for $p14^{ARF}$ expression. Single cell clones out of this pool are shown (PLC-p14 scc#1, PLC-p14 scc#3, PLC-p14 scc#4). (B) Macroscopic view of PLC, PLC-p14 scc#3 and PLC-p14 scc#4 tumors. (C) Weights of PLC, PLC-p14 scc#3 (#3) and PLC-p14 scc#4 (#4) tumors after 21 days. (D) Immunoblot of representative tumor cells after recultivation (xT) of PLC, PLC-p14 scc#3 and PLC-p14 scc#4 cells. PLC-p14 scc#4 cells (right) were used as control. Actin was used as loading control. (E) Representative H&E staining of subcutaneous tumors generated by PLC and PLC-p14 scc#4 cells, respectively.

5.8 The impact of STAT3 and/or p14 knockdown is cell line dependent

5.8.1 Knockdown of STAT3 in human Hep3B hepatoma cells

Deletion of STAT3 in murine hepatoma cells lacking $p19^{ARF}$ showed increased tumor growth (Fig. 2; Schneller et al. 2011). Based on these results, we investigated the influence of silencing STAT3 in Hep3B cells. Via lentiviral transmission of a shRNA construct targeting STAT3, Hep3B-shS3 cells were generated. Since several pools of shRNA oligos introduced in Hep3B cells did not achieved sufficient knockdown of STAT3, single cell clones were generated to select for cells with efficient silencing of STAT3 (designated in the following as Hep3B-shSTAT3 5 c9 and Hep3B-shSTAT3 2 c11; Fig. 18A). First, we analyzed the expression of $p14^{ARF}$ in Hep3B cells with a knockdown of STAT3. As shown in Figure 18B, expression level and localization in the nucleoli remained comparable between parental cells and those with STAT3 knockdown. In the next step, we applied a dense curve assay to examine possible differences in proliferation *in vitro*. Proliferation kinetics of all cell lines were similar until the third day. Afterwards, however, both shRNA bearing single cell clones showed a clearly decreased proliferation compared to parental cells and cells containing a non-target construct (Hep3B-sh_nt; Fig 18C). Finally, these cells were injected subcutaneously into SCID mice. While control cells exhibited tumor growth in well-known parameters, cells having a knockdown of STAT3 virtually did not form tumors (data not shown). In summary, these data show that STAT3 depletion does not influence $p14^{ARF}$ expression but exerts strong reduction of tumor growth.

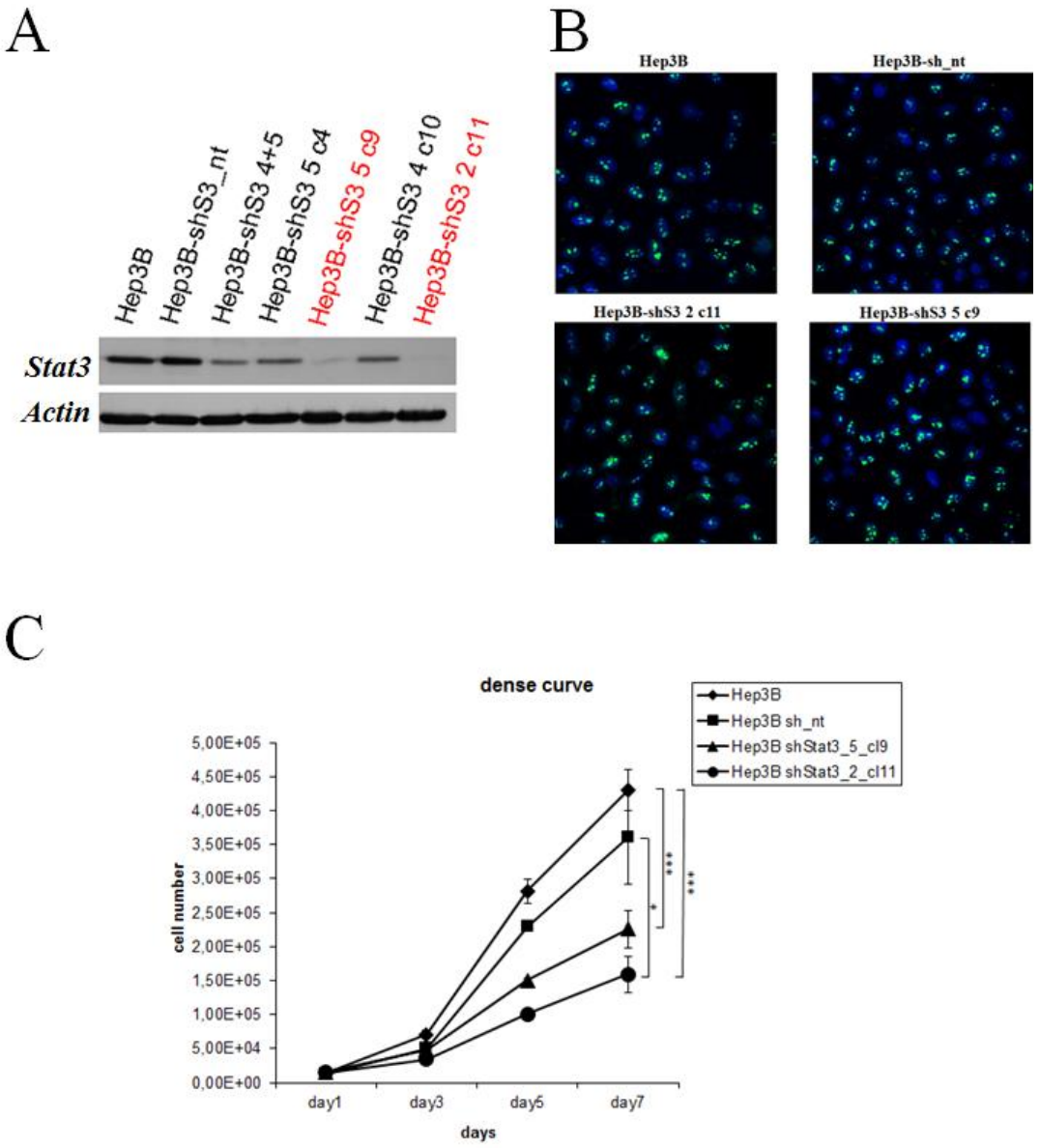

Fig. 18. Silencing of STAT3 in Hep3B cells reduces proliferation. (A) Single cell clone number 9 of cell pool infected with shRNA oligo number 5 and single cell clone number 11 of cell pool infected with shRNA oligo number 2, respectively, are indicated in red and show low expression of STAT3. Actin was used as loading control. (B) Immunofluorescence staining of Hep3B, Hep3B-sh_nt, Hep3B-shSTAT3 5 c9 and shSTAT3 2 c11 with an antibody against $p14^{ARF}$ (green). Cell nuclei were stained with DAPI (blue). (C) Proliferation kinetics. Cell number of triplicates were measured every second day. *P-value <0,05, ***P-value <0,005.

5.8.2 Hep3B-shSTAT3-shp14

As described above, the knockdown of STAT3 in Hep3B cells alone lead to attenuated proliferation *in vitro* and reduced tumor development. Noteworthy, these cells express endogenous $p14^{ARF}$. In our murine cell model, anti-oncogenic behavior of STAT3 emerged in $p19^{ARF}$ knockout cells. Therefore, we next generated Hep3B cells bearing both a knockdown

of both STAT3 and p14^{ARF}. For this purpose, Hep3B-shp14 cells were lenti-virally infected with shRNAs against STAT3. Since both vectors bearing the sh-p14 and sh-STAT3 construct, respectively, carried the same selection marker, single cell cloning was employed to select for cells with a double knockdown. As depicted in Fig. 19A, two promising clones were identified and were used for subsequent experiments. Proliferation kinetics of cells were assayed via dense curves. In both cases, the lack of STAT3 and p14^{ARF} resulted in a significant decline in cell growth which was already observed on day 3 (Fig. 19B). Upon subcutaneous injection of these cells into SCID mice, only 1 out of 4 tumors of each STAT3-targeted cell line appeared on day 30, whereas tumors from control cells emerged at an average of day 12 (data not shown). These results indicate that the knockdown of both STAT3 and p14^{ARF} leads to a dramatic decrease of proliferation *in vitro* and firmly impedes tumor formation *in vivo*. Remarkably, these findings are in contrast to data obtained in the p19^{ARF} mouse model.

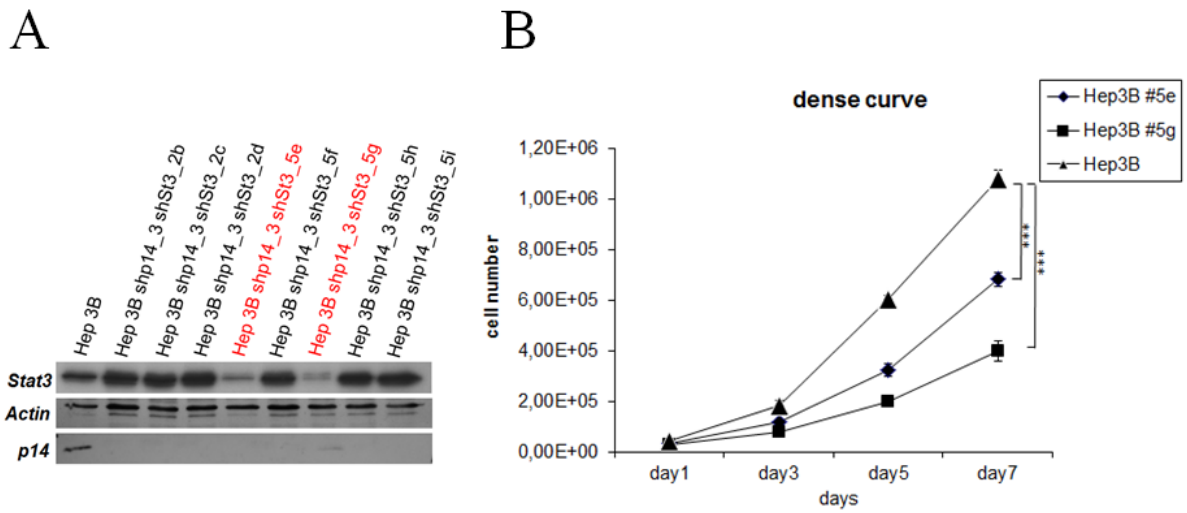

Fig. 19. STAT3 and p14^{ARF} double knockdown affects proliferation. (A) Immunoblot of several single cell clones generated of Hep3B-shp14 cells infected with sh-STAT3 oligos (shSt3-2, 5). Clones used for further experiments are marked in red. Actin was used as loading control. (B) Dense curves of Hep3B cells and cells with shRNA against STAT3 and p14^{ARF} (Hep3B #5e, Hep3B #5g). Cell number of triplicates were measured every second day. ***P-value <0,005.

5.8.3 PLC-shSTAT3

Exogenous expression of p14^{ARF} in PLC cells leads to decreased tumor formation. However, as described in section 5.7, levels of phosphorylated STAT3 remained the same compared to control cells upon recultivation of tumor cells. To elucidate the role of STAT3 in this hepatoma cell line, a knockdown of STAT3 via shRNA was performed. Lentiviral infection achieved a knockdown of approximately 70 percent (Fig. 20A, designated as PLC-shSt3 #4a).

To find out whether reduced STAT3 expression in PLC-shSt3 #4a cells showed an impact on proliferation, a dense curve assay was conducted. As observed in Fig. 20B, both parental and STAT3-targeted cells exhibited similar growth curves. Furthermore, a clonogenic assay was performed, revealing no difference in number of colony formation (data not shown). Finally, tumor formation of these cells upon subcutaneous injection into SCID mice disclosed rather similar tumor formation in both control and STAT3-targeted cells (data not shown). In conclusion, decreasing the expression of STAT3 in PLC cells by almost two thirds was not sufficient to induce an effect on proliferation and tumor formation.

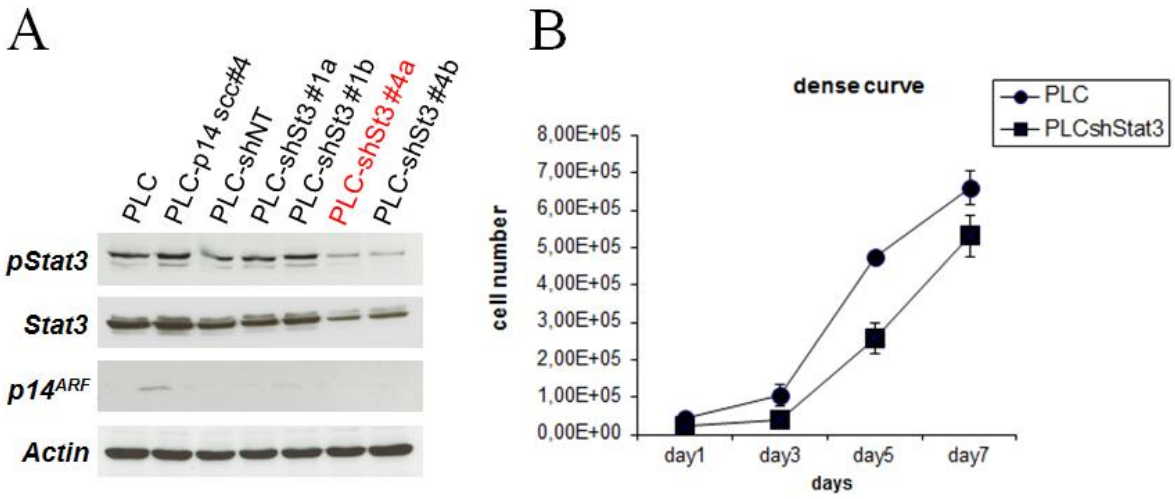

Fig. 20. Knockdown of STAT3 does not influence proliferation in PLC cells. (A) Expression of pY-STAT3, STAT3 and $p14^{ARF}$ in PLC control cells and those expressing shRNA against STAT3. Cells used for further experiments were marked in red. Actin was used as loading control. (B) Dense curve assay showing the proliferation kinetics of parental and shRNA treated PLC cells (PLC-shSt3 #4a, designated as PLCshStat3). Cell numbers of triplicates were measured every second day.

5.9 Detection of $p14^{ARF}$ in primary human HCC

Experiments described in section 5.7 and 5.8 demonstrated that modulation of $p14^{ARF}$ and STAT3 expression exhibits diverse effects, depending on which human hepatoma cell line has been employed. In the next step, we aimed to estimate a correlation between $p14^{ARF}$ expression and active STAT3 in human HCC samples, since interactions of $p14^{ARF}$ and STAT3 in single hepatoma cell lines are not conclusive regarding clinical relevance. According to results obtained in the murine cell model, $p14^{ARF}$-negative samples harboring active Stat3 might correlate with a more differentiated phenotype. In order to evaluate the quality of $p14^{ARF}$ antibodies, immunohistochemical analysis of xenografts, derived from human HCC cells that were subcutaneously injected into SCID mice, was performed. Both

Hep3B-shp14-2 cells and PLC cells have been confirmed as $p14^{ARF}$-negative prior to this assay. Fig. 21 exemplifies tumors generated from $p14^{ARF}$-positive Hep3B cells, Hep3B-shp14-2 cells and PLC cells that were stained with $p14^{ARF}$ antibody. However, the specificity of antibody was lacking as no differences in staining intensities were observed in $p14^{ARF}$-positive versus $p14^{ARF}$-negative heptoma cells. Noteworthy, all three $p14^{ARF}$ antibodies that were tested for evaluation (Sigma St.Louis, MO, clone #DCS-240; Cell Signaling Technology, Beverly, MA, clone #2407; Novus Biologicals, Littleton, CO, clone #NB100-91905) failed to generate specific staining, regardless of which modifications of the staining protocol has been exerted. As an alternative, RNA isolation of formalin-fixed, paraffin-embedded HCC patient tissue and subsequent evaluation of $p14^{ARF}$ expression via quantitative Real-Time PCR (qRT-PCR) assays was intended. For this purpose, the "High Pure RNA Paraffin Kit" (Roche, Basel, Swizerland) has been employed. However, low yield and low amount of RNA due to a high fragmentation rate impeded a proper analysis of human HCC cases regarding $p14^{ARF}$ expression.

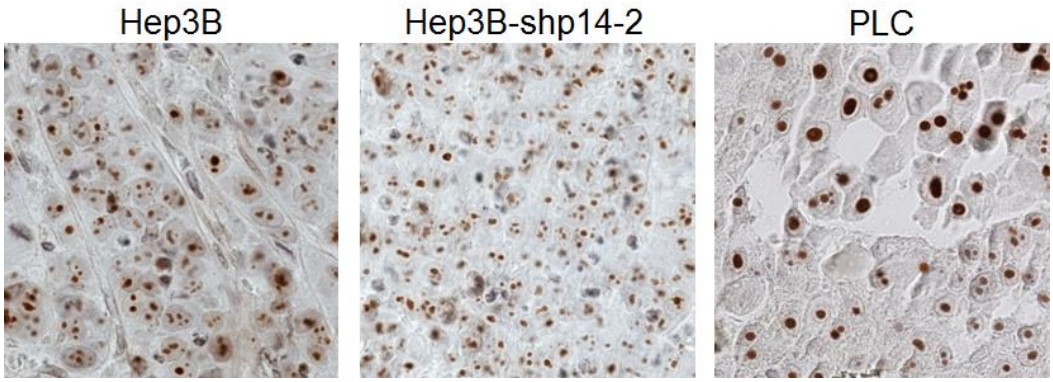

Fig. 21. Available $p14^{ARF}$ antibodies do not provide specific staining. Exemplified immunohistochemical stainings using anti-$p14^{ARF}$ (Novus Biologicals) of Hep3B, Hep3B-shp14-2 and PLC-derived tumors that have developed after subcutaneous injection into SCID mice.

5.10 The TGF-β-Smad pathway is crucial in murine, but dispensable in human hepatoma cells

Fischer et al. showed that hepatocytes which have been immortalized via knockout of $p19^{ARF}$ exhibited cell death upon TGF-β treatment (designated as MIM cells; Fischer et al. 2007). Interestingly, those cells overcome apoptosis upon expression of oncogenic Ha-Ras (termed MIM-R cells). Moreover, MIM-R cells treated with TGF-β undergo an epithelial to mesenchymal transition (EMT) that is accompanied by an increase in malignancy (Fischer et al. 2005). To figure out the impact of TGF-β on the proliferation of STAT3 deficient cells,

cumulative proliferation kinetics were determined. As shown in Fig. 22 left, STAT3 knockout cells (MIM-STAT3$^{\Delta hc}$-1, -2)-were able to overcome TGF-β-driven cell death. Re-introduction of wild-type STAT3 (wtSTAT3) diminished the escape from anti-proliferative effects of TGF-β, resulting in cytostasis. Next, we performed proliferation assays of MIM cells expressing oncogenic Ras and harboring a loss of STAT3 (MIM-R-STAT3$^{\Delta hep}$). Although MIM-R cells overcome apoptosis, treatment of TGF-β led to decrease in proliferation, irrespective of the presence of STAT3. However, proliferation was significantly lower in TGF-β treated cells expressing endogenous STAT3 (Fig. 22, right). In summary, these data suggest that STAT3 sensitizes the anti-proliferative effect of the TGF-β/Smad signaling in murine p19^{ARF} deficient hepatoma cells.

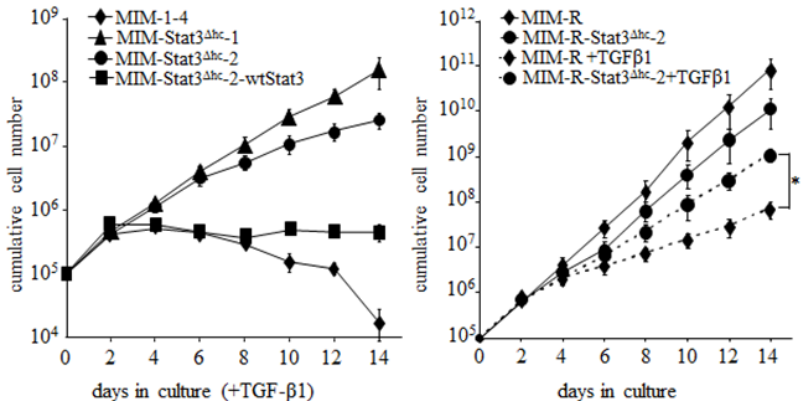

Fig. 22. Ambiguous role of the Smad pathway in murine and human-HCC cells. Cumulative cell proliferation assay showing p19^{ARF} and/or p19^{ARF}/STAT3-deficient cells with (right) or without (left) oncogenic Ras transformation. Cells were treated with 1 ng/ml TGF-β. Error bars depict standard deviation from at least five individual experiments; *P-value <0,05. By courtesy of Dr. Doris Schneller.

5.11 Phosphorylation of STAT3 is independent of PTEN

The tumor suppressor PTEN is capable to govern the pro- or anti-oncogenic activity of STAT3 via downstream effectors in glioblastoma (de la Iglesia et al. 2008). To figure out a possible interaction with STAT3 in hepatoma cells, Hep3B cells harboring a knockdown of PTEN were generated. To provide efficient silencing, single cell clones were isolated from shPTEN infected cell pools and designated as Hep3B shPTEN-1 and 2 (Fig. 23A). First, a dense curve assay was performed to examine the impact of PTEN knockdown on proliferation. Both clones used for the experiment exhibited a significant reduction in cell growth compared to the parental cell line (Fig. 23B). To observe effects *in vivo*, a subcutaneous injection into SCID mice was performed. Consistently, cells bearing the

knockdown of PTEN showed a strongly reduced tumor kinetic (data not shown). In the next step, we investigated whether loss of PTEN influenced the canonical activation of STAT3. For this purpose, cells were treated with IL-6 and Tyr^{705} phosphorylation of STAT3 was evaluated. As shown in Fig. 23C, cells lacking PTEN showed comparable pY-STAT3 levels to parental Hep3B cells, indicating no effect on canonical STAT3 pathway. Furthermore, immunofluorescence staining revealed no change in the cytoskeletal phenotype upon treatment with IL-6 (Fig. 23D). Altogether, these results suggest a role of PTEN in cell proliferation and cytoskeletal structure. However, these effects are independent of STAT3 activation.

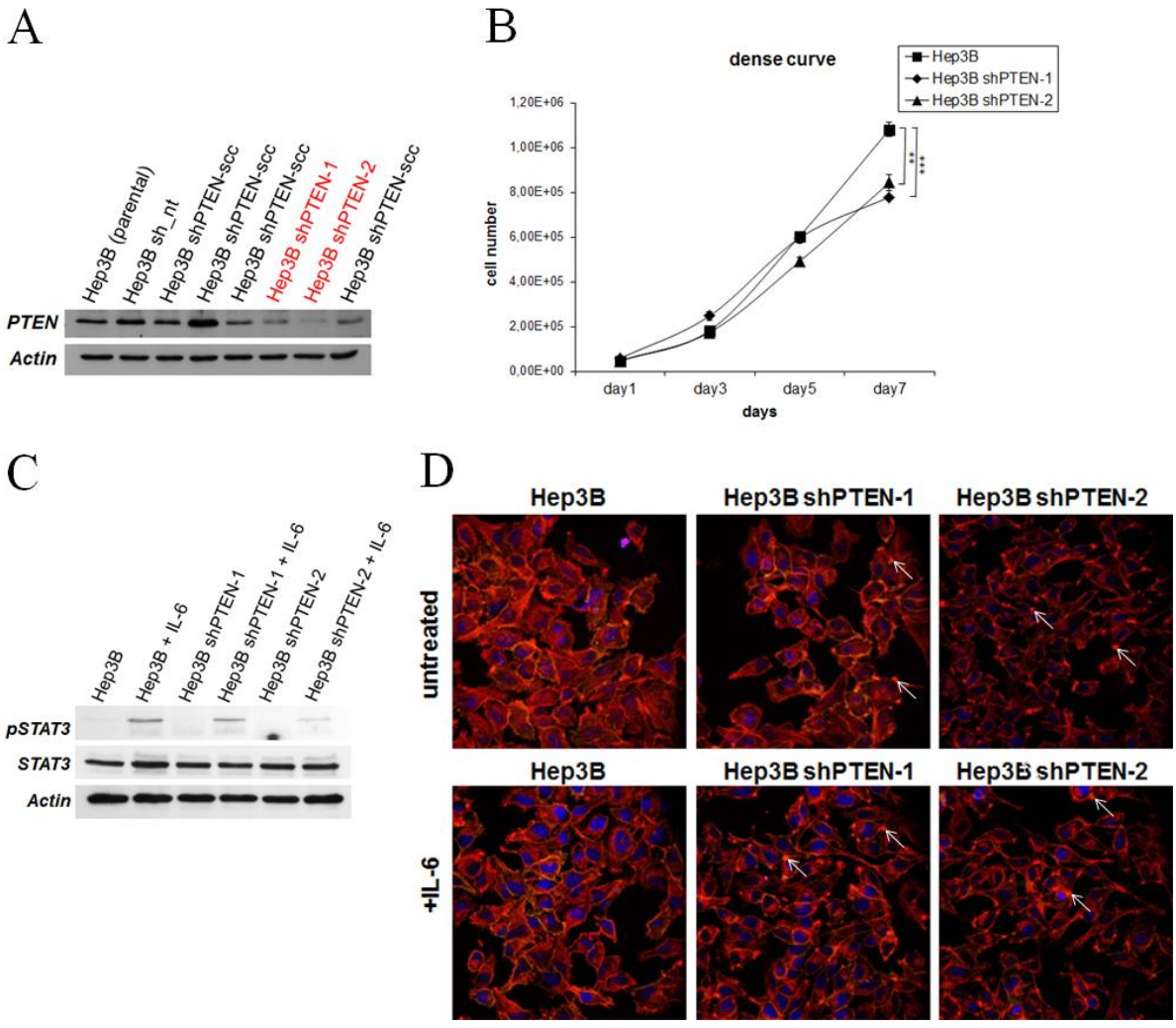

Fig. 23. Knockdown of PTEN leads to reduced proliferation. (A) Western blot analysis of control Hep3B cells and single cell clones raised from Hep3B cells transmitted with shRNA oligos against PTEN Cells used for further experiments were marked in red. (B) Dense curves showing the proliferation of Hep3B, Hep3B shPTEN-1 and HEP3B shPTEN-2 cells. **P-value <0,01, ***P-value <0,005. (C) Western blot analysis showing the expression of pY705-STAT3 (pSTAT3) and STAT3 in Hep3B, Hep3B shPTEN-1 and HEP3B shPTEN-2 cells, before and after treatment with IL-6. Actin was used as loading control. 20 ng/ml IL-6 was administered for 20

minutes. (D) Immunofluorescence staining of control and IL-6 treated cells. Arrows indicate actin foci. Red, phalloidin; blue, Top-Pro3.

6 Discussion

6.1 $p19^{ARF}$/$p14^{ARF}$ Controls Oncogenic Functions of STAT3 in HCC – in retrospect

In section 4, the publication of Schneller et al. demonstrated a differential role of STAT3 in liver cancer, as both the knockout and the overexpression of the STAT3β isoform that could not be phosphorylated displayed enhanced tumor growth in $p19^{ARF}$-deficient, Ras-transformed hepatoma cells. In contrast, overexpression of STAT3 constructs harboring a mutation in the SH2-domain leading to dimerization without prior phosphorylation on tyrosine 705 (pY705) attenuated malignancy (Fig. 1M; note: numeration referring to the manuscript of Schneller et al. is marked with "M"). A phenotype similar to U-STAT3β overexpression has been observed employing STAT3 knockout in this setting (Fig. 2M; MIM-R-$STAT3^{\Delta hc}$). Importantly, another oncogenic Ras-transformed murine cell line expressing $p19^{ARF}$, termed MMH-R, reversed this phenotype (Fig. 3M). A further link between STAT3 and $p19^{ARF}$ has been discovered in malignant liver tissues gained from DEN treated mice. A clear up-regulation of $p19^{ARF}$ was observed in STAT3 wild-type mice, whereas expression levels remained undetectable in both STAT3 knockout and in non-treated control mice (Fig. 4M).

The study by Schneller et al. further aimed to examine the interplay of STAT3 and $p14/p19^{ARF}$ in human HCC by focusing on the human hepatoma cell line Hep3B. This cell line shows pronounced $p14^{ARF}$ expression and is capable for canonical STAT3 activation. Upon efficient knockdown of $p14^{ARF}$, it appeared to be an adequate human model for the comparison with the approach in murine hepatoma cells. However, tumor kinetics comparable to the mouse experiments yielded no variation in tumor sizes, regardless of $p14^{ARF}$ expression. Remarkably, reduced levels of pY705-STAT3 were observed in $p14^{ARF}$ depleted Hep3B hepatoma cells (Fig. 5M). Finally, kinases participating in the canonical activation of STAT3 (JAK1, JAK2, JAK3, TYK2) were excluded to cooperate with $p14^{ARF}$ in the human HCC models (Fig. 6M).

Based on these facts, we devised a working model by integration of the obtained results (Fig. 7M). In this model, STAT3 activities were linked to an anti- or pro-oncogenic fate dependent on the presence of $p14/p19^{ARF}$. In more detail, both canonical and constitutive activation of STAT3 increases tumorigenesis in a $p14/p19^{ARF}$ positive background. Furthermore, $p14/p19^{ARF}$ is interacting with the putative factor ARF-X. ARF-X is released upon $p14/p19^{ARF}$ depletion and might bind to U-STAT3 and trigger its transcriptional activation.

Given that exogenous expression of constitutive active STAT3 acts in an anti-oncogenic manner, it is further hypothesized that canonical activation of STAT3 is circumvented, explaining the depletion of pY705-STAT3 observed in Hep3B cells.

Although the described model delineates only a couple of scenarios, it already includes a large complexity. For example, tumor kinetics of $p19^{ARF}$-proficient hepatoma cells (MMH-R) have only been evaluated by overexpressing caSTAT3β and U-STAT3β (a dominant negative form of STAT3β, designated as U-STAT3 in the manuscript of Schneller et al.), respectively. In contrast to MIM cells that were immortalized by deletion of $p19^{ARF}$, MMH cells became immortal upon overexpression of the cytoplasmic domain of the c-Met receptor. Given the importance of c-Met in HCC and the distinct functions observed for STAT3 isoforms, it might be interesting to complete tumor kinetic experiments with the STAT3α-isoform in this setting (Ueki et al. 1997; Ng et al. 2012).

It is important to mention that in the experiments employing overexpression of caSTAT3 and U-STAT3, the cells lines (MIM-R and MMH-R) used also expressed endogenous STAT3 (Fig. 1M and Fig. 3M). As mentioned above, latent STAT3 is able to shuttle between the cytoplasmic and nuclear compartments and shows transcriptional activity (Vogt et al. 2011). Neither hetero-dimerization of wild-type and exogenously expressed STAT3, nor expression of factors upregulated by endogenous STAT3 that interact with exogenous STAT3 can be excluded. Unfortunately, MMH cells bearing a STAT3 knockout were not available, since such cells would help completing the picture.

Another finding described in the manuscript illustrated an upregulation of $p19^{ARF}$ in DEN-treated control mice, whereas this augmentation failed to appear in mice lacking STAT3 in the liver ($STAT3^{\Delta hc}$; Fig. 4M). Additionally, decreased tumor formation has been stated in STAT3 deficient livers. Interestingly, this is contradictory to a recent publication, which showed enhanced tumor development in $STAT3^{\Delta hc}$ mice upon DEN induction by using the same mouse strain and DEN dosage (Bard-Chapeau et al. 2011). Both publications extend the ambiguous findings of the role STAT3 in hepatocarcinogenesis.

The publication by Schneller et al. also addresses the role of STAT3 in human HCC. At least in the used HCC cell line, the striking differences regarding tumor kinetics in the presence or absence of $p14^{ARF}$ could not be observed (further experiments in this respect were described in section 5 and will be later discussed). An alternative approach to hepatoma cell lines aimed to screen human HCC specimen in terms of their expression of (pY705-) STAT3 and $p14^{ARF}$. Profiling and subsequent correlation might result in a pattern regarding grading or etiology,

and might therefore help to identify HCC subtypes. Such analysis is ongoing in collaboration with D. Calvisi, University of Greifswald, Germany.

As provided by an editorial dealing with Schneller et al., D. Calvisi suggested a modified arrangement of the players interacting in the model (Fig. 7M). He included oncogenic Ras being "upstream" of STAT3 and suggested that Ras might orchestrate the tumorigenic outcome (Fig. 24; Calvisi 2011). Both cell lines used for murine experiments in the manuscript were transfected with oncogenic Ha-Ras and consequently acquired a transformed phenotype (Gotzmann et al. 2002; Fischer et al. 2005). This step was necessary to gain cells with oncogenic potential. Accordingly, abundant activation of the JAK-STAT3 pathway and Ras has been observed via screening of an HCC library (Calvisi et al. 2006). This awareness is stimulating for further investigations of Ras, STAT3 and p14/p19^{ARF} regarding both direct interactions and interactions of downstream effectors. Calvisi also proposed a tumor-suppressive role upon loss of STAT3 in the p19^{ARF}-positive background (Fig. 24A, "Stat3$^{-/-}$"). Notably, this statement referred to the general description of STAT3 as an oncogene, as respective experiments have not been performed by Schneller et al.

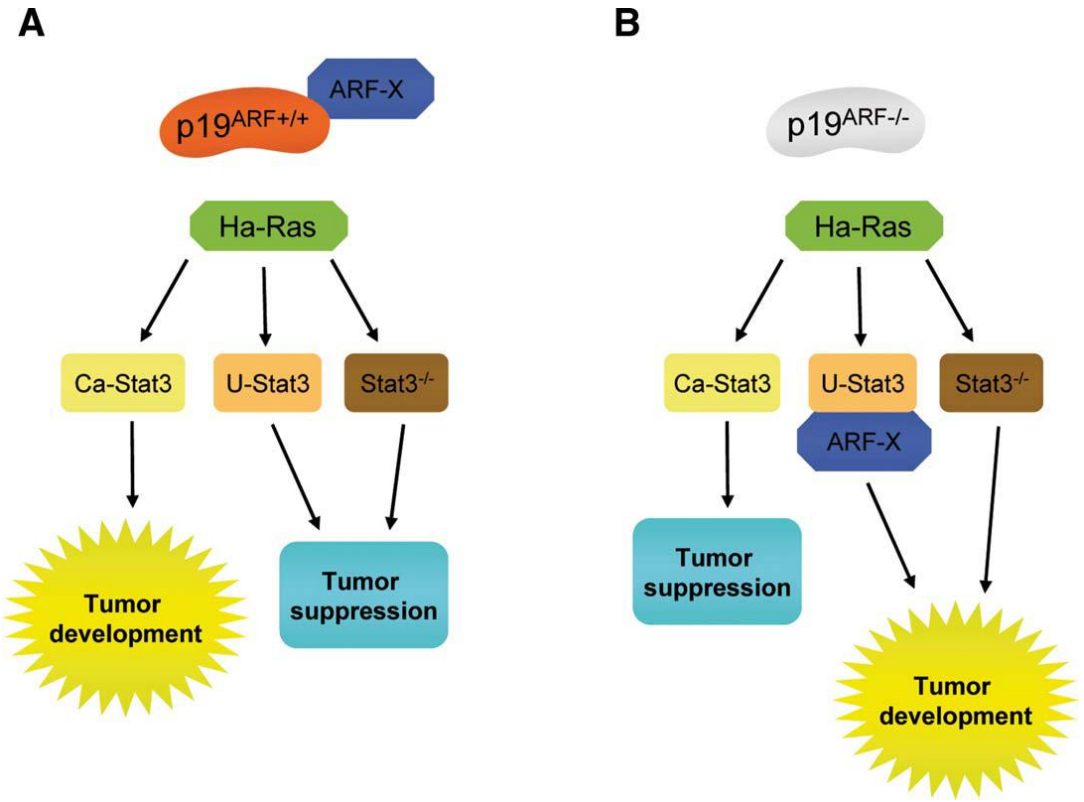

Fig. 24. Alternative view of the anti- and pro-oncogenic STAT3 regulation dependent on p19^{ARF}. Ha-Ras orchestrates tumor outcome via setting of STAT3, in the presence (A) and in the absence (B) of p19^{ARF}. Cartoon taken from Calvisi, 2011.

The effect of $p14^{ARF}$ on the canonical activation of STAT3 was investigated (Fig. 6M). Phosphorylation of STAT3 upon IL-6 treatment was prevented using transcriptional and translational inhibitors, suggesting the requirement of a factor that either maintains active STAT3 levels or avoids de-phosphorylation of STAT3. In this respect, the activity and presence of phosphatases, such as SHP-1 and SHP-2, should be evaluated. However, although this finding was obtained in two established hepatoma cell lines, it appeared to be independent of $p14^{ARF}$. Likewise, the same cell lines, Hep3B and PLC/PRF/5 (PLC), were employed for JAK inhibitor assays and showed $p14^{ARF}$ independent results. In addition, several assays using specific JAK inhibitors were performed, figuring out that JAK1 might be the responsible kinase (data not shown). Notably, this statement is solely based on indirect evidence, as JAK2, JAK3 and TYK2 could be excluded, but no JAK1 inhibitor was available. Therefore, assays employing depletion of JAK1 via knockdown or knockout are required to fully confirm this conclusion.

Altogether, the manuscript provided interesting insights into STAT3 functions in a murine liver cancer model. In addition, it presented a novel hypothesis for a possible crosstalk between various powerful regulators in tumorigenesis. However, further evaluation of this model has not been sufficiently done so far. Thus, based on the results of the manuscript, a multitude of experiments have been consequently performed both in murine and human systems (section 5) and will be discussed below.

6.2 Further investigations of murine model systems

6.2.1 Microarray analysis

As described briefly in the results section (5.1), STAT3- and $p19^{ARF}$- double deficient hepatocytes (MIM-R-$STAT3^{\Delta hc}$) have been employed to analyze the expression of STAT3 isoforms by profiling of the transcriptome. Therefore, caSTAT3α and STAT3β as well as wtSTAT3 were exogenously expressed in MIM-R- $STAT3^{\Delta hc}$ hepatocytes, as all these cells showed interesting tumor kinetics (Fig. 1M, 2M). However, no significant differences of the gene expression patterns could be observed as compared to control cells (MIM-R-$STAT3^{\Delta hc}$). This surprising result underlines the importance of paracrine signaling *in vivo*. Treatment with IL-6 to induce canonical activation of STAT3 is considered as a prerequisite for the functionality of STAT3. With respect to the profiling of caSTAT3α and caSTAT3β expression, a prior phosphorylation on tyrosine 705 would therefore be necessary for their

functionality. Liddle and co-workers demonstrated the importance of tyrosine 705 phosphorylation by using constitutive active constructs additionally harboring a mutation on tyrosine 705 (caSTAT3 (Y > F)). This study used SOCS3, a target gene known for being activated by canonical STAT3, for evaluation of transcriptional activity (Liddle et al. 2006). CaSTAT3α (Y > F) represents U-STAT3α. Therefore, caSTAT3 (Y > F)-expressing cells might be used to identify novel U-STAT3 target genes, as several publications have found the ability of U-STAT3 to bind both to GAS and alternative elements (Yang et al. 2005; Timofeeva et al. 2012). In this scenario, the currently running microarray analysis of MIM-R-STAT3$^{\Delta hc}$ hepatocytes exogenously expressing U-STAT3α and U-STAT3β is highly promising to get fundamental insights into the target genes of U-STAT3 isoforms.

6.2.2 p53 functionality

We addressed the question whether p53 could be responsible for differential actions of STAT3 in Ras-transformed MIM-R (tumor-suppressive, Fig. 1M, 2M) and in Ras-transformed MMH-R (tumor-promoting, Fig. 3M) hepatocytes. Therefore, we examined p53 functionality by chemotoxicants. For this purpose, we administered the chemotherapeutic drug etoposide to induce p53 expression (Fig. 12). In addition we evaluated the expression of p21^{WAF1}, a known target gene of p53 that indicates functionality of p53. Interestingly, p53 induction was displayed in regular levels in both hepatocytic cell types, as excessive up-regulation would indicate the existence of mutated forms (personal notification of V. Sexl, VetMed, Vienna). In general, although MIM-R cells (but not MMH-R cells) harbor a knockout of p19^{ARF}, an important upstream regulator of p53, it can be concluded that the phenotype observed in these models have developed independent of p53.

6.2.3 U-STAT3 localization and transactivation

To corroborate our proposed model, two issues regarding U-STAT3 had to be analyzed. First, we addressed the question whether U-STAT3 is able to translocate into the nucleus and second, whether it is capable to induce transactivation. Shuttling of U-STAT3 has been frequently shown, for both isoforms as well as for mono- and dimers (Vogt et al. 2011). However, evidence that U-STAT3 induces gene expression is still rare. George Stark's group appeared to be pioneers in this regard. They identified several genes being exclusively up-regulated by U-STAT3 but not by pY705-STAT3, including oncogenes (Yang et al. 2005). Cellular fractionation revealed nuclear localization of U-STAT3 and reporter assays showed

transcriptional activity. However, some differences between recent observations by Stark´s group and our results have to be mentioned. Most notably, while their work reported genes to be up-regulated by both wild-type STAT3 and U-STAT3, we solely observed reporter activity by the latter (Fig. 13B). Furthermore, genes referred in their publication were induced by U-STAT3α. RT-PCR analyzing genes being induced in their study (*mras, met, IL-6, IL-8, Rantes*) showed no results in MIM-R-STAT3$^{\Delta hc}$-U-STAT3β cells (data not shown), underlining the complex-network of gene expression underlying STAT3 isoforms. In addition, Stark and co-workers employed human mammary epithelial (hTERT-HME1) cells and mouse embryo fibroblasts (MEFs) in their study. Notably, the authors comment on the "limited congruency" of induced genes between these cell models (Yang et al. 2005). This statement emphasizes the hazard comparing mouse and human models and underlines the cell type specificity of U-STAT3 actions.

6.2.4 The interaction of NFkB and U-STAT3

Unphosphorylated NFκB can utilize the NLS of U-STAT3 to enter the nucleus (Yang et al. 2007). However, our studies did not reveal a correlation between the nuclear translocation of U-STAT3 and NFκB in Ras transformed hepatocytes (Fig. 14B), suggesting that the molecular collaboration of U-STAT3 and NFκB might depend on the cell type. Furthermore, we solely investigated U-STAT3β and results derived from U-STAT3α expression are lacking. Importantly, transcriptional activation by U-STAT3 of genes independent of NFκB has been also reported (Yang et al. 2007). This finding is encouraging to identify novel genes regulated by U-STAT3, independent of NFκB. Besides, several studies showed interactions of NFκB with both p19^{ARF} and Ras (Jo et al. 2000; Rocha et al. 2003). Therefore, it is conceivable that the lack of p19^{ARF} and the expression of oncogenic Ras in MIM-R cells might influence NFκB actions and its interaction with U-STAT3 in our cell model.

6.2.5 Conclusions and outlook

The employed murine cellular model revealed novel insights into the role of STAT3 in HCC, but some important questions are still open. To further analyze the role of p19^{ARF} in this context, it has to be re-expressed in MIM-R cells. Consequently, the STAT3-dependent phenotype in these cells should reverse. Thus far, this procedure failed, since MIM-R-STAT3$^{\Delta hc}$ cells expressing STAT3 versions already require four selection markers, making it difficult to find a suitable method for further selections. Moreover, re-introduction of p19^{ARF}

causes senescence, as it has been shown in several cell types (Serrano et al. 1997; Lin and Lowe 2001). As an alternative, $p19^{ARF}$ will be silenced via shRNA in $p19^{ARF}$-proficient MMH-R cells, which is currently in progress. Inversion of tumor kinetics upon exogenous expression of U-STAT3 and caSTAT3 in these cells, respectively, would confirm $p19^{ARF}$ as a key regulator in these cells. Unfortunately, MMH cells bearing a knockout of STAT3 are not available. Therefore, the MIM-R-$STAT3^{\Delta hc}$ cell type cannot be fully reproduced with the MMH cell model. Transcriptome analysis of U-STAT3α and U-STAT3β is another ongoing approach and might clarify their specific role in this cell system. Bridging the results obtained in the mouse to human HCC will be discussed in the following section.

6.3 Investigation on human hepatoma cell lines – facing diversity

Despite the significance of the murine data, transmission of results obtained in the mouse model towards human relevance is indispensable. In this regard, available established HCC cell lines were genetically modified to resemble murine parameters. Furthermore, we further analyzed regulatory proteins which have been shown to be crucially involved in HCC, such as TGF-β and PTEN.

6.3.1 Early down-regulation of active STAT3 in Hep3B-shp14ARF cells

The knock-down of $p14^{ARF}$ in Hep3B cells showed no phenotypic change *in vitro*. Likewise, upon subcutaneous injection into immunodeficient mice, these cells showed a comparable tumor kinetic to control cells. However, a significant decrease of active STAT3 levels has been observed. This fact accounted for the hypothesis that active STAT3 acts tumor suppressive in the absence or depletion of $p14^{ARF}$ (Fig. 7M).

The embryonic lethality of total STAT3 knockout and the multitude of implications during tumorigenesis raised the question at which point of time pY705-STAT3 activation is switched off. We observed in Hep3B cells that downregulation of pY705 occurred early in tumor formation (Fig. 15). This supports the idea that Hep3B tumors keep active STAT3 levels low during entire tumor formation. Investigation *in vivo* using human hepatoma cells exogenously expressing caSTAT3 isoforms (in a $p14^{ARF}$ knockdown background) would address this question in more detail. An approach to tackle this question was performed by inducing STAT3 activation via IL-6. Proliferation kinetics revealed no differences (Fig. 16).This *in vitro* study did not reflect results from the xenograft model. In this respect, further

experiments are needed to confirm and to examine the molecular mechanism underlying the suppression of pY705-STAT3 in HCC development.

6.3.2 Impact of p14^{ARF} expression

As described above, silencing of p14^{ARF} prevents canonical STAT3 activation in human Hep3B xenografts. Hep3B hepatoma cells express high levels of p14^{ARF}, thus served as an appropriate tool for p14^{ARF} depletion and the analysis of the ensuing phenotype. Therefore, we raised the question whether constitutive expression of p14^{ARF} in a p14$^{ARF-/-}$ cell line would show a comparable effect. PLC/PRF/5 (PLC), a well-established cell line negative for p14^{ARF} expression was chosen to address this issue. Specifically, we aimed to investigate the impact of exogenous p14^{ARF} expression on (i) STAT3 activation, (ii) tumor kinetics and (iii) phenotypical changes. Notably, since the pool of cells yielded only moderate expression of p14^{ARF}, single cell clones were picked. Clone number 4 (PLC-shp14 scc #4) was selected to demonstrate our results. Another established clone confirmed our results obtained with PLC-shp14 scc #4 cells (data not shown). Subcutaneous injection into immunocompromized SCID mice revealed two important observations. First, while tumors of parental cells partly showed broad variations in size, cells harboring p14^{ARF} developed unambiguously smaller tumors on average (Fig. 17C). In contrast to Hep3B cells, re-cultivation of tumor cells did not show a difference in activated STAT3 levels dependent on p14^{ARF} (Fig. 17D). Unfortunately, the available STAT3 antibody recognized both human and mouse homologues. Therefore, direct extraction of tumors was not feasible in this cell line as tumors derived from parental PLC cells contained much higher murine STAT3 due to elevated vascularization. Secondly, PLC cells exogenously expressing p14^{ARF} exhibited a marked decrease in vascularization, as macroscopically visible (Fig. 17B) and confirmed by H&E staining (Fig. 17E). In line with this finding, p14^{ARF} has been shown to negatively regulate neo-angiogenesis via upregulation of TIMP-3 and HIF-1α inhibition, respectively (Fatyol and Szalay 2001; Zerrouqi et al. 2012). HIF-1α has been also found down-regulated via STAT3 in a thyroid cancer model (Couto et al. 2012), indicating that both p14^{ARF} and STAT3 might regulate vascularization. In conclusion, the PLC cell model provided conflicting results compared to other hepatoma cell models under investigation. It showed neither characteristics of Hep3B cells nor results comparable to the murine cell model (MMH-R). Regarding vascularization, the results obtained in PLC cells could help to understand the role of STAT3 and p14^{ARF} in neo-angiogenesis in tumorigenesis.

6.3.3 Intervention with STAT3

In order to get new insights into the cooperation of $p14^{ARF}$ and STAT3, we silenced STAT3 in Hep3B cells (Hep3B-shSTAT3). Two single cell clones displayed satisfying knockdown of STAT3 (Fig. 18A). Since Hep3B cells exhibited a correlation between $p14^{ARF}$ and activated STAT3 (Fig. 5M, A-C), we next aimed to analyze a possible mutuality of this interplay. Interestingly, silencing of STAT3 revealed no down-regulation of $p14^{ARF,}$ in contrast to the *vice versa* approach. Remarkably, Hep3B cells lacking STAT3 showed no change in phenotype, however, proliferation kinetics revealed significantly lower growth rates of STAT3-deficient cells (Fig. 18C). Moreover, xenograft tumor formation failed without STAT3. Similar to PLC cells exogenously expressing $p14^{ARF}$ tumor suppressor, Hep3B cells lacking oncogenic STAT3 exhibited the expected phenotype, i.e. a decreased malignancy. Interestingly, knockdown of STAT3 in PLC cells showed no differences to parental cells (Fig. 21). This might be argued with remaining STAT3 in PLC cells treated with shRNA, as single cell cloning failed in these cells. On the other hand, PLC cells might be more efficiently compensate the knockdown of STAT3. To figure this out, a closer look at differences in proliferative signals between parental and treated cells is needed. To assess a clear correlation between $p14^{ARF}$ and STAT3, intervention on both factors is required, as discussed below.

6.3.4 Double knockdown of STAT3/p14ARF in human hepatoma cells

Knockdown of $p14^{ARF}$ in Hep3B cells leads to attenuated levels of phosphorylated STAT3 *in vivo*. However, tumor kinetics are comparable to control cells. Therefore, we postulated that transcriptional activity of U-STAT3 compensated canonical activation, resulting in a similar tumor growth (Fig. 7M). We further addressed the question of what happens in the absence of STAT3 protein. To this end, a Hep3B cell line expressing shRNAs for both STAT3 and $p14^{ARF}$ was generated. Proliferation and tumor kinetics of Hep3B-shSTAT3-shp14 cells revealed greatly decreased levels (Fig. 19B). Comparing single $p14^{ARF}$ and STAT3 knockdown cells with these cells, the double knockdown cells showed a similar phenotype to the STAT3 knockdown model. However, by considering the murine model of MIM-R-$STAT3^{\Delta hc}$ cells, those human HCC cells are rather expected to exhibit increased tumor formation. As mouse cells additionally express oncogenic Ras direct comparisons of the mouse and human hepatoma model might be not feasible.

In conclusion, results obtained from human HCC cells that have been manipulated on STAT3 and/or $p14^{ARF}$ expression revealed valuable insights into their specific role in HCC progression. Notably, direct comparison of experiments performed with Hep3B and PLC cells

is rather inappropriate, as these cells acquired their tumorigenic properties by different events, at least regarding $p14^{ARF}$. Therefore, silencing of $p14^{ARF}$ in Hep3B cells can be utilized for alterations in signaling pathways within these cells rather than for direct comparison of tumorigenesis in $p14^{ARF}$-deficient cells, such as PLC cells. Experiments with other $p14^{ARF}$-proficient human hepatoma cells, such as HUH-7, might be more suitable to corroborate the present findings.

6.3.5 Analysis of p14ARF in primary human HCC

The analysis of $p14^{ARF}$ in human HCC samples elaborated a huge obstacle, since immunohistochemical evaluation remained hardly feasible. Presumably due to the hydrophobicity and small size of $p14^{ARF}$, this technique was not feasible, as described by other labs (Ozenne et al. 2010). Therefore, most data correspond to studies obtained from mRNA levels of $p14^{ARF}$. However, this method predicts its transient expression and does not reveal any information about post-transcriptional modification and co-localization with known and putative interacting partners, such as STAT3. Accordingly, co-immunoprecipitation of $p14^{ARF}$ and STAT3 would partly solve this problem. Yet, the presence of U-STAT3 and phosphorylated STAT3 in the cytoplasm and nucleus, respectively, describes another important issue of complexity which must be taken into consideration.

Fig. 21 illustrates the non-specific detection of $p14^{ARF}$ via immunohistochemical methods. To tackle this issue, we performed RNA isolation of human FFPE-HCC specimens for subsequent RT-PCR analysis. Generally, this method entails high rates of RNA fragmentation. This problem could be overcome by using RT-PCR-primers near the 3´-end of the target. Unfortunately, as depicted in Fig. 5, $p14^{ARF}$ shares this region with $p16^{INK4A}$. Therefore, designing primers specific for $p14^{ARF}$ near the 3´-end was not possible. As mentioned above, the group of D. Calvisi will analyze a large collection of frozen HCC samples for pY705-STAT3 and $p14^{ARF}$ expression. These data will help to correlate their expression with clinical records of HCC progression.

Another approach to bridge murine to human data would be the genetic modification of primary human hepatocytes. In other words, deletion of $p14^{ARF}$ and expression of oncogenic Ras in these cells would provide important aspects regarding the significance of the murine data. Concomitantly, introduction of $p14^{ARF}$ mutants lacking important sequences, such as the nucleolar localization signals or the binding to CtBP, might help to elucidate the exact role of $p14^{ARF}$, as it was already shown for murine $p19^{ARF}$ (Kamijo et al. 1998; Chen et al. 2008). Although isolation and maintenance of human primary hepatocytes is rather difficult,

promising protocols are upcoming (Zamule et al. 2008; Bhogal et al. 2011). Since this approach is costly and elaborating, further screening of human HCC samples and subsequent deciphering of their molecular signaling pattern seems more promising in near future.

6.3.6 The role of STAT3 in TGF-β signaling

Gotzmann and colleagues examined the ability of TGF-β to induce an epithelial to mesenchymal transition of MIM cells transformed with oncogenic Ras. Without expression of oncogenic Ras, the same cells exhibit cell cycle arrest and cell death upon TGF-β treatment (Gotzmann et al. 2002). These findings underline the importance of the collaboration between Ras and TGF-β for malignancy. D. Schneller investigated the role of STAT3 in TGF-β effects on immortalized MIM and Ras-transformed MIM-R hepatocytes. To this end, proliferation of MIM cells with or without a knockdown of STAT3 was determined upon TGF-β administration. MIM-STAT3$^{\Delta hc}$ cells remained growing unaffected by TGF-β, whereas cells endogenously expressing STAT3 underwent cell death. Remarkably, STAT3-deficient cells re-expressing wild-type STAT3 showed a moderate reduction in proliferation kinetics (Fig. 22, left). This experiment showed that STAT3 (i) plays a pivotal role in providing a response to TGF-β and (ii) exhibits anti-oncogenic properties in the absence of Ras. Accordingly, performing this experiment in the presence of Ras with MIM-R and MIM-R-STAT3$^{\Delta hc}$ cells, TGF-β treated cells lacking STAT3 exhibit significantly augmented proliferation, albeit the reduced cell growth was not as strong as STAT3 expressing MIM cells (Fig. 22, right). This finding raises the question of the role of STAT3β in the context of TGF-β, as re-introduction of wild-type STAT3 (i.e. STAT3α) did not fully rescue the phenotype of endogenously expressing cells (Fig. 22, left). Introduction of caSTAT3 and U-STAT3 constructs and concomitant administration of TGF-β and IL-6, respectively, might provide further insight into the interaction of STAT3 and TGF-β. In addition, analysis of proliferation kinetics with human hepatoma cell lines and long-term treatment with TGF-β are required to get a more complete picture.

The interaction of TGF-β and JAK/STAT3 pathway was already described. For example, inhibition of STAT3 suppressed growth exclusively in HCC cells bearing non-functional TGF-β signaling (Lin et al. 2009). Furthermore, another study reported TGF-β as a negative regulator of IL-6 in intestinal cells (Walia et al. 2003). In addition, the contrary situation was observed in a lung cancer model, exhibiting a promoting role of TGF-β towards IL-6 (Yao et al. 2010). These reports underline the complexity of this molecular collaboration and strengthen the crucial importance of both cell specificity and state of disease for its outcome.

6.3.7 Investigations on PTEN/STAT3 interactions in human HCC

PTEN is commonly described as a tumor suppressor, playing an important role in regulating the PI3/AKT pathway. Its deletion, hypermethylation or mutation has been observed in several malignancies (Blanco-Aparicio et al. 2007). A conditional knockout in hepatocytes caused a steatohepatitis mimicking phenotype and consequently HCC (Horie et al. 2004). Furthermore, miR-21 was observed to down-regulate PTEN in human HCC samples (Meng et al. 2007). PTEN became particularly interesting upon a report characterizing its crosstalk with STAT3 in glioblastoma. This study of de la Iglesia and co-workers described two antagonistic interactions of STAT3 that crucially regulated the progress of this cancer (de la Iglesia et al. 2008). More precisely, LIFRβ (leukemia inhibitory factor receptor β), which is upstream of STAT3 activation in astrocytes, is downregulated via the AKT/FOXO3 axis upon knockout of PTEN. These STAT3 signaling deprived cells exhibited increased proliferation and, together with silencing PTEN, enhanced tumor formation. In contrast, EGFRvIII, a constitutive variant of EGFR, was shown to be dependent on STAT3 for mediating pro-oncogenic features. Noteworthy, STAT3 protein appeared to interact physically with EGFRvIII both in cytoplasm and in the nucleus (Fig. 25; de la Iglesia et al. 2008). A subsequent study revealed IL-8 as a crucial target of STAT3 in this scenario (de la Iglesia et al. 2008).

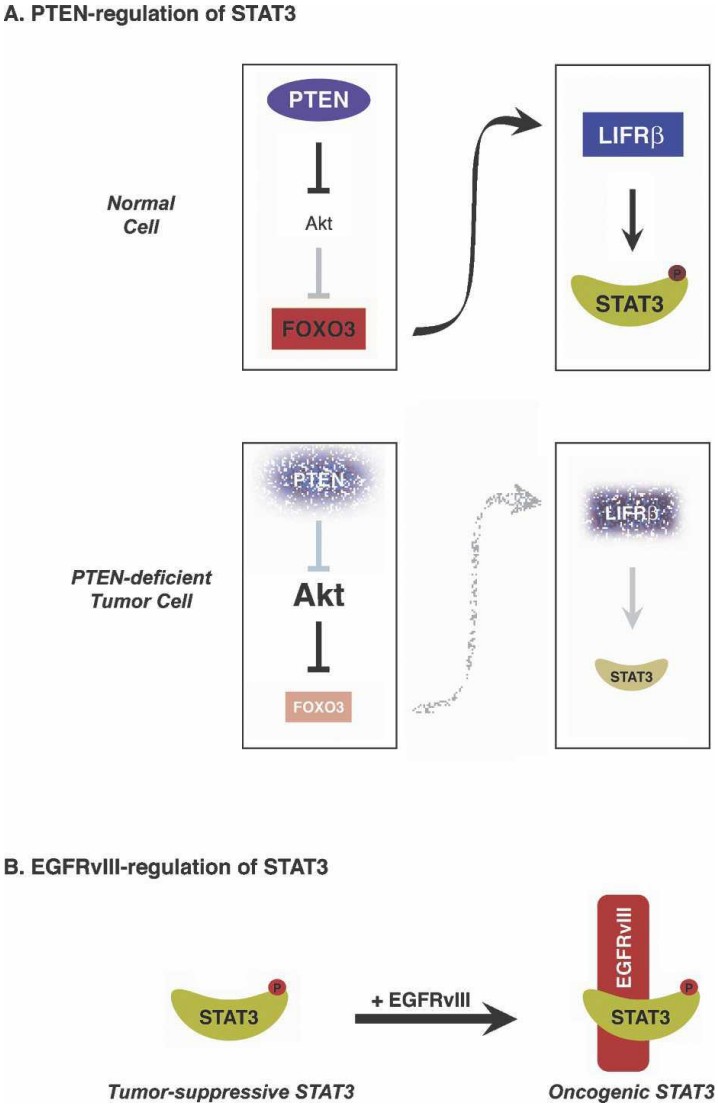

Fig. 25. Opposing roles of STAT3 dependent on cellular background. (A) Loss of PTEN in malignant cells indirectly diminishes STAT3 expression, thereby alleviating its anti-oncogenic effect in this genetic background. (B) In the context of EGFRvIII expressing glioblastoma, STAT3 is switched to pro-oncogenicity. Cartoon taken from de la Iglesia 2008.

Inspired by the findings observed in brain tumors, human hepatoma cells harboring a knockdown of PTEN were generated. Interestingly, this intervention caused a significant decrease in proliferation and tumor formation (Fig. 23B and data not shown). Hence, these results are in contrast to recent observations in glioblastoma and results observed in HCC, as mentioned earlier. Regarding the data obtained in glioblastoma, it has to be pointed out that activation of STAT3 via LIFRβ does not represent the major pathway in liver cancer, thus the PTEN/STAT3 axis might be distinct in HCC cells. Accordingly, IL-6 stimulation of PTEN-knockdown cells exhibited STAT3 activation (Fig. 23C). Nonetheless, the dramatic decrease in proliferation and tumor kinetic upon knockdown of the tumor suppressor PTEN remained unexpected, given the effect of specific deletion in a steatosis/HCC mouse model and the

frequent absence of PTEN observed in human HCC both accompanied by increased tumorigenicity (Dong-Dong et al. 2003; Horie et al. 2004).

The impact of PTEN deficiency in Hep3B-shPTEN cells became visible upon fluorescence staining of the cytoskeleton (Fig. 23D), showing actin foci structures at the cell membranes. It has been long known that PTEN also regulates Rac, a small GTPase that plays a role in cell migration and invasion (Mareel and Leroy 2003). Up-regulation of Rac is usually attributed to enhanced motility during malignancy (Parri and Chiarugi 2010). This alteration suggests an influence of the PTEN knockdown in these cells, yet the overall results obtained so far are not conclusive and would be subject of further investigations. For example, double knockout of both PTEN and STAT3 might elucidate whether the anti-proliferative effects of PTEN deficiency is dependent on total STAT3 protein.

6.4 Concluding remarks

Recently, Feng et al. reported paradox data obtained from various publications describing the development of liver cancer (Feng 2012). A proposed model how regulatory factors can contribute to HCC, even if they are missing, is shown in Figure 26. The author relied on their differential role in HCC pathogenesis, especially focusing on the lack of survival signals upon their deletion, leading to chronic hepatic burden. Consequently, infiltrating inflammatory mediators, such as Kupffer cells convey compensatory proliferation and neoplastic development. Therefore, investigations concerning pre-cancerous stages might provide more insights into the establishment of malignancies induced by the loss of a putative oncogene. Referring to available models in our lab, DEN induction in $p19^{ARF}$- and STAT3/$p19^{ARF}$-deficient mice, respectively, might reveal important observations from the onset of tumorigenesis.

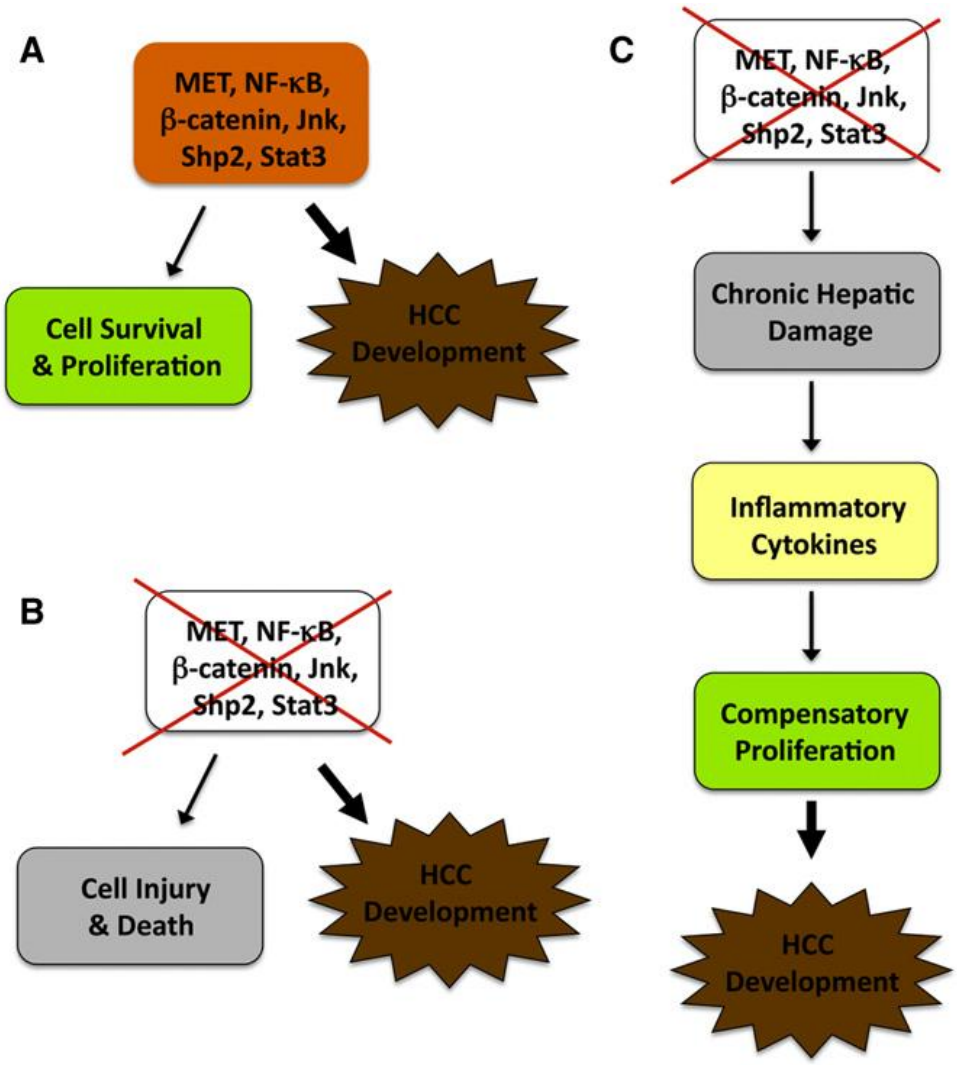

Fig. 26. Conflicting action of tumor promoters in HCC. (A), (B) MET, NFkB, β-catenin, JNK, SHP2 and STAT3 promote hepatocarcinogenesis both in their presence and absence. (C) Proposal of pathogenesis induced by the lack of these factors. Scheme taken from.Feng 2012.

The review further discussed the translatability of these phenomena to humans, since all results presented herein have been discovered in murine models. Accordingly, it was mentioned that mutations in the candidate genes resulting in loss of function have not yet been reported in humans. Indeed, this also accounts for STAT3, as rather activating than corrupting mutations have been commonly observed (Calvisi et al. 2006; Yang et al. 2007). Furthermore, although the human data refer to hepatoma cell lines, our results are in line towards different outcomes between murine and human HCC. As also mentioned in this review, the real-life situation might be much more complex than the straight-forward model depicted in the cartoon. Numerous regulatory molecules are able to interfere in each of this multi-stage cancer. As shown in Fig. 15, down-regulation of STAT3 occurred early in tumor development of Hep3B-shp14 cells that were subcutaneously injected into immunocompromised mice.

However, since Hep3B cells already acquired full tumorigenicity, it is certainly not an appropriate model for performing pre-malignant studies. Instead, screening for inflammatory markers in low-grade human HCC samples might reveal patterns predicting the prognosis of the tumor. With this kind of studies, deeper insights into the interaction of $p14^{ARF}$ and STAT3 in human HCC might be possible.

This study revealed interesting findings, such as the identification of both U-STAT3 isoforms for being able for nuclear translocation and transcriptional activity and the impact of STAT3 and $p14^{ARF}$ in various human hepatoma cell lines. However, the mechanistic link between these molecules has not yet been demonstrated. A recent paper revealed $p14^{ARF}$ being upstream of STAT3 activation, leading to the onset of a pro-apoptotic pathway in a lung cancer model bearing a common EGFR mutation. Interestingly, the latter was shown to attenuate $p14^{ARF}$ expression (Ozenne et al. 2012). Although the authors did not provide a mechanism addressing $p14^{ARF}$ and STAT3 actions, unpublished data regarding Tat-interacting protein (Tip60), a histone acetyl transferase, as a STAT3 activator has been mentioned. However, studies in human embryonic kidney (HEK) and, notably, in the hepatoma cell line HepG2 showed Tip60 as a co-repressor of STAT3, underlining the cell specificity of interactions (Xiao et al. 2003). Noteworthy, Tip60 belongs to the "ARF harem" (Pollice et al. 2008). Hence, Tip60 might also be considered in our cell models for implications in STAT3-dependent mechanisms.

In summary, the publication of Schneller et al. and further studies of the PhD thesis allowed deeper insights into the role of several important players in hepatocarcinogenesis, in particular $p14^{ARF}$ and STAT3. Currently, microarray analysis of STAT3 and $p19^{ARF}$-deficient, Ras-transformed hepatocytes (MIM-R-$STAT3^{\Delta hc}$) expressing U-STAT3α and U-STAT3β, respectively, is performed and the analysis will facilitate the understanding of unphosphorylated STAT3 proteins. Besides translating murine into human data, cell specificity of different cancers describes an important issue, as interactions of STAT3 with putative binding partners might be alternatively regulated. Therefore, the genetic background of the used models must be evaluated. In future, personalized "-omics" methods, such as ChIP-seq and RNA-seq will raise quality of information and will be helpful to avoid misappropriate and ineffective application of drugs (Montgomery and Dermitzakis 2011). Accordingly, this study suggests to determine the expression of $p14^{ARF}$ in HCC patients, as this indication might influence therapies targeting STAT3.

7 References

Abraham, R. T. (2001). "Cell cycle checkpoint signaling through the ATM and ATR kinases." Genes Dev **15**(17): 2177-2196.

Agger, K., P. A. Cloos, L. Rudkjaer, K. Williams, G. Andersen, J. Christensen and K. Helin (2009). "The H3K27me3 demethylase JMJD3 contributes to the activation of the INK4A-ARF locus in response to oncogene- and stress-induced senescence." Genes Dev **23**(10): 1171-1176.

Akira, S. (1999). "Functional roles of STAT family proteins: lessons from knockout mice." Stem Cells **17**(3): 138-146.

Akira, S., Y. Nishio, M. Inoue, X. J. Wang, S. Wei, T. Matsusaka, K. Yoshida, T. Sudo, M. Naruto and T. Kishimoto (1994). "Molecular cloning of APRF, a novel IFN-stimulated gene factor 3 p91-related transcription factor involved in the gp130-mediated signaling pathway." Cell **77**(1): 63-71.

Alazawi, W., M. Cunningham, J. Dearden and G. R. Foster (2010). "Systematic review: outcome of compensated cirrhosis due to chronic hepatitis C infection." Aliment Pharmacol Ther **32**(3): 344-355.

Altekruse, S. F., K. A. McGlynn and M. E. Reichman (2009). "Hepatocellular carcinoma incidence, mortality, and survival trends in the United States from 1975 to 2005." J Clin Oncol **27**(9): 1485-1491.

Amann, T., F. Bataille, T. Spruss, K. Dettmer, P. Wild, C. Liedtke, M. Muhlbauer, P. Kiefer, P. J. Oefner, C. Trautwein, A. K. Bosserhoff and C. Hellerbrand (2010). "Reduced expression of fibroblast growth factor receptor 2IIIb in hepatocellular carcinoma induces a more aggressive growth." Am J Pathol **176**(3): 1433-1442.

Anzola, M., N. Cuevas, M. Lopez-Martinez, A. Saiz, J. J. Burgos and M. Martinez de Pancorboa (2004). "P14ARF gene alterations in human hepatocellular carcinoma." Eur J Gastroenterol Hepatol **16**(1): 19-26.

Arany, I., D. K. Reed, S. C. Grifoni, K. Chandrashekar, G. W. Booz and L. A. Juncos (2012). "A novel U-STAT3-dependent mechanism mediates the deleterious effects of chronic nicotine exposure on renal injury." Am J Physiol Renal Physiol **302**(6): F722-729.

Ascha, M. S., I. A. Hanouneh, R. Lopez, T. A. Tamimi, A. F. Feldstein and N. N. Zein (2010). "The incidence and risk factors of hepatocellular carcinoma in patients with nonalcoholic steatohepatitis." Hepatology **51**(6): 1972-1978.

Awuah, P. K., B. H. Rhieu, S. Singh, A. Misse and S. P. Monga (2012). "beta-Catenin Loss in Hepatocytes Promotes Hepatocellular Cancer after Diethylnitrosamine and Phenobarbital Administration to Mice." PLoS One **7**(6): e39771.

Bard-Chapeau, E. A., S. Li, J. Ding, S. S. Zhang, H. H. Zhu, F. Princen, D. D. Fang, T. Han, B. Bailly-Maitre, V. Poli, N. M. Varki, H. Wang and G. S. Feng (2011). "Ptpn11/Shp2 acts as a tumor suppressor in hepatocellular carcinogenesis." Cancer Cell **19**(5): 629-639.

Barnes, P. J. and M. Karin (1997). "Nuclear factor-kappaB: a pivotal transcription factor in chronic inflammatory diseases." N Engl J Med **336**(15): 1066-1071.

Barra, V., T. Schillaci, L. Lentini, G. Costa and A. Di Leonardo (2012). "Bypass of cell cycle arrest induced by transient DNMT1 post-transcriptional silencing triggers aneuploidy in human cells." Cell Div **7**(1): 2.

Begitt, A., T. Meyer, M. van Rossum and U. Vinkemeier (2000). "Nucleocytoplasmic translocation of Stat1 is regulated by a leucine-rich export signal in the coiled-coil domain." Proc Natl Acad Sci U S A **97**(19): 10418-10423.

Bhogal, R. H., J. Hodson, D. C. Bartlett, C. J. Weston, S. M. Curbishley, E. Haughton, K. T. Williams, G. M. Reynolds, P. N. Newsome, D. H. Adams and S. C. Afford (2011). "Isolation of primary human hepatocytes from normal and diseased liver tissue: a one hundred liver experience." PLoS One **6**(3): e18222.

Blanco-Aparicio, C., O. Renner, J. F. Leal and A. Carnero (2007). "PTEN, more than the AKT pathway." Carcinogenesis **28**(7): 1379-1386.

Blivet-Van Eggelpoel, M. J., H. Chettouh, L. Fartoux, L. Aoudjehane, V. Barbu, C. Rey, S. Priam, C. Housset, O. Rosmorduc and C. Desbois-Mouthon (2012). "Epidermal growth factor receptor and HER-3 restrict cell response to sorafenib in hepatocellular carcinoma cells." J Hepatol **57**(1): 108-115.

Bowman, T., R. Garcia, J. Turkson and R. Jove (2000). "STATs in oncogenesis." Oncogene **19**(21): 2474-2488.

Brabletz, T., A. Jung, S. Reu, M. Porzner, F. Hlubek, L. A. Kunz-Schughart, R. Knuechel and T. Kirchner (2001). "Variable beta-catenin expression in colorectal cancers indicates tumor progression driven by the tumor environment." Proc Natl Acad Sci U S A **98**(18): 10356-10361.

Braunstein, J., S. Brutsaert, R. Olson and C. Schindler (2003). "STATs dimerize in the absence of phosphorylation." J Biol Chem **278**(36): 34133-34140.

Bromberg, J. F., C. M. Horvath, D. Besser, W. W. Lathem and J. E. Darnell, Jr. (1998). "Stat3 activation is required for cellular transformation by v-src." Mol Cell Biol **18**(5): 2553-2558.

Bromberg, J. F., M. H. Wrzeszczynska, G. Devgan, Y. Zhao, R. G. Pestell, C. Albanese and J. E. Darnell, Jr. (1999). "Stat3 as an oncogene." Cell **98**(3): 295-303.

Buckley, A. F., L. J. Burgart, V. Sahai and S. Kakar (2008). "Epidermal growth factor receptor expression and gene copy number in conventional hepatocellular carcinoma." Am J Clin Pathol **129**(2): 245-251.

Buontempo, F., T. Ersahin, S. Missiroli, S. Senturk, D. Etro, M. Ozturk, S. Capitani, R. Cetin-Atalay and M. L. Neri (2011). "Inhibition of Akt signaling in hepatoma cells induces apoptotic cell death independent of Akt activation status." Invest New Drugs **29**(6): 1303-1313.

Cabrera, R. and D. R. Nelson (2010). "Review article: the management of hepatocellular carcinoma." Aliment Pharmacol Ther **31**(4): 461-476.

Cai, B., J. Li, J. Wang, X. Luo, J. Ai, Y. Liu, N. Wang, H. Liang, M. Zhang, N. Chen, G. Wang, S. Xing, X. Zhou, B. Yang, X. Wang and Y. Lu (2012). "microRNA-124 Regulates Cardiomyocyte Differentiation of Bone Marrow-Derived Mesenchymal Stem Cells Via Targeting STAT3 Signaling." Stem Cells **30**(8): 1746-1755.

Cai, Q. W., J. Li, X. Q. Li, J. Q. Wang and Y. Huang (2012). "Expression of STAT3, MMP-1 and TIMP-1 in gastric cancer and correlation with pathological features." Mol Med Report **5**(6): 1438-1442.

Caldenhoven, E., T. B. van Dijk, R. Solari, J. Armstrong, J. A. Raaijmakers, J. W. Lammers, L. Koenderman and R. P. de Groot (1996). "STAT3beta, a splice variant of transcription factor STAT3, is a dominant negative regulator of transcription." J Biol Chem **271**(22): 13221-13227.

Calone, I. and S. Souchelnytskyi (2012). "Inhibition of TGFbeta signaling and its implications in anticancer treatments." Exp Oncol **34**(1): 9-16.

Calvisi, D. F. (2011). "Dr. Jekyll and Mr. Hyde: a paradoxical oncogenic and tumor suppressive role of signal transducer and activator of transcription 3 in liver cancer." Hepatology **54**(1): 9-12.

Calvisi, D. F., S. Ladu, E. A. Conner, D. Seo, J. T. Hsieh, V. M. Factor and S. S. Thorgeirsson (2011). "Inactivation of Ras GTPase-activating proteins promotes unrestrained activity of wild-type Ras in human liver cancer." J Hepatol **54**(2): 311-319.

Calvisi, D. F., S. Ladu, A. Gorden, M. Farina, E. A. Conner, J. S. Lee, V. M. Factor and S. S. Thorgeirsson (2006). "Ubiquitous activation of Ras and Jak/Stat pathways in human HCC." Gastroenterology **130**(4): 1117-1128.

Campbell, J. S., S. D. Hughes, D. G. Gilbertson, T. E. Palmer, M. S. Holdren, A. C. Haran, M. M. Odell, R. L. Bauer, H. P. Ren, H. S. Haugen, M. M. Yeh and N. Fausto (2005). "Platelet-derived growth factor C induces liver fibrosis, steatosis, and hepatocellular carcinoma." Proc Natl Acad Sci U S A **102**(9): 3389-3394.

Castillo, J., E. Erroba, M. J. Perugorria, M. Santamaria, D. C. Lee, J. Prieto, M. A. Avila and C. Berasain (2006). "Amphiregulin contributes to the transformed phenotype of human hepatocellular carcinoma cells." Cancer Res **66**(12): 6129-6138.

Catlett-Falcone, R., T. H. Landowski, M. M. Oshiro, J. Turkson, A. Levitzki, R. Savino, G. Ciliberto, L. Moscinski, J. L. Fernandez-Luna, G. Nunez, W. S. Dalton and R. Jove (1999). "Constitutive activation of Stat3 signaling confers resistance to apoptosis in human U266 myeloma cells." Immunity **10**(1): 105-115.

Chatterjee-Kishore, M., K. L. Wright, J. P. Ting and G. R. Stark (2000). "How Stat1 mediates constitutive gene expression: a complex of unphosphorylated Stat1 and IRF1 supports transcription of the LMP2 gene." EMBO J **19**(15): 4111-4122.

Chen, D., N. Kon, M. Li, W. Zhang, J. Qin and W. Gu (2005). "ARF-BP1/Mule is a critical mediator of the ARF tumor suppressor." Cell **121**(7): 1071-1083.

Chen, K. F., H. L. Chen, C. Y. Liu, W. T. Tai, K. Ichikawa, P. J. Chen and A. L. Cheng (2012). "Dovitinib sensitizes hepatocellular carcinoma cells to TRAIL and tigatuzumab, a novel anti-DR5 antibody, through SHP-1-dependent inhibition of STAT3." Biochem Pharmacol **83**(6): 769-777.

Chen, K. F., W. T. Tai, T. H. Liu, H. P. Huang, Y. C. Lin, C. W. Shiau, P. K. Li, P. J. Chen and A. L. Cheng (2010). "Sorafenib overcomes TRAIL resistance of hepatocellular carcinoma cells through the inhibition of STAT3." Clin Cancer Res **16**(21): 5189-5199.

Chen, L., Y. Shi, C. Y. Jiang, L. X. Wei, Y. L. Wang and G. H. Dai (2011). "Expression and prognostic role of pan-Ras, Raf-1, pMEK1 and pERK1/2 in patients with hepatocellular carcinoma." Eur J Surg Oncol **37**(6): 513-520.

Chen, W., X. Shen, X. Xia, G. Xu, T. Ma, X. Bai and T. Liang (2012). "NSC 74859-mediated inhibition of STAT3 enhances the anti-proliferative activity of cetuximab in hepatocellular carcinoma." Liver Int **32**(1): 70-77.

Chen, X., L. F. Barton, Y. Chi, B. E. Clurman and J. M. Roberts (2007). "Ubiquitin-independent degradation of cell-cycle inhibitors by the REGgamma proteasome." Mol Cell **26**(6): 843-852.

Chen, X., U. Vinkemeier, Y. Zhao, D. Jeruzalmi, J. E. Darnell, Jr. and J. Kuriyan (1998). "Crystal structure of a tyrosine phosphorylated STAT-1 dimer bound to DNA." Cell **93**(5): 827-839.

Chen, Y. W., S. Paliwal, K. Draheim, S. R. Grossman and B. C. Lewis (2008). "p19Arf inhibits the invasion of hepatocellular carcinoma cells by binding to C-terminal binding protein." Cancer Res **68**(2): 476-482.

Cheng, A. L., Y. C. Shen and A. X. Zhu (2011). "Targeting fibroblast growth factor receptor signaling in hepatocellular carcinoma." Oncology **81**(5-6): 372-380.

Chung, J., E. Uchida, T. C. Grammer and J. Blenis (1997). "STAT3 serine phosphorylation by ERK-dependent and -independent pathways negatively modulates its tyrosine phosphorylation." Mol Cell Biol **17**(11): 6508-6516.

Cimica, V., H. C. Chen, J. K. Iyer and N. C. Reich (2011). "Dynamics of the STAT3 transcription factor: nuclear import dependent on Ran and importin-beta1." PLoS One **6**(5): e20188.

Colombo, E., P. Martinelli, R. Zamponi, D. C. Shing, P. Bonetti, L. Luzi, S. Volorio, L. Bernard, G. Pruneri, M. Alcalay and P. G. Pelicci (2006). "Delocalization and destabilization of the Arf tumor suppressor by the leukemia-associated NPM mutant." Cancer Res **66**(6): 3044-3050.

Colomiere, M., A. C. Ward, C. Riley, M. K. Trenerry, D. Cameron-Smith, J. Findlay, L. Ackland and N. Ahmed (2009). "Cross talk of signals between EGFR and IL-6R through JAK2/STAT3 mediate epithelial-mesenchymal transition in ovarian carcinomas." Br J Cancer **100**(1): 134-144.

Couto, J. P., L. Daly, A. Almeida, J. A. Knauf, J. A. Fagin, M. Sobrinho-Simoes, J. Lima, V. Maximo, P. Soares, D. Lyden and J. F. Bromberg (2012). "STAT3 negatively regulates thyroid tumorigenesis." Proc Natl Acad Sci U S A **109**(35): E2361-2370.

Crawford, Y. and N. Ferrara (2009). "VEGF inhibition: insights from preclinical and clinical studies." Cell Tissue Res **335**(1): 261-269.

Cully, M., H. You, A. J. Levine and T. W. Mak (2006). "Beyond PTEN mutations: the PI3K pathway as an integrator of multiple inputs during tumorigenesis." Nat Rev Cancer **6**(3): 184-192.

Dahmani, R., P. A. Just and C. Perret (2011). "The Wnt/beta-catenin pathway as a therapeutic target in human hepatocellular carcinoma." Clin Res Hepatol Gastroenterol **35**(11): 709-713.

Dang, C. V. (2012). "MYC on the path to cancer." Cell **149**(1): 22-35.

Daniele, G., J. Corral, L. R. Molife and J. S. de Bono (2012). "FGF receptor inhibitors: role in cancer therapy." Curr Oncol Rep **14**(2): 111-119.

Darnell, J. E., Jr., I. M. Kerr and G. R. Stark (1994). "Jak-STAT pathways and transcriptional activation in response to IFNs and other extracellular signaling proteins." Science **264**(5164): 1415-1421.

Datta, A., J. Sen, J. Hagen, C. K. Korgaonkar, M. Caffrey, D. E. Quelle, D. E. Hughes, T. J. Ackerson, R. H. Costa and P. Raychaudhuri (2005). "ARF directly binds DP1: interaction with DP1 coincides with the G1 arrest function of ARF." Mol Cell Biol **25**(18): 8024-8036.

de la Iglesia, N., G. Konopka, K. L. Lim, C. L. Nutt, J. F. Bromberg, D. A. Frank, P. S. Mischel, D. N. Louis and A. Bonni (2008). "Deregulation of a STAT3-interleukin 8 signaling pathway promotes human glioblastoma cell proliferation and invasiveness." J Neurosci **28**(23): 5870-5878.

de la Iglesia, N., G. Konopka, S. V. Puram, J. A. Chan, R. M. Bachoo, M. J. You, D. E. Levy, R. A. Depinho and A. Bonni (2008). "Identification of a PTEN-regulated STAT3 brain tumor suppressor pathway." Genes Dev **22**(4): 449-462.

Dechow, T. N., L. Pedranzini, A. Leitch, K. Leslie, W. L. Gerald, I. Linkov and J. F. Bromberg (2004). "Requirement of matrix metalloproteinase-9 for the transformation of human mammary epithelial cells by Stat3-C." Proc Natl Acad Sci U S A **101**(29): 10602-10607.

Decker, T., D. J. Lew, J. Mirkovitch and J. E. Darnell, Jr. (1991). "Cytoplasmic activation of GAF, an IFN-gamma-regulated DNA-binding factor." EMBO J **10**(4): 927-932.

Demaria, M., C. Giorgi, M. Lebiedzinska, G. Esposito, L. D'Angeli, A. Bartoli, D. J. Gough, J. Turkson, D. E. Levy, C. J. Watson, M. R. Wieckowski, P. Provero, P. Pinton and V. Poli (2010). "A STAT3-mediated metabolic switch is involved in tumour transformation and STAT3 addiction." Aging (Albany NY) **2**(11): 823-842.

Dewilde, S., A. Vercelli, R. Chiarle and V. Poli (2008). "Of alphas and betas: distinct and overlapping functions of STAT3 isoforms." Front Biosci **13**: 6501-6514.

Dolled-Filhart, M., R. L. Camp, D. P. Kowalski, B. L. Smith and D. L. Rimm (2003). "Tissue microarray analysis of signal transducers and activators of transcription 3 (Stat3) and phospho-Stat3 (Tyr705) in node-negative breast cancer shows nuclear localization is associated with a better prognosis." Clin Cancer Res **9**(2): 594-600.

Dominguez-Brauer, C., Y. J. Chen, P. M. Brauer, J. Pimkina and P. Raychaudhuri (2009). "ARF stimulates XPC to trigger nucleotide excision repair by regulating the repressor complex of E2F4." EMBO Rep **10**(9): 1036-1042.

Dong-Dong, L., Z. Xi-Ran and C. Xiang-Rong (2003). "Expression and significance of new tumor suppressor gene PTEN in primary liver cancer." J Cell Mol Med **7**(1): 67-71.

Dumoutier, L., C. de Meester, J. Tavernier and J. C. Renauld (2009). "New activation modus of STAT3: a tyrosine-less region of the interleukin-22 receptor recruits STAT3 by interacting with its coiled-coil domain." J Biol Chem **284**(39): 26377-26384.

El-Serag, H. B. (2011). "Hepatocellular carcinoma." N Engl J Med **365**(12): 1118-1127.

El-Serag, H. B. (2012). "Epidemiology of viral hepatitis and hepatocellular carcinoma." Gastroenterology **142**(6): 1264-1273 e1261.

Epling-Burnette, P. K., J. H. Liu, R. Catlett-Falcone, J. Turkson, M. Oshiro, R. Kothapalli, Y. Li, J. M. Wang, H. F. Yang-Yen, J. Karras, R. Jove and T. P. Loughran, Jr. (2001). "Inhibition of STAT3 signaling leads to apoptosis of leukemic large granular lymphocytes and decreased Mcl-1 expression." J Clin Invest **107**(3): 351-362.

Eymin, B., P. Claverie, C. Salon, C. Leduc, E. Col, E. Brambilla, S. Khochbin and S. Gazzeri (2006). "p14ARF activates a Tip60-dependent and p53-independent ATM/ATR/CHK pathway in response to genotoxic stress." Mol Cell Biol **26**(11): 4339-4350.

Eymin, B., L. Karayan, P. Seite, C. Brambilla, E. Brambilla, C. J. Larsen and S. Gazzeri (2001). "Human ARF binds E2F1 and inhibits its transcriptional activity." Oncogene **20**(9): 1033-1041.

Ezzoukhry, Z., C. Louandre, E. Trecherel, C. Godin, B. Chauffert, S. Dupont, M. Diouf, J. C. Barbare, J. C. Maziere and A. Galmiche (2012). "EGFR activation is a potential determinant of primary resistance of hepatocellular carcinoma cells to sorafenib." Int J Cancer.

Farazi, P. A., J. Glickman, J. Horner and R. A. Depinho (2006). "Cooperative interactions of p53 mutation, telomere dysfunction, and chronic liver damage in hepatocellular carcinoma progression." Cancer Res **66**(9): 4766-4773.

Fatyol, K. and A. A. Szalay (2001). "The p14ARF tumor suppressor protein facilitates nucleolar sequestration of hypoxia-inducible factor-1alpha (HIF-1alpha) and inhibits HIF-1-mediated transcription." J Biol Chem **276**(30): 28421-28429.

Feng, G. S. (2012). "Conflicting roles of molecules in hepatocarcinogenesis: paradigm or paradox." Cancer Cell **21**(2): 150-154.

Feng, X. H. and R. Derynck (2005). "Specificity and versatility in tgf-beta signaling through Smads." Annu Rev Cell Dev Biol **21**: 659-693.

Firmbach-Kraft, I., M. Byers, T. Shows, R. Dalla-Favera and J. J. Krolewski (1990). "tyk2, prototype of a novel class of non-receptor tyrosine kinase genes." Oncogene **5**(9): 1329-1336.

Fischer, A. N., E. Fuchs, M. Mikula, H. Huber, H. Beug and W. Mikulits (2007). "PDGF essentially links TGF-beta signaling to nuclear beta-catenin accumulation in hepatocellular carcinoma progression." Oncogene **26**(23): 3395-3405.

Fischer, A. N., B. Herrera, M. Mikula, V. Proell, E. Fuchs, J. Gotzmann, R. Schulte-Hermann, H. Beug and W. Mikulits (2005). "Integration of Ras subeffector signaling in TGF-beta mediated late stage hepatocarcinogenesis." Carcinogenesis **26**(5): 931-942.

Forner, A., J. M. Llovet and J. Bruix (2012). "Hepatocellular carcinoma." Lancet **379**(9822): 1245-1255.

Fukai, K., O. Yokosuka, F. Imazeki, M. Tada, R. Mikata, M. Miyazaki, T. Ochiai and H. Saisho (2005). "Methylation status of p14ARF, p15INK4b, and p16INK4a genes in human hepatocellular carcinoma." Liver Int **25**(6): 1209-1216.

Garcia, M. A., M. Collado, C. Munoz-Fontela, A. Matheu, L. Marcos-Villar, J. Arroyo, M. Esteban, M. Serrano and C. Rivas (2006). "Antiviral action of the tumor suppressor ARF." EMBO J **25**(18): 4284-4292.

Garcia, R., C. L. Yu, A. Hudnall, R. Catlett, K. L. Nelson, T. Smithgall, D. J. Fujita, S. P. Ethier and R. Jove (1997). "Constitutive activation of Stat3 in fibroblasts transformed

by diverse oncoproteins and in breast carcinoma cells." Cell Growth Differ **8**(12): 1267-1276.

Gauglhofer, C., S. Sagmeister, W. Schrottmaier, C. Fischer, C. Rodgarkia-Dara, T. Mohr, S. Stattner, C. Bichler, D. Kandioler, F. Wrba, R. Schulte-Hermann, K. Holzmann, M. Grusch, B. Marian, W. Berger and B. Grasl-Kraupp (2011). "Up-regulation of the fibroblast growth factor 8 subfamily in human hepatocellular carcinoma for cell survival and neoangiogenesis." Hepatology **53**(3): 854-864.

Georgiades, C. S., K. Hong, M. D'Angelo and J. F. Geschwind (2005). "Safety and efficacy of transarterial chemoembolization in patients with unresectable hepatocellular carcinoma and portal vein thrombosis." J Vasc Interv Radiol **16**(12): 1653-1659.

Gotzmann, J., H. Huber, C. Thallinger, M. Wolschek, B. Jansen, R. Schulte-Hermann, H. Beug and W. Mikulits (2002). "Hepatocytes convert to a fibroblastoid phenotype through the cooperation of TGF-beta1 and Ha-Ras: steps towards invasiveness." J Cell Sci **115**(Pt 6): 1189-1202.

Gough, D. J., A. Corlett, K. Schlessinger, J. Wegrzyn, A. C. Larner and D. E. Levy (2009). "Mitochondrial STAT3 supports Ras-dependent oncogenic transformation." Science **324**(5935): 1713-1716.

Greenman, C., P. Stephens, R. Smith, G. L. Dalgliesh, C. Hunter, G. Bignell, H. Davies, J. Teague, A. Butler, C. Stevens, S. Edkins, S. O'Meara, I. Vastrik, E. E. Schmidt, T. Avis, S. Barthorpe, G. Bhamra, G. Buck, B. Choudhury, J. Clements, J. Cole, E. Dicks, S. Forbes, K. Gray, K. Halliday, R. Harrison, K. Hills, J. Hinton, A. Jenkinson, D. Jones, A. Menzies, T. Mironenko, J. Perry, K. Raine, D. Richardson, R. Shepherd, A. Small, C. Tofts, J. Varian, T. Webb, S. West, S. Widaa, A. Yates, D. P. Cahill, D. N. Louis, P. Goldstraw, A. G. Nicholson, F. Brasseur, L. Looijenga, B. L. Weber, Y. E. Chiew, A. DeFazio, M. F. Greaves, A. R. Green, P. Campbell, E. Birney, D. F. Easton, G. Chenevix-Trench, M. H. Tan, S. K. Khoo, B. T. Teh, S. T. Yuen, S. Y. Leung, R. Wooster, P. A. Futreal and M. R. Stratton (2007). "Patterns of somatic mutation in human cancer genomes." Nature **446**(7132): 153-158.

Gu, F. M., Q. L. Li, Q. Gao, J. H. Jiang, K. Zhu, X. Y. Huang, J. F. Pan, J. Yan, J. H. Hu, Z. Wang, Z. Dai, J. Fan and J. Zhou (2011). "IL-17 induces AKT-dependent IL-6/JAK2/STAT3 activation and tumor progression in hepatocellular carcinoma." Mol Cancer **10**: 150.

Guo, G. G., K. Patel, V. Kumar, M. Shah, V. A. Fried, J. D. Etlinger and P. B. Sehgal (2002). "Association of the chaperone glucose-regulated protein 58 (GRP58/ER-60/ERp57) with Stat3 in cytosol and plasma membrane complexes." J Interferon Cytokine Res **22**(5): 555-563.

Hanahan, D. and R. A. Weinberg (2011). "Hallmarks of cancer: the next generation." Cell **144**(5): 646-674.

Harimoto, N., K. Taguchi, K. Shirabe, E. Adachi, Y. Sakaguchi, Y. Toh, T. Okamura, H. Kayashima, A. Taketomi and Y. Maehara (2010). "The significance of fibroblast growth factor receptor 2 expression in differentiation of hepatocellular carcinoma." Oncology **78**(5-6): 361-368.

He, G., G. Y. Yu, V. Temkin, H. Ogata, C. Kuntzen, T. Sakurai, W. Sieghart, M. Peck-Radosavljevic, H. L. Leffert and M. Karin (2010). "Hepatocyte IKKbeta/NF-kappaB

inhibits tumor promotion and progression by preventing oxidative stress-driven STAT3 activation." Cancer Cell **17**(3): 286-297.

Helin, K., E. Harlow and A. Fattaey (1993). "Inhibition of E2F-1 transactivation by direct binding of the retinoblastoma protein." Mol Cell Biol **13**(10): 6501-6508.

Higashiyama, S., H. Iwabuki, C. Morimoto, M. Hieda, H. Inoue and N. Matsushita (2008). "Membrane-anchored growth factors, the epidermal growth factor family: beyond receptor ligands." Cancer Sci **99**(2): 214-220.

Ho, C., C. Wang, S. Mattu, G. Destefanis, S. Ladu, S. Delogu, J. Armbruster, L. Fan, S. A. Lee, L. Jiang, F. Dombrowski, M. Evert, X. Chen and D. F. Calvisi (2012). "AKT (v-akt murine thymoma viral oncogene homolog 1) and N-Ras (neuroblastoma ras viral oncogene homolog) coactivation in the mouse liver promotes rapid carcinogenesis by way of mTOR (mammalian target of rapamycin complex 1), FOXM1 (forkhead box M1)/SKP2, and c-Myc pathways." Hepatology **55**(3): 833-845.

Horie, Y., A. Suzuki, E. Kataoka, T. Sasaki, K. Hamada, J. Sasaki, K. Mizuno, G. Hasegawa, H. Kishimoto, M. Iizuka, M. Naito, K. Enomoto, S. Watanabe, T. W. Mak and T. Nakano (2004). "Hepatocyte-specific Pten deficiency results in steatohepatitis and hepatocellular carcinomas." J Clin Invest **113**(12): 1774-1783.

Horvath, C. M., Z. Wen and J. E. Darnell, Jr. (1995). "A STAT protein domain that determines DNA sequence recognition suggests a novel DNA-binding domain." Genes Dev **9**(8): 984-994.

Hosui, A., A. Kimura, D. Yamaji, B. M. Zhu, R. Na and L. Hennighausen (2009). "Loss of STAT5 causes liver fibrosis and cancer development through increased TGF-{beta} and STAT3 activation." J Exp Med **206**(4): 819-831.

Hou, J., U. Schindler, W. J. Henzel, T. C. Ho, M. Brasseur and S. L. McKnight (1994). "An interleukin-4-induced transcription factor: IL-4 Stat." Science **265**(5179): 1701-1706.

Hou, J., J. Xu, R. Jiang, Y. Wang, C. Chen, L. Deng, X. Huang, X. Wang and B. Sun (2012). "Estrogen sensitive PTPRO expression represses hepatocellular carcinoma progression by control of STAT3." Hepatology.

Huang, S. (2007). "Regulation of metastases by signal transducer and activator of transcription 3 signaling pathway: clinical implications." Clin Cancer Res **13**(5): 1362-1366.

Huang, S. and P. J. Houghton (2001). "Mechanisms of resistance to rapamycins." Drug Resist Updat **4**(6): 378-391.

Huang, Y., J. Qiu, S. Dong, M. S. Redell, V. Poli, M. A. Mancini and D. J. Tweardy (2007). "Stat3 isoforms, alpha and beta, demonstrate distinct intracellular dynamics with prolonged nuclear retention of Stat3beta mapping to its unique C-terminal end." J Biol Chem **282**(48): 34958-34967.

Humphrey, P. A., A. J. Wong, B. Vogelstein, M. R. Zalutsky, G. N. Fuller, G. E. Archer, H. S. Friedman, M. M. Kwatra, S. H. Bigner and D. D. Bigner (1990). "Anti-synthetic peptide antibody reacting at the fusion junction of deletion-mutant epidermal growth factor receptors in human glioblastoma." Proc Natl Acad Sci U S A **87**(11): 4207-4211.

Huynh, H., R. Ong and K. C. Soo (2012). "Foretinib demonstrates anti-tumor activity and improves overall survival in preclinical models of hepatocellular carcinoma." Angiogenesis **15**(1): 59-70.

Hwang, Y. H., J. Y. Choi, S. Kim, E. S. Chung, T. Kim, S. S. Koh, B. Lee, S. H. Bae, J. Kim and Y. M. Park (2004). "Over-expression of c-raf-1 proto-oncogene in liver cirrhosis and hepatocellular carcinoma." Hepatol Res **29**(2): 113-121.

Itahana, K., K. P. Bhat, A. Jin, Y. Itahana, D. Hawke, R. Kobayashi and Y. Zhang (2003). "Tumor suppressor ARF degrades B23, a nucleolar protein involved in ribosome biogenesis and cell proliferation." Mol Cell **12**(5): 1151-1164.

Ito, T., N. Nishida, Y. Fukuda, T. Nishimura, T. Komeda and K. Nakao (2004). "Alteration of the p14(ARF) gene and p53 status in human hepatocellular carcinomas." J Gastroenterol **39**(4): 355-361.

Ivanov, V. N., A. Bhoumik, M. Krasilnikov, R. Raz, L. B. Owen-Schaub, D. Levy, C. M. Horvath and Z. Ronai (2001). "Cooperation between STAT3 and c-jun suppresses Fas transcription." Mol Cell **7**(3): 517-528.

Ivanovska, I., C. Zhang, A. M. Liu, K. F. Wong, N. P. Lee, P. Lewis, U. Philippar, D. Bansal, C. Buser, M. Scott, M. Mao, R. T. Poon, S. T. Fan, M. A. Cleary, J. M. Luk and H. Dai (2011). "Gene signatures derived from a c-MET-driven liver cancer mouse model predict survival of patients with hepatocellular carcinoma." PLoS One **6**(9): e24582.

Jamieson, C., M. Sharma and B. R. Henderson (2012). "Wnt signaling from membrane to nucleus: beta-catenin caught in a loop." Int J Biochem Cell Biol **44**(6): 847-850.

Jenkins, B. J., D. Grail, T. Nheu, M. Najdovska, B. Wang, P. Waring, M. Inglese, R. M. McLoughlin, S. A. Jones, N. Topley, H. Baumann, L. M. Judd, A. S. Giraud, A. Boussioutas, H. J. Zhu and M. Ernst (2005). "Hyperactivation of Stat3 in gp130 mutant mice promotes gastric hyperproliferation and desensitizes TGF-beta signaling." Nat Med **11**(8): 845-852.

Jiang, R., Z. Tan, L. Deng, Y. Chen, Y. Xia, Y. Gao, X. Wang and B. Sun (2011). "Interleukin-22 promotes human hepatocellular carcinoma by activation of STAT3." Hepatology **54**(3): 900-909.

Jo, H., R. Zhang, H. Zhang, T. A. McKinsey, J. Shao, R. D. Beauchamp, D. W. Ballard and P. Liang (2000). "NF-kappa B is required for H-ras oncogene induced abnormal cell proliferation and tumorigenesis." Oncogene **19**(7): 841-849.

Johnson, D. E. and L. T. Williams (1993). "Structural and functional diversity in the FGF receptor multigene family." Adv Cancer Res **60**: 1-41.

Johnson, G. L. and R. Lapadat (2002). "Mitogen-activated protein kinase pathways mediated by ERK, JNK, and p38 protein kinases." Science **298**(5600): 1911-1912.

Jorissen, R. N., F. Walker, N. Pouliot, T. P. Garrett, C. W. Ward and A. W. Burgess (2003). "Epidermal growth factor receptor: mechanisms of activation and signalling." Exp Cell Res **284**(1): 31-53.

Jung, K. H., M. J. Choi, S. Hong, H. Lee, S. W. Hong, H. M. Zheng, H. S. Lee and S. S. Hong (2012). "HS-116, a novel phosphatidylinositol 3-kinase inhibitor induces apoptosis and suppresses angiogenesis of hepatocellular carcinoma through inhibition of the PI3K/AKT/mTOR pathway." Cancer Lett **316**(2): 187-195.

Kamijo, T., J. D. Weber, G. Zambetti, F. Zindy, M. F. Roussel and C. J. Sherr (1998). "Functional and physical interactions of the ARF tumor suppressor with p53 and Mdm2." Proc Natl Acad Sci U S A **95**(14): 8292-8297.

Kamijo, T., F. Zindy, M. F. Roussel, D. E. Quelle, J. R. Downing, R. A. Ashmun, G. Grosveld and C. J. Sherr (1997). "Tumor suppression at the mouse INK4a locus mediated by the alternative reading frame product p19ARF." Cell **91**(5): 649-659.

Kaposi-Novak, P., J. S. Lee, L. Gomez-Quiroz, C. Coulouarn, V. M. Factor and S. S. Thorgeirsson (2006). "Met-regulated expression signature defines a subset of human hepatocellular carcinomas with poor prognosis and aggressive phenotype." J Clin Invest **116**(6): 1582-1595.

Kelly-Spratt, K. S., K. E. Gurley, Y. Yasui and C. J. Kemp (2004). "p19Arf suppresses growth, progression, and metastasis of Hras-driven carcinomas through p53-dependent and -independent pathways." PLoS Biol **2**(8): E242.

Khan, K. N., H. Yatsuhashi, K. Yamasaki, M. Yamasaki, O. Inoue, M. Koga and M. Yano (2000). "Prospective analysis of risk factors for early intrahepatic recurrence of hepatocellular carcinoma following ethanol injection." J Hepatol **32**(2): 269-278.

Kim, D. H., D. D. Sarbassov, S. M. Ali, J. E. King, R. R. Latek, H. Erdjument-Bromage, P. Tempst and D. M. Sabatini (2002). "mTOR interacts with raptor to form a nutrient-sensitive complex that signals to the cell growth machinery." Cell **110**(2): 163-175.

Kishimoto, T., S. Akira, M. Narazaki and T. Taga (1995). "Interleukin-6 family of cytokines and gp130." Blood **86**(4): 1243-1254.

Kondo, S., H. Ojima, H. Tsuda, J. Hashimoto, C. Morizane, M. Ikeda, H. Ueno, K. Tamura, K. Shimada, Y. Kanai and T. Okusaka (2012). "Clinical impact of c-Met expression and its gene amplification in hepatocellular carcinoma." Int J Clin Oncol.

Kortylewski, M., M. Kujawski, T. Wang, S. Wei, S. Zhang, S. Pilon-Thomas, G. Niu, H. Kay, J. Mule, W. G. Kerr, R. Jove, D. Pardoll and H. Yu (2005). "Inhibiting Stat3 signaling in the hematopoietic system elicits multicomponent antitumor immunity." Nat Med **11**(12): 1314-1321.

Kuan, C. T., C. J. Wikstrand and D. D. Bigner (2001). "EGF mutant receptor vIII as a molecular target in cancer therapy." Endocr Relat Cancer **8**(2): 83-96.

Law, P. T., A. K. Ching, A. W. Chan, Q. W. Wong, C. K. Wong, K. F. To and N. Wong (2012). "MiR-145 modulates multiple components of the insulin-like growth factor pathway in hepatocellular carcinoma." Carcinogenesis **33**(6): 1-8.

Lechel, A., H. Holstege, Y. Begus, A. Schienke, K. Kamino, U. Lehmann, S. Kubicka, P. Schirmacher, J. Jonkers and K. L. Rudolph (2007). "Telomerase deletion limits progression of p53-mutant hepatocellular carcinoma with short telomeres in chronic liver disease." Gastroenterology **132**(4): 1465-1475.

Lee, J., J. C. Kim, S. E. Lee, C. Quinley, H. Kim, S. Herdman, M. Corr and E. Raz (2012). "Signal transducer and activator of transcription 3 (STAT3) protein suppresses adenoma-to-carcinoma transition in Apcmin/+ mice via regulation of Snail-1 (SNAI) protein stability." J Biol Chem **287**(22): 18182-18189.

Lee, T. K., A. Castilho, V. C. Cheung, K. H. Tang, S. Ma and I. O. Ng (2011). "CD24(+) liver tumor-initiating cells drive self-renewal and tumor initiation through STAT3-mediated NANOG regulation." Cell Stem Cell **9**(1): 50-63.

Leite de Oliveira, R., A. Hamm and M. Mazzone (2011). "Growing tumor vessels: more than one way to skin a cat - implications for angiogenesis targeted cancer therapies." Mol Aspects Med **32**(2): 71-87.

Levine, A. J., N. Reich and R. Thomas (1983). "The regulation of a cellular protein, p53, in normal and transformed cells." Prog Clin Biol Res **119**: 159-169.

Levy, D. E. and J. E. Darnell, Jr. (2002). "Stats: transcriptional control and biological impact." Nat Rev Mol Cell Biol **3**(9): 651-662.

Levy, D. E. and C. K. Lee (2002). "What does Stat3 do?" J Clin Invest **109**(9): 1143-1148.

Li, Q. L., F. M. Gu, Z. Wang, J. H. Jiang, L. Q. Yao, C. J. Tan, X. Y. Huang, A. W. Ke, Z. Dai, J. Fan and J. Zhou (2012). "Activation of PI3K/AKT and MAPK pathway through a PDGFRbeta-dependent feedback loop is involved in rapamycin resistance in hepatocellular carcinoma." PLoS One **7**(3): e33379.

Li, T., Y. Zhu, C. Y. Qin, Z. Yang, A. Fang, S. Xu and W. Ren (2012). "Expression and prognostic significance of vascular endothelial growth factor receptor 1 in hepatocellular carcinoma." J Clin Pathol.

Li, W. C., S. L. Ye, R. X. Sun, Y. K. Liu, Z. Y. Tang, Y. Kim, J. G. Karras and H. Zhang (2006). "Inhibition of growth and metastasis of human hepatocellular carcinoma by antisense oligonucleotide targeting signal transducer and activator of transcription 3." Clin Cancer Res **12**(23): 7140-7148.

Li, Z. and S. R. Hann (2009). "The Myc-nucleophosmin-ARF network: a complex web unveiled." Cell Cycle **8**(17): 2703-2707.

Liddle, F. J., J. V. Alvarez, V. Poli and D. A. Frank (2006). "Tyrosine phosphorylation is required for functional activation of disulfide-containing constitutively active STAT mutants." Biochemistry **45**(17): 5599-5605.

Lin, A. W. and S. W. Lowe (2001). "Oncogenic ras activates the ARF-p53 pathway to suppress epithelial cell transformation." Proc Natl Acad Sci U S A **98**(9): 5025-5030.

Lin, H. Y., S. C. Hou, S. C. Chen, M. C. Kao, C. C. Yu, S. Funayama, C. T. Ho and T. D. Way (2012). "(-)-Epigallocatechin gallate induces Fas/CD95-mediated apoptosis through inhibiting constitutive and IL-6-induced JAK/STAT3 signaling in head and neck squamous cell carcinoma cells." J Agric Food Chem **60**(10): 2480-2489.

Lin, L., R. Amin, G. I. Gallicano, E. Glasgow, W. Jogunoori, J. M. Jessup, M. Zasloff, J. L. Marshall, K. Shetty, L. Johnson, L. Mishra and A. R. He (2009). "The STAT3 inhibitor NSC 74859 is effective in hepatocellular cancers with disrupted TGF-beta signaling." Oncogene **28**(7): 961-972.

Liu, P., H. Cheng, T. M. Roberts and J. J. Zhao (2009). "Targeting the phosphoinositide 3-kinase pathway in cancer." Nat Rev Drug Discov **8**(8): 627-644.

Liu, X., G. W. Robinson, F. Gouilleux, B. Groner and L. Hennighausen (1995). "Cloning and expression of Stat5 and an additional homologue (Stat5b) involved in prolactin signal transduction in mouse mammary tissue." Proc Natl Acad Sci U S A **92**(19): 8831-8835.

Liu, Z., I. Hazan-Halevy, D. M. Harris, P. Li, A. Ferrajoli, S. Faderl, M. J. Keating and Z. Estrov (2011). "STAT-3 activates NF-kappaB in chronic lymphocytic leukemia cells." Mol Cancer Res **9**(4): 507-515.

Llanos, S., P. A. Clark, J. Rowe and G. Peters (2001). "Stabilization of p53 by p14ARF without relocation of MDM2 to the nucleolus." Nat Cell Biol **3**(5): 445-452.

Llovet, J. M., S. Ricci, V. Mazzaferro, P. Hilgard, E. Gane, J. F. Blanc, A. C. de Oliveira, A. Santoro, J. L. Raoul, A. Forner, M. Schwartz, C. Porta, S. Zeuzem, L. Bolondi, T. F. Greten, P. R. Galle, J. F. Seitz, I. Borbath, D. Haussinger, T. Giannaris, M. Shan, M. Moscovici, D. Voliotis and J. Bruix (2008). "Sorafenib in advanced hepatocellular carcinoma." N Engl J Med **359**(4): 378-390.

Lo, H. W., S. C. Hsu, W. Xia, X. Cao, J. Y. Shih, Y. Wei, J. L. Abbruzzese, G. N. Hortobagyi and M. C. Hung (2007). "Epidermal growth factor receptor cooperates with signal transducer and activator of transcription 3 to induce epithelial-mesenchymal transition in cancer cells via up-regulation of TWIST gene expression." Cancer Res **67**(19): 9066-9076.

Loges, S., M. Mazzone, P. Hohensinner and P. Carmeliet (2009). "Silencing or fueling metastasis with VEGF inhibitors: antiangiogenesis revisited." Cancer Cell **15**(3): 167-170.

Luwor, R. B., B. Baradaran, L. E. Taylor, J. Iaria, T. V. Nheu, N. Amiry, C. M. Hovens, B. Wang, A. H. Kaye and H. J. Zhu (2012). "Targeting Stat3 and Smad7 to restore TGF-beta cytostatic regulation of tumor cells in vitro and in vivo." Oncogene.

Ma, J. and X. Cao (2006). "Regulation of Stat3 nuclear import by importin alpha5 and importin alpha7 via two different functional sequence elements." Cell Signal **18**(8): 1117-1126.

Maass, T., F. R. Thieringer, A. Mann, T. Longerich, P. Schirmacher, D. Strand, T. Hansen, P. R. Galle, A. Teufel and S. Kanzler (2011). "Liver specific overexpression of platelet-derived growth factor-B accelerates liver cancer development in chemically induced liver carcinogenesis." Int J Cancer **128**(6): 1259-1268.

MacDonald, B. T., K. Tamai and X. He (2009). "Wnt/beta-catenin signaling: components, mechanisms, and diseases." Dev Cell **17**(1): 9-26.

Machado-Silva, A., S. Perrier and J. C. Bourdon (2010). "p53 family members in cancer diagnosis and treatment." Semin Cancer Biol **20**(1): 57-62.

Machida, K., H. Tsukamoto, J. C. Liu, Y. P. Han, S. Govindarajan, M. M. Lai, S. Akira and J. H. Ou (2010). "c-Jun mediates hepatitis C virus hepatocarcinogenesis through signal transducer and activator of transcription 3 and nitric oxide-dependent impairment of oxidative DNA repair." Hepatology **52**(2): 480-492.

Mak, G. W., W. L. Lai, Y. Zhou, M. Li, I. O. Ng and Y. P. Ching (2012). "CDK5RAP3 Is a Novel Repressor of p14(ARF) in Hepatocellular Carcinoma Cells." PLoS One **7**(7): e42210.

Malumbres, M. and M. Barbacid (2003). "RAS oncogenes: the first 30 years." Nat Rev Cancer **3**(6): 459-465.

Mareel, M. and A. Leroy (2003). "Clinical, cellular, and molecular aspects of cancer invasion." Physiol Rev **83**(2): 337-376.

Maritano, D., M. L. Sugrue, S. Tininini, S. Dewilde, B. Strobl, X. Fu, V. Murray-Tait, R. Chiarle and V. Poli (2004). "The STAT3 isoforms alpha and beta have unique and specific functions." Nat Immunol **5**(4): 401-409.

Masuda, M., M. Shimomura, K. Kobayashi, S. Kojima and T. Nakatsura (2011). "Growth inhibition by NVP-BEZ235, a dual PI3K/mTOR inhibitor, in hepatocellular carcinoma cell lines." Oncol Rep **26**(5): 1273-1279.

Matsuda, T., T. Nakamura, K. Nakao, T. Arai, M. Katsuki, T. Heike and T. Yokota (1999). "STAT3 activation is sufficient to maintain an undifferentiated state of mouse embryonic stem cells." EMBO J **18**(15): 4261-4269.

Meng, F., R. Henson, H. Wehbe-Janek, K. Ghoshal, S. T. Jacob and T. Patel (2007). "MicroRNA-21 regulates expression of the PTEN tumor suppressor gene in human hepatocellular cancer." Gastroenterology **133**(2): 647-658.

Meyer, T. and U. Vinkemeier (2004). "Nucleocytoplasmic shuttling of STAT transcription factors." Eur J Biochem **271**(23-24): 4606-4612.

Mima, K., H. Okabe, T. Ishimoto, H. Hayashi, S. Nakagawa, H. Kuroki, M. Watanabe, T. Beppu, M. Tamada, O. Nagano, H. Saya and H. Baba (2012). "CD44s Regulates the TGF-beta-Mediated Mesenchymal Phenotype and Is Associated with Poor Prognosis in Patients with Hepatocellular Carcinoma." Cancer Res **72**(13): 3414-3423.

Mitin, N., K. L. Rossman and C. J. Der (2005). "Signaling interplay in Ras superfamily function." Curr Biol **15**(14): R563-574.

Miura, S., N. Mitsuhashi, H. Shimizu, F. Kimura, H. Yoshidome, M. Otsuka, A. Kato, T. Shida, D. Okamura and M. Miyazaki (2012). "Fibroblast growth factor 19 expression correlates with tumor progression and poorer prognosis of hepatocellular carcinoma." BMC Cancer **12**: 56.

Miyazono, K. (2009). "Transforming growth factor-beta signaling in epithelial-mesenchymal transition and progression of cancer." Proc Jpn Acad Ser B Phys Biol Sci **85**(8): 314-323.

Montgomery, S. B. and E. T. Dermitzakis (2011). "From expression QTLs to personalized transcriptomics." Nat Rev Genet **12**(4): 277-282.

Morris, S. M., J. Y. Baek, A. Koszarek, S. Kanngurn, S. E. Knoblaugh and W. M. Grady (2012). "Transforming growth factor-beta signaling promotes hepatocarcinogenesis induced by p53 loss." Hepatology **55**(1): 121-131.

Mu, Y., S. K. Gudey and M. Landstrom (2012). "Non-Smad signaling pathways." Cell Tissue Res **347**(1): 11-20.

Mui, A. L., H. Wakao, A. M. O'Farrell, N. Harada and A. Miyajima (1995). "Interleukin-3, granulocyte-macrophage colony stimulating factor and interleukin-5 transduce signals through two STAT5 homologs." EMBO J **14**(6): 1166-1175.

Musteanu, M., L. Blaas, M. Mair, M. Schlederer, M. Bilban, S. Tauber, H. Esterbauer, M. Mueller, E. Casanova, L. Kenner, V. Poli and R. Eferl (2010). "Stat3 is a negative regulator of intestinal tumor progression in Apc(Min) mice." Gastroenterology **138**(3): 1003-1011 e1001-1005.

Nagaraj, N. S. and P. K. Datta (2010). "Targeting the transforming growth factor-beta signaling pathway in human cancer." Expert Opin Investig Drugs **19**(1): 77-91.

Ndubuisi, M. I., G. G. Guo, V. A. Fried, J. D. Etlinger and P. B. Sehgal (1999). "Cellular physiology of STAT3: Where's the cytoplasmic monomer?" J Biol Chem **274**(36): 25499-25509.

Ng, I. H., D. C. Ng, D. A. Jans and M. A. Bogoyevitch (2012). "Selective STAT3-alpha or -beta expression reveals spliceform-specific phosphorylation kinetics, nuclear retention and distinct gene expression outcomes." Biochem J.

Niu, G., K. H. Shain, M. Huang, R. Ravi, A. Bedi, W. S. Dalton, R. Jove and H. Yu (2001). "Overexpression of a dominant-negative signal transducer and activator of transcription 3 variant in tumor cells leads to production of soluble factors that induce apoptosis and cell cycle arrest." Cancer Res **61**(8): 3276-3280.

Niu, G., K. L. Wright, Y. Ma, G. M. Wright, M. Huang, R. Irby, J. Briggs, J. Karras, W. D. Cress, D. Pardoll, R. Jove, J. Chen and H. Yu (2005). "Role of Stat3 in regulating p53 expression and function." Mol Cell Biol **25**(17): 7432-7440.

Nordenstedt, H., D. L. White and H. B. El-Serag (2010). "The changing pattern of epidemiology in hepatocellular carcinoma." Dig Liver Dis **42 Suppl 3**: S206-214.

O'Shea, J. J., M. Gadina and R. D. Schreiber (2002). "Cytokine signaling in 2002: new surprises in the Jak/Stat pathway." Cell **109 Suppl**: S121-131.

Oh, H. M., C. R. Yu, I. Dambuza, B. Marrero and C. E. Egwuagu (2012). "STAT3 interacts with Class O Forkhead transcription factors in the cytoplasm and regulates nuclear/cytoplasmic localization of FoxO1 and FoxO3a in CD4+ T cells." J Biol Chem.

Osborne, J. K., E. Zaganjor and M. H. Cobb (2012). "Signal control through Raf: in sickness and in health." Cell Res **22**(1): 14-22.

Ozenne, P., D. Dayde, E. Brambilla, B. Eymin and S. Gazzeri (2012). "p14(ARF) inhibits the growth of lung adenocarcinoma cells harbouring an EGFR L858R mutation by activating a STAT3-dependent pro-apoptotic signalling pathway." Oncogene.

Ozenne, P., B. Eymin, E. Brambilla and S. Gazzeri (2010). "The ARF tumor suppressor: structure, functions and status in cancer." Int J Cancer **127**(10): 2239-2247.

Park, E. J., J. H. Lee, G. Y. Yu, G. He, S. R. Ali, R. G. Holzer, C. H. Osterreicher, H. Takahashi and M. Karin (2010). "Dietary and genetic obesity promote liver inflammation and tumorigenesis by enhancing IL-6 and TNF expression." Cell **140**(2): 197-208.

Park, H. J., G. Gusarova, Z. Wang, J. R. Carr, J. Li, K. H. Kim, J. Qiu, Y. D. Park, P. R. Williamson, N. Hay, A. L. Tyner, L. F. Lau, R. H. Costa and P. Raychaudhuri (2011). "Deregulation of FoxM1b leads to tumour metastasis." EMBO Mol Med **3**(1): 21-34.

Park, O. K., L. K. Schaefer, W. Wang and T. S. Schaefer (2000). "Dimer stability as a determinant of differential DNA binding activity of Stat3 isoforms." J Biol Chem **275**(41): 32244-32249.

Parri, M. and P. Chiarugi (2010). "Rac and Rho GTPases in cancer cell motility control." Cell Commun Signal **8**: 23.

Pectasides, E., A. M. Egloff, C. Sasaki, P. Kountourakis, B. Burtness, G. Fountzilas, U. Dafni, T. Zaramboukas, T. Rampias, D. Rimm, J. Grandis and A. Psyrri (2010). "Nuclear localization of signal transducer and activator of transcription 3 in head and neck squamous cell carcinoma is associated with a better prognosis." Clin Cancer Res **16**(8): 2427-2434.

Pena, G., B. Cai, J. Liu, E. P. van der Zanden, E. A. Deitch, W. J. de Jonge and L. Ulloa (2010). "Unphosphorylated STAT3 modulates alpha 7 nicotinic receptor signaling and cytokine production in sepsis." Eur J Immunol **40**(9): 2580-2589.

Petitjean, A., M. I. Achatz, A. L. Borresen-Dale, P. Hainaut and M. Olivier (2007). "TP53 mutations in human cancers: functional selection and impact on cancer prognosis and outcomes." Oncogene **26**(15): 2157-2165.

Pinzani, M., F. Marra and V. Carloni (1998). "Signal transduction in hepatic stellate cells." Liver **18**(1): 2-13.

Pollak, M. (2012). "The insulin and insulin-like growth factor receptor family in neoplasia: an update." Nat Rev Cancer **12**(3): 159-169.

Pollice, A., M. Sepe, V. R. Villella, F. Tolino, M. Vivo, V. Calabro and G. La Mantia (2007). "TBP-1 protects the human oncosuppressor p14ARF from proteasomal degradation." Oncogene **26**(35): 5154-5162.

Pollice, A., M. Vivo and G. La Mantia (2008). "The promiscuity of ARF interactions with the proteasome." FEBS Lett **582**(23-24): 3257-3262.

Quelle, D. E., F. Zindy, R. A. Ashmun and C. J. Sherr (1995). "Alternative reading frames of the INK4a tumor suppressor gene encode two unrelated proteins capable of inducing cell cycle arrest." Cell **83**(6): 993-1000.

Ram, P. T. and R. Iyengar (2001). "G protein coupled receptor signaling through the Src and Stat3 pathway: role in proliferation and transformation." Oncogene **20**(13): 1601-1606.

Randerson-Moor, J. A., M. Harland, S. Williams, D. Cuthbert-Heavens, E. Sheridan, J. Aveyard, K. Sibley, L. Whitaker, M. Knowles, J. N. Bishop and D. T. Bishop (2001). "A germline deletion of p14(ARF) but not CDKN2A in a melanoma-neural system tumour syndrome family." Hum Mol Genet **10**(1): 55-62.

Ray, S., C. Lee, T. Hou, I. Boldogh and A. R. Brasier (2008). "Requirement of histone deacetylase1 (HDAC1) in signal transducer and activator of transcription 3 (STAT3) nucleocytoplasmic distribution." Nucleic Acids Res **36**(13): 4510-4520.

Reich, N., B. Evans, D. Levy, D. Fahey, E. Knight, Jr. and J. E. Darnell, Jr. (1987). "Interferon-induced transcription of a gene encoding a 15-kDa protein depends on an upstream enhancer element." Proc Natl Acad Sci U S A **84**(18): 6394-6398.

Reinhardt, H. C. and B. Schumacher (2012). "The p53 network: cellular and systemic DNA damage responses in aging and cancer." Trends Genet **28**(3): 128-136.

Ren, Z., X. Mao, C. Mertens, R. Krishnaraj, J. Qin, P. K. Mandal, M. J. Romanowski, J. S. McMurray and X. Chen (2008). "Crystal structure of unphosphorylated STAT3 core fragment." Biochem Biophys Res Commun **374**(1): 1-5.

Rizos, H., A. P. Darmanian, G. J. Mann and R. F. Kefford (2000). "Two arginine rich domains in the p14ARF tumour suppressor mediate nucleolar localization." Oncogene **19**(26): 2978-2985.

Roberts, P. J. and C. J. Der (2007). "Targeting the Raf-MEK-ERK mitogen-activated protein kinase cascade for the treatment of cancer." Oncogene **26**(22): 3291-3310.

Rocha, S., K. J. Campbell and N. D. Perkins (2003). "p53- and Mdm2-independent repression of NF-kappa B transactivation by the ARF tumor suppressor." Mol Cell **12**(1): 15-25.

Rocha, S., M. D. Garrett, K. J. Campbell, K. Schumm and N. D. Perkins (2005). "Regulation of NF-kappaB and p53 through activation of ATR and Chk1 by the ARF tumour suppressor." EMBO J **24**(6): 1157-1169.

Salmena, L., A. Carracedo and P. P. Pandolfi (2008). "Tenets of PTEN tumor suppression." Cell **133**(3): 403-414.

Samani, A. A., S. Yakar, D. LeRoith and P. Brodt (2007). "The role of the IGF system in cancer growth and metastasis: overview and recent insights." Endocr Rev **28**(1): 20-47.

Saporita, A. J., L. B. Maggi, Jr., A. J. Apicelli and J. D. Weber (2007). "Therapeutic targets in the ARF tumor suppressor pathway." Curr Med Chem **14**(17): 1815-1827.

Sawey, E. T., M. Chanrion, C. Cai, G. Wu, J. Zhang, L. Zender, A. Zhao, R. W. Busuttil, H. Yee, L. Stein, D. M. French, R. S. Finn, S. W. Lowe and S. Powers (2011). "Identification of a therapeutic strategy targeting amplified FGF19 in liver cancer by Oncogenomic screening." Cancer Cell **19**(3): 347-358.

Schaefer, T. S., L. K. Sanders and D. Nathans (1995). "Cooperative transcriptional activity of Jun and Stat3 beta, a short form of Stat3." Proc Natl Acad Sci U S A **92**(20): 9097-9101.

Schindler, C., X. Y. Fu, T. Improta, R. Aebersold and J. E. Darnell, Jr. (1992). "Proteins of transcription factor ISGF-3: one gene encodes the 91-and 84-kDa ISGF-3 proteins that are activated by interferon alpha." Proc Natl Acad Sci U S A **89**(16): 7836-7839.

Schneller, D., G. Machat, A. Sousek, V. Proell, F. van Zijl, G. Zulehner, H. Huber, M. Mair, M. K. Muellner, S. M. Nijman, R. Eferl, R. Moriggl and W. Mikulits (2011). "p19(ARF) /p14(ARF) controls oncogenic functions of signal transducer and activator of transcription 3 in hepatocellular carcinoma." Hepatology **54**(1): 164-172.

Schroder, M., K. M. Kroeger, H. D. Volk, K. A. Eidne and G. Grutz (2004). "Preassociation of nonactivated STAT3 molecules demonstrated in living cells using bioluminescence resonance energy transfer: a new model of STAT activation?" J Leukoc Biol **75**(5): 792-797.

Schroer, N., J. Pahne, B. Walch, C. Wickenhauser and S. Smola (2011). "Molecular pathobiology of human cervical high-grade lesions: paracrine STAT3 activation in tumor-instructed myeloid cells drives local MMP-9 expression." Cancer Res **71**(1): 87-97.

Semenza, G. L. (2000). "Hypoxia, clonal selection, and the role of HIF-1 in tumor progression." Crit Rev Biochem Mol Biol **35**(2): 71-103.

Serrano, M., H. Lee, L. Chin, C. Cordon-Cardo, D. Beach and R. A. DePinho (1996). "Role of the INK4a locus in tumor suppression and cell mortality." Cell **85**(1): 27-37.

Serrano, M., A. W. Lin, M. E. McCurrach, D. Beach and S. W. Lowe (1997). "Oncogenic ras provokes premature cell senescence associated with accumulation of p53 and p16INK4a." Cell **88**(5): 593-602.

Shao, Y. Y., C. C. Huang, S. D. Lin, C. H. Hsu and A. L. Cheng (2012). "Serum insulin-like growth factor-1 levels predict outcomes of patients with advanced hepatocellular carcinoma receiving antiangiogenic therapy." Clin Cancer Res **18**(14): 3992-3997.

Sharma, D., J. Wang, P. P. Fu, S. Sharma, A. Nagalingam, J. Mells, J. Handy, A. J. Page, C. Cohen, F. A. Anania and N. K. Saxena (2010). "Adiponectin antagonizes the

oncogenic actions of leptin in hepatocellular carcinogenesis." Hepatology **52**(5): 1713-1722.

Shin, D. H., H. Y. Min, A. K. El-Naggar, S. M. Lippman, B. Glisson and H. Y. Lee (2011). "Akt/mTOR counteract the antitumor activities of cixutumumab, an anti-insulin-like growth factor I receptor monoclonal antibody." Mol Cancer Ther **10**(12): 2437-2448.

Shuai, K., G. R. Stark, I. M. Kerr and J. E. Darnell, Jr. (1993). "A single phosphotyrosine residue of Stat91 required for gene activation by interferon-gamma." Science **261**(5129): 1744-1746.

Simboeck, E., J. D. Ribeiro, S. Teichmann and L. Di Croce (2011). "Epigenetics and senescence: learning from the INK4-ARF locus." Biochem Pharmacol **82**(10): 1361-1370.

Stott, F. J., S. Bates, M. C. James, B. B. McConnell, M. Starborg, S. Brookes, I. Palmero, K. Ryan, E. Hara, K. H. Vousden and G. Peters (1998). "The alternative product from the human CDKN2A locus, p14(ARF), participates in a regulatory feedback loop with p53 and MDM2." EMBO J **17**(17): 5001-5014.

Strehlow, I. and C. Schindler (1998). "Amino-terminal signal transducer and activator of transcription (STAT) domains regulate nuclear translocation and STAT deactivation." J Biol Chem **273**(43): 28049-28056.

Sun, X., J. Zhang, L. Wang and Z. Tian (2008). "Growth inhibition of human hepatocellular carcinoma cells by blocking STAT3 activation with decoy-ODN." Cancer Lett **262**(2): 201-213.

Tai, W. T., A. L. Cheng, C. W. Shiau, H. P. Huang, J. W. Huang, P. J. Chen and K. F. Chen (2011). "Signal transducer and activator of transcription 3 is a major kinase-independent target of sorafenib in hepatocellular carcinoma." J Hepatol **55**(5): 1041-1048.

Takahashi, T. and T. Shirasawa (1994). "Molecular cloning of rat JAK3, a novel member of the JAK family of protein tyrosine kinases." FEBS Lett **342**(2): 124-128.

Tang, S. H., D. H. Yang, W. Huang, H. K. Zhou, X. H. Lu and G. Ye (2006). "Hypomethylated P4 promoter induces expression of the insulin-like growth factor-II gene in hepatocellular carcinoma in a Chinese population." Clin Cancer Res **12**(14 Pt 1): 4171-4177.

Tang, Y., K. Kitisin, W. Jogunoori, C. Li, C. X. Deng, S. C. Mueller, H. W. Ressom, A. Rashid, A. R. He, J. S. Mendelson, J. M. Jessup, K. Shetty, M. Zasloff, B. Mishra, E. P. Reddy, L. Johnson and L. Mishra (2008). "Progenitor/stem cells give rise to liver cancer due to aberrant TGF-beta and IL-6 signaling." Proc Natl Acad Sci U S A **105**(7): 2445-2450.

Tannapfel, A., K. Anhalt, P. Hausermann, F. Sommerer, M. Benicke, D. Uhlmann, H. Witzigmann, J. Hauss and C. Wittekind (2003). "Identification of novel proteins associated with hepatocellular carcinomas using protein microarrays." J Pathol **201**(2): 238-249.

Tannapfel, A., C. Busse, L. Weinans, M. Benicke, A. Katalinic, F. Geissler, J. Hauss and C. Wittekind (2001). "INK4a-ARF alterations and p53 mutations in hepatocellular carcinomas." Oncogene **20**(48): 7104-7109.

Tannapfel, A., K. John, N. Mise, A. Schmidt, S. Buhlmann, S. M. Ibrahim and B. M. Putzer (2008). "Autonomous growth and hepatocarcinogenesis in transgenic mice expressing the p53 family inhibitor DNp73." Carcinogenesis **29**(1): 211-218.

Timofeeva, O. A., S. Chasovskikh, I. Lonskaya, N. I. Tarasova, L. Khavrutskii, S. G. Tarasov, X. Zhang, V. R. Korostyshevskiy, A. Cheema, L. Zhang, S. Dakshanamurthy, M. L. Brown and A. Dritschilo (2012). "Mechanisms of unphosphorylated STAT3 transcription factor binding to DNA." J Biol Chem **287**(17): 14192-14200.

Tkach, M., L. Coria, C. Rosemblit, M. A. Rivas, C. J. Proietti, M. C. Diaz Flaque, W. Beguelin, I. Frahm, E. H. Charreau, J. Cassataro, P. V. Elizalde and R. Schillaci (2012). "Targeting Stat3 Induces Senescence in Tumor Cells and Elicits Prophylactic and Therapeutic Immune Responses against Breast Cancer Growth Mediated by NK Cells and CD4+ T Cells." J Immunol **189**(3): 1162-1172.

Tovar, V., C. Alsinet, A. Villanueva, Y. Hoshida, D. Y. Chiang, M. Sole, S. Thung, S. Moyano, S. Toffanin, B. Minguez, L. Cabellos, J. Peix, M. Schwartz, V. Mazzaferro, J. Bruix and J. M. Llovet (2010). "IGF activation in a molecular subclass of hepatocellular carcinoma and pre-clinical efficacy of IGF-1R blockage." J Hepatol **52**(4): 550-559.

Trierweiler, C., H. E. Blum and P. Hasselblatt (2012). "The Transcription Factor c-Jun Protects against Liver Damage following Activated beta-Catenin Signaling." PLoS One **7**(7): e40638.

Ueki, T., J. Fujimoto, T. Suzuki, H. Yamamoto and E. Okamoto (1997). "Expression of hepatocyte growth factor and its receptor c-met proto-oncogene in hepatocellular carcinoma." Hepatology **25**(4): 862-866.

Vinkemeier, U., S. L. Cohen, I. Moarefi, B. T. Chait, J. Kuriyan and J. E. Darnell, Jr. (1996). "DNA binding of in vitro activated Stat1 alpha, Stat1 beta and truncated Stat1: interaction between NH2-terminal domains stabilizes binding of two dimers to tandem DNA sites." EMBO J **15**(20): 5616-5626.

Vogt, M., T. Domoszlai, D. Kleshchanok, S. Lehmann, A. Schmitt, V. Poli, W. Richtering and G. Muller-Newen (2011). "The role of the N-terminal domain in dimerization and nucleocytoplasmic shuttling of latent STAT3." J Cell Sci **124**(Pt 6): 900-909.

Walia, B., L. Wang, D. Merlin and S. V. Sitaraman (2003). "TGF-beta down-regulates IL-6 signaling in intestinal epithelial cells: critical role of SMAD-2." FASEB J **17**(14): 2130-2132.

Wang, B., S. H. Hsu, W. Frankel, K. Ghoshal and S. T. Jacob (2012). "Stat3-mediated activation of microRNA-23a suppresses gluconeogenesis in hepatocellular carcinoma by down-regulating Glucose-6-phosphatase and peroxisome proliferator-activated receptor gamma, coactivator 1 alpha." Hepatology **56**(1): 186-197.

Wang, H., F. Lafdil, L. Wang, O. Park, S. Yin, J. Niu, A. M. Miller, Z. Sun and B. Gao (2011). "Hepatoprotective versus oncogenic functions of STAT3 in liver tumorigenesis." Am J Pathol **179**(2): 714-724.

Wang, T., G. Niu, M. Kortylewski, L. Burdelya, K. Shain, S. Zhang, R. Bhattacharya, D. Gabrilovich, R. Heller, D. Coppola, W. Dalton, R. Jove, D. Pardoll and H. Yu (2004). "Regulation of the innate and adaptive immune responses by Stat-3 signaling in tumor cells." Nat Med **10**(1): 48-54.

Wang, Z., A. Ahmad, Y. Li, D. Kong, A. S. Azmi, S. Banerjee and F. H. Sarkar (2010). "Emerging roles of PDGF-D signaling pathway in tumor development and progression." Biochim Biophys Acta **1806**(1): 122-130.

Wang, Z., D. Kong, Y. Li and F. H. Sarkar (2009). "PDGF-D signaling: a novel target in cancer therapy." Curr Drug Targets **10**(1): 38-41.

Weber, J. D., J. R. Jeffers, J. E. Rehg, D. H. Randle, G. Lozano, M. F. Roussel, C. J. Sherr and G. P. Zambetti (2000). "p53-independent functions of the p19(ARF) tumor suppressor." Genes Dev **14**(18): 2358-2365.

Wegenka, U. M., C. Lutticken, J. Buschmann, J. Yuan, F. Lottspeich, W. Muller-Esterl, C. Schindler, E. Roeb, P. C. Heinrich and F. Horn (1994). "The interleukin-6-activated acute-phase response factor is antigenically and functionally related to members of the signal transducer and activator of transcription (STAT) family." Mol Cell Biol **14**(5): 3186-3196.

Wen, Z., Z. Zhong and J. E. Darnell, Jr. (1995). "Maximal activation of transcription by Stat1 and Stat3 requires both tyrosine and serine phosphorylation." Cell **82**(2): 241-250.

Wilks, A. F., A. G. Harpur, R. R. Kurban, S. J. Ralph, G. Zurcher and A. Ziemiecki (1991). "Two novel protein-tyrosine kinases, each with a second phosphotransferase-related catalytic domain, define a new class of protein kinase." Mol Cell Biol **11**(4): 2057-2065.

Willems, L., J. Tamburini, N. Chapuis, C. Lacombe, P. Mayeux and D. Bouscary (2012). "PI3K and mTOR signaling pathways in cancer: new data on targeted therapies." Curr Oncol Rep **14**(2): 129-138.

Wu, W. Y., J. Li, Z. S. Wu, C. L. Zhang and X. L. Meng (2011). "STAT3 activation in monocytes accelerates liver cancer progression." BMC Cancer **11**: 506.

Xiao, H., J. Chung, H. Y. Kao and Y. C. Yang (2003). "Tip60 is a co-repressor for STAT3." J Biol Chem **278**(13): 11197-11204.

Xie, C., W. Wang, F. Yang, M. Wu and Y. Mei (2012). "RUVBL2 is a novel repressor of ARF transcription." FEBS Lett **586**(4): 435-441.

Xirodimas, D. P., J. Chisholm, J. M. Desterro, D. P. Lane and R. T. Hay (2002). "P14ARF promotes accumulation of SUMO-1 conjugated (H)Mdm2." FEBS Lett **528**(1-3): 207-211.

Xu, Q., J. Briggs, S. Park, G. Niu, M. Kortylewski, S. Zhang, T. Gritsko, J. Turkson, H. Kay, G. L. Semenza, J. Q. Cheng, R. Jove and H. Yu (2005). "Targeting Stat3 blocks both HIF-1 and VEGF expression induced by multiple oncogenic growth signaling pathways." Oncogene **24**(36): 5552-5560.

Xue, W., L. Zender, C. Miething, R. A. Dickins, E. Hernando, V. Krizhanovsky, C. Cordon-Cardo and S. W. Lowe (2007). "Senescence and tumour clearance is triggered by p53 restoration in murine liver carcinomas." Nature **445**(7128): 656-660.

Yang, E., M. A. Henriksen, O. Schaefer, N. Zakharova and J. E. Darnell, Jr. (2002). "Dissociation time from DNA determines transcriptional function in a STAT1 linker mutant." J Biol Chem **277**(16): 13455-13462.

Yang, E., Z. Wen, R. L. Haspel, J. J. Zhang and J. E. Darnell, Jr. (1999). "The linker domain of Stat1 is required for gamma interferon-driven transcription." Mol Cell Biol **19**(7): 5106-5112.

Yang, J., M. Chatterjee-Kishore, S. M. Staugaitis, H. Nguyen, K. Schlessinger, D. E. Levy and G. R. Stark (2005). "Novel roles of unphosphorylated STAT3 in oncogenesis and transcriptional regulation." Cancer Res **65**(3): 939-947.

Yang, J., X. Liao, M. K. Agarwal, L. Barnes, P. E. Auron and G. R. Stark (2007). "Unphosphorylated STAT3 accumulates in response to IL-6 and activates transcription by binding to NFkappaB." Genes Dev **21**(11): 1396-1408.

Yang, J. and G. R. Stark (2008). "Roles of unphosphorylated STATs in signaling." Cell Res **18**(4): 443-451.

Yang, S. F., S. N. Wang, C. F. Wu, Y. T. Yeh, C. Y. Chai, S. C. Chunag, M. C. Sheen and K. T. Lee (2007). "Altered p-STAT3 (tyr705) expression is associated with histological grading and intratumour microvessel density in hepatocellular carcinoma." J Clin Pathol **60**(6): 642-648.

Yao, Z., S. Fenoglio, D. C. Gao, M. Camiolo, B. Stiles, T. Lindsted, M. Schlederer, C. Johns, N. Altorki, V. Mittal, L. Kenner and R. Sordella (2010). "TGF-beta IL-6 axis mediates selective and adaptive mechanisms of resistance to molecular targeted therapy in lung cancer." Proc Natl Acad Sci U S A **107**(35): 15535-15540.

Yi, Z. Y., L. J. Feng, Z. Xiang and H. Yao (2011). "Vascular endothelial growth factor receptor-1 activation mediates epithelial to mesenchymal transition in hepatocellular carcinoma cells." J Invest Surg **24**(2): 67-76.

Yip-Schneider, M. T., P. J. Klein, S. C. Wentz, A. Zeni, A. Menze and C. M. Schmidt (2009). "Resistance to mitogen-activated protein kinase kinase (MEK) inhibitors correlates with up-regulation of the MEK/extracellular signal-regulated kinase pathway in hepatocellular carcinoma cells." J Pharmacol Exp Ther **329**(3): 1063-1070.

Yoshikawa, H., K. Matsubara, G. S. Qian, P. Jackson, J. D. Groopman, J. E. Manning, C. C. Harris and J. G. Herman (2001). "SOCS-1, a negative regulator of the JAK/STAT pathway, is silenced by methylation in human hepatocellular carcinoma and shows growth-suppression activity." Nat Genet **28**(1): 29-35.

Yoshizawa, H. (2002). "Hepatocellular carcinoma associated with hepatitis C virus infection in Japan: projection to other countries in the foreseeable future." Oncology **62 Suppl 1**: 8-17.

Yue, H., W. Li, R. Desnoyer and S. S. Karnik (2010). "Role of nuclear unphosphorylated STAT3 in angiotensin II type 1 receptor-induced cardiac hypertrophy." Cardiovasc Res **85**(1): 90-99.

Yue, H., K. Tanaka, T. Furukawa, S. S. Karnik and W. Li (2012). "Thymidine phosphorylase inhibits vascular smooth muscle cell proliferation via upregulation of STAT3." Biochim Biophys Acta **1823**(8): 1316-1323.

Yun, U. J., S. E. Park, Y. S. Jo, J. Kim and D. Y. Shin (2012). "DNA damage induces the IL-6/STAT3 signaling pathway, which has anti-senescence and growth-promoting functions in human tumors." Cancer Lett **323**(2): 155-160.

Zammarchi, F., E. de Stanchina, E. Bournazou, T. Supakorndej, K. Martires, E. Riedel, A. D. Corben, J. F. Bromberg and L. Cartegni (2011). "Antitumorigenic potential of STAT3 alternative splicing modulation." Proc Natl Acad Sci U S A **108**(43): 17779-17784.

Zamule, S. M., S. C. Strom and C. J. Omiecinski (2008). "Preservation of hepatic phenotype in lentiviral-transduced primary human hepatocytes." Chem Biol Interact **173**(3): 179-186.

Zeng, Y., Y. Kotake, X. H. Pei, M. D. Smith and Y. Xiong (2011). "p53 binds to and is required for the repression of Arf tumor suppressor by HDAC and polycomb." Cancer Res **71**(7): 2781-2792.

Zerrouqi, A., B. Pyrzynska, M. Febbraio, D. J. Brat and E. G. Van Meir (2012). "P14ARF inhibits human glioblastoma-induced angiogenesis by upregulating the expression of TIMP3." J Clin Invest **122**(4): 1283-1295.

Zhang, C., X. Guo, L. Zhang, Z. Lu, N. Ma, Y. Cheng, F. Shen, B. Zhang, M. Wu and L. Wei (2008). "Methylation-related silencing of p14ARF gene correlates with telomerase activity and mRNA expression of human telomerase reverse transcriptase in hepatocellular carcinoma." J Surg Oncol **98**(6): 462-468.

Zhang, J. F., M. L. He, W. M. Fu, H. Wang, L. Z. Chen, X. Zhu, Y. Chen, D. Xie, P. Lai, G. Chen, G. Lu, M. C. Lin and H. F. Kung (2011). "Primate-specific microRNA-637 inhibits tumorigenesis in hepatocellular carcinoma by disrupting signal transducer and activator of transcription 3 signaling." Hepatology **54**(6): 2137-2148.

Zhang, J. J., U. Vinkemeier, W. Gu, D. Chakravarti, C. M. Horvath and J. E. Darnell, Jr. (1996). "Two contact regions between Stat1 and CBP/p300 in interferon gamma signaling." Proc Natl Acad Sci U S A **93**(26): 15092-15096.

Zhang, L., J. N. Wang, J. M. Tang, X. Kong, J. Y. Yang, F. Zheng, L. Y. Guo, Y. Z. Huang, L. Tian, S. F. Cao, C. H. Tuo, H. L. Guo and S. Y. Chen (2012). "VEGF is essential for the growth and migration of human hepatocellular carcinoma cells." Mol Biol Rep **39**(5): 5085-5093.

Zhang, W., X. D. Zhu, H. C. Sun, Y. Q. Xiong, P. Y. Zhuang, H. X. Xu, L. Q. Kong, L. Wang, W. Z. Wu and Z. Y. Tang (2010). "Depletion of tumor-associated macrophages enhances the effect of sorafenib in metastatic liver cancer models by antimetastatic and antiangiogenic effects." Clin Cancer Res **16**(13): 3420-3430.

Zhong, Z., Z. Wen and J. E. Darnell, Jr. (1994). "Stat3 and Stat4: members of the family of signal transducers and activators of transcription." Proc Natl Acad Sci U S A **91**(11): 4806-4810.

Zhong, Z., Z. Wen and J. E. Darnell, Jr. (1994). "Stat3: a STAT family member activated by tyrosine phosphorylation in response to epidermal growth factor and interleukin-6." Science **264**(5155): 95-98.

Zugowski, C., F. Lieder, A. Muller, J. Gasch, F. M. Corvinus, R. Moriggl and K. Friedrich (2011). "STAT3 controls matrix metalloproteinase-1 expression in colon carcinoma cells by both direct and AP-1-mediated interaction with the MMP-1 promoter." Biol Chem **392**(5): 449-459.

8 Materials and Methods

Immunoblotting

Dishes containing adherent cells were put on ice, washed twice with ice-cold PBS (phosphate buffer saline), lysed with RIPA buffer (containing freshly added protease inhibitors) and immediately collected by a rubber policeman scraper. After a freeze and thaw step with liquid nitrogen, the suspension was incubated on ice for 10 minutes and centrifuged at full speed for 15 minutes at 4°C. The supernatant containing the protein extract was used to determine the concentration using the Bradford assay according to the manufacturer's description (BioRad Laboratories, Hercules, CA, USA). 30 µg of protein extract mixed with 5 x SDS sample buffer was boiled at 95°C for 5 minutes and loaded to a polyacrylamide (PAA) gel. Depending on the size of proteins, 10% or 15% separation gel and a 5% stacking gel were prepared. The gel was run in electrophoresis buffer at 16-25 mA (approx. 100 V). Then, separated proteins were transferred to a nitro-cellulose membrane (Protran, Whatman, Kent, UK) in blotting buffer for 1 hour at 100 V const. Next, the membrane was stained with Ponceau S (0.1% in 5% acetic acid), blocked with blocking solution (5% BSA dissolved in TBST (Tris-Buffered Saline Tween-20) for 1 hour and incubated with the primary antibody (anti-STAT3, anti-pY705-STAT3, all Cell Signaling, Beverly, MA, USA; anti-p53, anti-$p21^{Waf}$, anti-NFκB, all Santa Cruz Biotechnologicals, Santa Cruz, CA, USA; anti-actin, anti-$p14^{ARF}$ all Sigma, St.Louis, MO, USA; anti-PTEN, Abcam, Milton, Cambridge, UK; dissolved 1:100 in blocking solution) at 4°C overnight. After 3 washing steps with TBST for 10 minutes, the membrane was incubated with the respective secondary antibody (peroxidase-labeled rabbit IgG and mouse IgG, Vector Laboratories, Burlingame, CA, USA; dissolved 1:10.000 in TBST) for 1 hour at room temperature (RT) and washed 3 times with TBST for 10 minutes. Signal detection was accomplished by incubation with chemoluminescent luminol/coumarin solution for 2 minutes and exposed to X-ray films.

Solutions and Buffers

RIPA buffer (pH 7.4)

- 50 mM Tris (pH 7.4)
- 150 mM NaCl
- 1 mM ß-glycerophosphat (pH 7.2)
- 0.5% DOC (Na-deoxycholate)

- 1% Nonidet P-40

Protease inhibitors
- Leupeptin 10 µg/ml
- Aprotinin 10 µg/ml
- PMSF 1 mM

Phosphatase inhibitors
- NaF 1 mM
- Na_3VO_4 1 mM

5 x SDS sample buffer
- 250 mM Tris (pH 6.8)
- 10% SDS
- 30% glycerol
- 5% ß-mercaptoethanol
- 100 nM dithiotitol
- Bromphenolblue (some granules)

10% separation gel	***15% separation gel***	***5% stacking gel***
- 4.45 ml 30% PAA	- 6.25 ml 30% PAA	- 0.5 ml 30% PAA
- 2.5 ml 2 M Tris pH 8.8	- 3.125 ml 2 M Tris pH 8.8	- 0.5 ml 2M Tris, pH 6.8
- 6.2 ml ddH_2O	- 3.125 ml ddH_2O	- 3 ml ddH_2O

Composition for 2 gels each; add 50 µl 10% APS and 8µl TEMED to separation gels and 20 µl 10% APS and 4µl TEMED to stacking gel, respectively

Electrophoresis Buffer
- 25 mM Tris
- 192 mM glycine
- 0.1% SDS

Blotting Buffer
- 25 mM Tris
- 192 mM glycine
- 0.02% SDS
- 15% Methanol

Luminol/coumarin solution
- 200 ml 0.1 M Tris (pH 8.8)
- 500 µl p-coumarin acid (340 ng/26 ml DMSO)
- 1ml luminol (2.26 g in 51 ml DMSO)
- freshly added 3% H_2O_2 3 µl/ml

TBST
- 10 ml 10% Tween in 1 l 1xTBS (final 0.1% Tween)

PBS
- 8 g NaCl
- 0.2 g KCl
- 1.44 g Na_2HPO_4
- 0.24 g of KH_2PO_4
- ddH_2O to 1 l; adjust to pH 7.4

Cell fractionation

After two washing steps with ice-cold PBS, cells were harvested from a 100 mm plate by resuspending in 500 µl PBS and centrifugation at 500 g for 5 minutes. Nuclear and cytoplasmic extraction was performed according to the manufacturer's instruction (NE-PER®, Thermo Scientific, Waltham, MA, USA). Briefly, the cell pellet was suspended in ice-cold cytoplasmic extraction reagent (CER) I. After an incubation step and addition of CER II the cell suspension was centrifuged for 5 minutes at maximum speed (16.000 g). The supernatant containing the cytoplasmic fraction was carefully decanted. Next, the insoluble pellet was suspended to ice-cold nuclear extraction reagent. During incubation for 40 minutes including vortexing every 10 minutes, the nuclear fraction was extracted from the pellet. Finally, supernatant containing the nuclear fraction was harvested by centrifugation at maximum speed (16.000 g) for 10 minutes. Extract integrity was monitored by immunoblotting using nucleoporin (BD Biosciences, Franklin Lakes, NJ, USA) and tubulin (Calbiochem, LaJolla, CA, USA) antibodies for nuclear and cytoplasmic fraction, respectively. All incubation and centrifugation steps were performed at 4°C.

Transient transfection and reporter assays

Cells were plated on 6-well plates and transiently transfected after 24 hours with 1 µg of control β-Galactosidase reporter plasmid (pAD-CMV1-βgal) and 2 µg STAT3 minimal (m)CMV-Luc promoter. Transfection was performed with Lipofectamine Plus according to the protocol of the manufacturer (Invitrogen, Carlsbad, CA, USA). After 48 hours, cells were lysed in lysis buffer (250 mM Tris/HCl, pH 7.5, 0.5% Triton X-100, Roth Lactan, Graz, Austria) and centrifuged at full speed (16.000 g) for 10 minutes at 4°C. Supernatant containing the cell extract were used for reporter assays. Transfection efficiency was evaluated by β-Galactosidase activity. Luciferase activity was then normalized to β-

Galactosidase activity. Assays were performed in triplicate and results represent the average of 3 independent experiments.

ß-Galactosidase assay

After incubation at 37°C for 30 minutes β-galactosidase activity was photometrically determined using onitrophenyl-β-d-galactopyranoside (ONPG) and transfection efficiency was measured by ELISA (Roche, Mannheim, Germany) according to the instructions of the manufacturer.

20 µl Cell extract was mixed in proportions depicted below:

- 4 µl 100x Mg solution
- 88 µl x ONPG
- 268 µl 0.1 M sodium phosphate

Solutions and Buffers

100 x $MgCl_2$ solution

- 0.1 M $MgCl_2$
- 4.5 M ß-Mercaptoethanol

1x ONPG (Sigma, St. Louis, MO, USA)

- 4 mg/ml of ONPG dissolved in 0.1 M sodium phosphate pH 7.5

0.1 M sodium phosphate solution pH 7.5

- 16.4 ml 0.5 M Na_2HPO_4
- 9 ml 0.2 M NaH_2PO_4
- ddH_2O to 100 ml

Luciferase Assay

20 µl of cell extract was mixed with 50 µl assay buffer in a 96 well plate. Luciferase activity was measured with a Luminoskan microplate reader (Labsystems, Farnborough, UK) according to the protocol of the manufacturer.

Solutions and Buffers

10 ml Assay Buffer

- 2.5 ml 0.1 M glycylglycine pH 7.8
- 150 µl 1 M $MgSO_4$
- 500 µl 0.1 M ATP
- ddH_2O to 10 ml

10 ml Injection Buffer
- 6 ml H_2O
- 2 ml 0.1 M glycylglycine pH 7.8
- 2 ml 1 mM luciferin

1 mM Luciferin
- D-Luciferin Sodium salt (Sigma)
- 10 mg luciferin dissolved in 33 ml ddH_2O

0.1 M ATP
- ATP Disodium salt (Böhringer, Ingelheim, Germany), 1 g ATP dissolved in 16.5 ml ddH_2O

Immunofluorescence

Adherent cells on glass slides (Superfrost microscope slides, Menzel, Braunschweig, Germany) were washed twice with ice-cold PBS. 4% formaldehyde solution (Histofix, Roth Lactan, Graz, Austria) was used to fix cells (30 minutes, RT). After another washing step, formaldehyde was inactivated by using NH_4Cl (125 mg dissolved in 50 ml ddH_2O) for 5 minutes. In the next step, 0.05% Triton X-100 (Roth Lactan, Graz, Austria) in PBS was applied for permabilization and 0.2% fish gelatin (Sigma, St.Louis, MO, USA) in PBS was performed for blocking. Afterwards, 150 µl of primary antibody (anti-$p14^{ARF}$, Sigma; anti-STAT3, Cell Signaling Technology, Beverly, MA, USA; anti-NFκB, Santa Cruz Biotechnology, Santa Cruz, CA, USA; anti-Smad2/3, Upstate Biotechnology, Lake Placid, NY, USA; diluted 1:1.000 in blocking solution) was applied for 1 hour. After three washing steps with PBS, the secondary antibody mix provided in blocking solution containing secondary antibodies (diluted 1:1.000; anti-rabbit-Alexa-546; anti-rabbit-Alexa-488; anti-mouse-Alexa-488; all Invitrogen, Carlsbad, CA, USA), Phalloidin (diluted 1:500; Sigma) and DAPI (diluted 1:5.000; Invitrogen) was incubated for 45 minutes in the dark. Finally, slides were mounted with mowiol (Sigma), covered with a cover slip and stored in the dark. Analysis was performed with a confocal microscope (Zeiss, LSM 700, Oberkochen, Germany). Washing steps were performed with PBS for 5 minutes each.

Immunohistochemistry

Formalin-fixed, paraffin-embedded tumor sections of 4 µm were rehydrated in staining jaws by a set of alcohols with decreasing concentration (two times Xylol for 20 minutes, two times 100% Isopropanol (10 minutes), 96%, 80% 70%, 60%, (2 minutes each)). Afterwards, the epitopes were unmasked by boiling the slides in 0.01 M citric acid pH 6.0 for 20 minutes and cooled down for 20 minutes. Digestion of peroxidases was performed by 2% H_2O_2 (dissolved

in PBS) incubation for 10 minutes. After washing with PBS for 5 minutes, cells were permeabilized with 0.1% solution of Triton-X 100 (dissolved in PBS) for 5 minutes. Blocking, antibody incubation and signal detection were performed according to the instruction of the manufacturer (VECTASTAIN ABC kit; DAB Peroxidase Substrate Kit; Vector Laboratories, Burlingame, CA, USA. Primary antibodies: anti-STAT3, Cell Signaling Technology, Beverly, MA, USA; anti-$p14^{ARF}$, Sigma, St. Louis, MO, USA; Cell Signaling Technology; Novus Biologicals, Littleton, CO, USA.Primary antibody dilution was at 1:100). Next, a counterstain with Hematoxilin for 1 min (Hemalaun, Merck, Darmstadt, Germany) was performed. Finally the sample was dehydrated by an increasing set of alcohols and mounted with Entellan (Merck).

Proliferation Assays

Dense curve

12 x 10^4 cells were seeded in 12-well plates, each in triplicates for 4 timepoints (day 1, 3, 5, 7) in the respective growth medium as described. Every second day, cells were detached and re-suspended in 1 ml medium. An aliquot (50 to 250 µl, depending on cell number) was used to measure the cell number (Casy Cell Counter, Schärfe Systems, Reutlingen, Germany).

Cumulative cell number

2 x 10^5 cells were seeded in 6-well plates, each in triplicates in the respective growth medium as described. Every second day, an aliquot of 50 µl was used to measure the cell number (Casy Cell Counter, Schärfe Systems).

Microarray Expression profiling

Total RNA was isolated from triplicates of cells using the RNeasy Mini kit (Qiagen, Valencia, CA, USA). The integrity and quantity of RNA was analyzed by Agilent Bioanalyzer (Agilent Technologies, Santa Clara, CA, USA). Labeling and hybridization on Affymetrix Gene-Chip mouse gene 1.0 ST Array (Affymetrix, Santa Clara, CA, USA) as well as scanning of signal intensities was done according to the manufacturer's protocol.

(Note: remaining materials and methods are described in the manuscript of Schneller et al. in section 4.4)

9 Acknowledgements

First of all I want to thank my supervisor Wolfgang Mikulits for giving me the opportunity to be part of this exciting project. Without his guidance, expertise and patience the realization of this thesis would have been barely possible.

I am also very thankful to join his fantastic lab, whose spirit greatly contributed to scientific discourses. I would like to give special mention to Alexandra Sousek for the essential reflections on our project, Heidemarie Huber for her indispensable help in various experiments, Doris Schneller, who introduced me to and build up the project and Michaela Petz and Markus Grubinger for their helpful advice and assistance to overcome one or the other problem. Furthermore, I want to appreciate Christine Haider, Franziska van Zijl, Nicole Them, Sara Doppler, Sabine Mall, Patrick Reichl, Gerhard Führlinger, Christoph Kornauth and the ones I forgot for discussions and activities in- and outside the lab and for creating a nice working atmosphere.

Last but not least I would like to express my gratitude to my friends, to my family and to B-Trix for having supported and encouraged me beyond the lab.

10 Curriculum Vitae

PERSONAL DATA

Name:	Georg Machat
Date of birth:	20. December 1978
Place of birth:	Vienna
Nationality:	Austria
Family status:	single
Address:	Degengasse 63/21 1160 Wien Tel: +43-699-19687757 E-mail: georgmachat@hotmail.com

EDUCATION

2008 – 2012	Doctoral thesis at the Institute for Cancer Research, Department of Inner Medicine I, Medical University Vienna
2009 – 2012	TOXICOLOGY University Course for Postgraduates
2008	Final exam of diploma thesis
2007 – 2008	Diploma thesis at the Institute of Medical Biochemistry, Max F. Perutz Laboratories, Division of Molecular Biology, under the supervision of Prof. Dr. Christian Seiser
2005	Semester abroad at the Humboldt University of Berlin, Germany, within the ERASMUS framework, supported by the European Union
2002 - 2006	Study of Biology – Microbiology/Genetics at the University of Vienna

1999 - 2002:	Study of Food- and Biotechnology, at the University of Agricultural Sciences
1998	Alternative civilian service at the Volkshilfe Wien
1997	Final secondary-school examinations at the Bundesrealgymnasium 18, Vienna

PUBLICATIONS

p19(ARF) /p14(ARF) controls oncogenic functions of signal transducer and activator of transcription 3 in hepatocellular carcinoma.
Schneller D, Machat G, Sousek A, Proell V, van Zijl F, Zulehner G, Huber H, Mair M, Muellner MK, Nijman SM, Eferl R, Moriggl R, Mikulits W.
Hepatology. 2011 Jul;54(1):164-72. doi: 10.1002/hep.24329.

A human model of epithelial to mesenchymal transition to monitor drug efficacy in hepatocellular carcinoma progression.
van Zijl F, Mall S, Machat G, Pirker C, Zeillinger R, Weinhaeusel A, Bilban M, Berger W, Mikulits W.
Mol Cancer Ther. 2011 May;10(5):850-60. Epub 2011 Mar 1.

Epithelial-mesenchymal transition in hepatocellular carcinoma.
van Zijl F, Zulehner G, Petz M, Schneller D, Kornauth C, Hau M, Machat G, Grubinger M, Huber H, Mikulits W.
Future Oncol. 2009 Oct;5(8):1169-79. Review.